Distribution Agreement

In presenting this thesis or dissertation as a partial fulfillment of the requirements for an advanced degree from Emory University, I hereby grant to Emory University and its agents the non-exclusive license to archive, make accessible, and display my thesis or dissertation in whole or in part in all forms of media, now or hereafter known, including display on the world wide web. I understand that I may select some access restrictions as part of the online submission of this thesis or dissertation. I retain all ownership rights to the copyright of the thesis or dissertation. I also retain the right to use in future works (such as articles or books) all or part of this thesis or dissertation.

Signature:

_____ April 6, 2018

Ashley Jacqueline Swain Date

Structural Plasticity of GABAergic and Glutamatergic Terminals in the Ventral Motor and Caudal Intralaminar Thalamic Nuclei in MPTP-treated Parkinsonian Monkeys

By

Ashley J. Swain

Doctor of Philosophy

Graduate Division of Biological and Biomedical Sciences

Neuroscience

_____

Yoland Smith, Ph.D.

Advisor

_____

Thomas Wichmann, Ph.D.

Advisor

_____

Paul Bolam, Ph.D.

Committee Member

_____

Dieter Jaeger, Ph.D.

Committee Member

_____

Malu Tansey, Ph.D.

Committee Member

Accepted:

_____

Lisa A. Tedesco, Ph.D.

Dean of the James T. Laney School of Graduate Studies

2018

Structural Plasticity of GABAergic and Glutamatergic Terminals in the Ventral Motor and Caudal Intralaminar Thalamic Nuclei in MPTP-treated Parkinsonian Monkeys

By

Ashley J. Swain

B.S. in Mathematics

Spelman College, 2009

M.S. in Mathematics

University of Nebraska-Lincoln, 2011

Advisors: Yoland Smith, Ph.D. and Thomas Wichmann, M.D.

An abstract of a dissertation submitted to the Faculty of the James T. Laney School of Graduate Studies of Emory University in partial fulfillment of the requirements for the degree of Doctor of Philosophy in the Graduate Division of Biological and Biomedical Sciences in Neuroscience

2018

Abstract

Structural Plasticity of GABAergic and Glutamatergic Terminals in the Ventral Motor and Caudal Intralaminar Thalamic Nuclei in MPTP-treated Parkinsonian Monkeys

By Ashley J. Swain

In primates, the parvocellular part of the ventral anterior nucleus (VApc) and the centromedian nucleus (CM) are the thalamic targets of inputs from the internal globus pallidus (GPi). Neurons in VApc and CM also receive glutamatergic projections from the cerebral cortex, and GABAergic inputs from the reticular nucleus (RTN) and interneurons. In MPTP-treated monkeys, the firing rate and pattern of VApc neurons is altered. To examine whether structural changes in synaptic connectivity are associated with these dysfunctions, we used light- and electron microscopy (LM and EM) immunohistochemical and tracing methods to assess changes in GABAergic and glutamatergic synaptic networks of the VApc and CM in parkinsonian monkeys.

At the LM level, the intensity of immunostaining for GABAergic markers in VApc and CM did not significantly differ between normal and parkinsonian monkeys, suggesting that there are no gross changes in the GABAergic innervation to these nuclei in the parkinsonian state. At the EM level, we identified 3 types of terminals in VApc and CM: Terminals forming asymmetric synapses (As-type), which originate mostly from the cerebral cortex, terminals forming single symmetric synapses (S1-type), representing GABAergic inputs from the RTN and interneurons, and terminals forming multiple symmetric synapses (S2-type) which originate from the GPi. The average density of As-type terminals outnumbered that of S1 and S2-type terminals in VApc and CM of normal and parkinsonian monkeys. Compared to untreated animals, the density of As-type terminals was lower in the VApc of parkinsonian monkeys, while that of S1 and S2-type terminals was the same. The pattern of synaptic connectivity of the three terminal subtypes did not differ between both groups. However, the proportion of S2-type terminals in contact with vesicle-filled dendrites of GABAergic interneurons was higher in VApc and CM of parkinsonian monkeys. Preliminary evidence from 20 reconstructed pallidothalamic terminals suggest an increase in the flat area and surface area of GABAergic synapses in parkinsonian animals. Together, these findings suggest that the parkinsonian state is associated with plasticity in the prevalence and microcircuitry of glutamatergic corticothalamic afferents and GABAergic pallidothalamic inputs, which may contribute to the pathophysiology of the basal ganglia-thalamocortical system in parkinsonism.

Structural Plasticity of GABAergic and Glutamatergic Terminals in the Ventral Motor and Caudal Intralaminar Thalamic Nuclei in MPTP-treated Parkinsonian Monkeys

By

Ashley J. Swain

B.S. in Mathematics

Spelman College, 2009

M.S. in Mathematics

University of Nebraska-Lincoln, 2011

Advisors: Yoland Smith, Ph.D. and Thomas Wichmann, M.D.

A dissertation submitted to the Faculty of the

James T. Laney School of Graduate Studies of Emory University

in partial fulfillment of the requirements for the degree of Doctor

of Philosophy in the Graduate Division of Biological and

Biomedical Sciences in Neuroscience

2018

Acknowledgements

First and foremost, I would like to thank my Lord and Savior, Jesus Christ, for continuing to bless, support, encourage, and strengthen me throughout my graduate career. It is by his grace and mercy that I am where I am today. I would like to express my sincere gratitude to my advisors, Drs. Yoland Smith and Thomas Wichmann, for their unconditional support, guidance, and dedication to my achievement of a doctoral degree in neuroscience. Their scientific training and mentorship have been more valuable to me than I could ever imagine, and I am forever grateful to them. I appreciate them for molding me into a scientist who I never imagined I could become and for seeing the potential in me when I could not see it in myself. In addition, my thesis committee has significantly contributed to my success by providing unwavering support and mentoring. I sincerely thank them. Also thank you to all of my science and lab colleagues, especially Jeff, Susan, Rosa and Adriana. A special thank you to the Emory Neuroscience Program and Gary Longstreet, for constantly uplifting and guiding me through these last six years.

I am also very grateful for my social supports, which includes my family and friends. To my close friends, thank you for reminding and encouraging me that I could do this, and that I am not alone. I am very much appreciative of your constant, love, support, laughs, motivation, and inspirational quotes. To my family, each individual member has supported me in one way or another and greatly contributed to my success. I know for certain I could not have continued towards this path of success without certain people who always saw my potential and pushed me beyond my comfort level. A special thank you to: my mother, Jackie, my sister, Nikki, my Nana, Carrie, my Uncle Poochie, my father, John, my Atlanta parents/mentors Drs. Sylvia and Robert Bozeman, best friend's, godparents, aunts, cousins and in-laws. Mom, I thank you so much for instilling in me perseverance, determination, and the importance of education. It is because of your selfless nature that I observed when I was a child that I am where I am today, a first-

generation college graduate with a master's degree in mathematics and a doctoral degree in neuroscience.

Finally, I extend my utmost gratitude and appreciation to my immediate family, Auden and Michael. Auden, I was blessed to have you enter my life at a crucial period. Not only did you teach me how to be a mother and what it meant to be selfless but you motivated me to do more and to excel every step of the way. When you entered my life, I found a work ethic like no other and I became driven because I knew that you were watching every move I made from the moment you opened your eyes. I thank you so much for being an easy going, playful, friendly and happy child. You provided light in the time of darkness and gave me strength to keep pushing forward. My husband, Michael, words cannot express the amount of appreciation and love I have for you. You have endured the most throughout my graduate school experience. I know you had no idea of what you were getting into when you signed up to be by my side during this journey. Thank you for stepping up when needed, thank you for allowing me to work late and travel while you took care of our son. You have spent countless nights staying up with me when I had to work extremely late. I literally could not have done this without you. You have always been there to encourage me through the tough times and reminded me to keep pushing forward and to fight through the tears. My number one supporter that have helped me to celebrate every success, thank you for never giving up on me. Michael, God blessed me with a perfectly patient person to travel this journey with. I thank you with all of my heart and soul, for this degree is yours just as much as it is mines. You have been a wonderful father and husband throughout my graduate experiences. You are the real MVP!

Graduate school has not been an easy road for me, but with love and support from my family, friends, advisors, mentors, committee members, and colleagues I have finally made it! Thanks to all of you from the bottom of my heart. I am eternally grateful. GOD designed me for accomplishment, engineered me for success, and endowed me with the seeds of greatness.

Table of Contents

List of Figures

List of Tables

Chapter 1: Introduction & Background

Contains excerpts from:

Bogenpohl JW, Swain AJ, and Smith Y. (2017) Direct Pathway. In: Neuroscience and biobehavioral psychology. Elsevier: Oxford, UK (in press).

1.1 Introduction

Our current knowledge of information processing in the brain along the basal ganglia-thalamacortical loops is limited despite the tremendous developments in our understanding of the functional anatomy of the basal ganglia over the past decades. Today, we are still uncertain as to what happens with information that leaves the internal segment of the globus pallidus (GPi) or substantia nigra reticulata (SNr) and enters the thalamus or other basal ganglia output nuclei. In addition, loss of nigrostriatal dopamine (DA) in Parkinson's disease (PD) is thought to increase basal ganglia (BG) inhibition of thalamus from the GPi and SNr, resulting in reduced thalamic activity, which may then lead to decreased cortical activity and motoric slowing. However, the functional impact of the increased BG outflow on the thalamocortical system proposed in this model remains highly speculative. In fact, data gathered from PD patients and various animal models of parkinsonism suggest that the situation is far more complex and heterogeneous than what would be predicted by this model. Thus, an in-depth knowledge of the anatomy and physiology of the interconnections between various nodes of the basal ganglia-thalamocortical loops in normal and diseased states is a prerequisite to a deeper understanding of the functional network changes that underlie the pathophysiology of these loops in PD. Here, we aim to fill this gap of knowledge by using anatomical methods to determine potential changes in synaptic connectivity and morphology of GPi terminals in the parvocellular part of the ventral anterior (VApc) and centromedian (CM) thalamic nuclei in control and MPTP-treated parkinsonian monkeys. These findings provide a solid foundation for potential changes in structure-function relationships that may underlie some aspects of the pathophysiology of the pallidothalamic and corticothalamic systems in Parkinson's disease.

1.2 Functional Circuitry of the Basal Ganglia

1.2.1 General Organization of the Basal Ganglia

In the brain, there are a collection of interconnected subcortical nuclei, known as the basal ganglia, that influence and are influenced by cortical and brainstem functions. The core function of the basal ganglia is to regulate motor and non-motor activity. Various interconnected subcortical structures that consist of the caudate nucleus and putamen (also known as the striatum), the internal and external segment of the globus pallidus (GPe and GPi), the substantia nigra, and the subthalamic nucleus (STN), all of which are involved in intricate information processing, make up the basal ganglia (Wichmann and DeLong, 1996). The striatum is separated into two primary parts: the dorsal striatum, that is composed of the caudate nucleus and the putamen separated by fibers of the internal capsule in primates, and the ventral striatum, that consists of the nucleus accumbens and olfactory tubercle (Carpenter et al., 1976). Unlike primates, the dorsal striatum in rodents consists of a single mass of gray matter referred to as the caudate-putamen complex (Chronister et al., 1976). The pallidum in primates is divided into two parts, the internal and external segments of the globus pallidus also known as GPi and GPe, respectively. Since there is no GPi component in rodents, the homologue of GPi is known as the entopeduncular nucleus (EPN) and that of GPe is the globus pallidus (GP). Together, the putamen and globus pallidus make up a nucleus called the lenticular nucleus, which is lateral to the internal capsule. Another key basal ganglia structure is the STN, a small almond-shaped nucleus located just below the thalamus, that is an important modulator of the basal ganglia output. The STN is primarily composed of glutamatergic neurons. At the basis of the mesencephalon is the substantia nigra (that has a black pigment), which is divided into two major components; the substantia nigra pars compacta (SNc) and the substantia nigra pars reticulata (SNr). Both the SNc and SNr have different connections and use different neurotransmitters. The SNc is made up of dopaminergic neurons, while the SNr is made up of GABAergic projection neurons. Another group of

mesencephalic neurons located along the midline is the ventral tegmental area (VTA). The VTA also contains dopaminergic neurons and is known to play a key role in cognition and motivation.

The basal ganglia primarily receive information originating from glutamatergic projections from the cortex and thalamus that is sent to several sub-cortical nuclei. Cortical information gains access to the BG circuits through its substantial, highly topographic and segregated connections with the whole striatum i.e. projections from sensorimotor cortical areas terminate in the posterior putamen, associative cortical inputs terminate in the anterior putamen and caudate nucleus, and limbic inputs terminate in the ventral striatum (Alexander et al., 1986; Alexander et al., 1990; Hoover and Strick, 1993; Parent and Hazrati, 1995a). After processing through a complex synaptic network between striatal projection neurons (referred to as medium spiny neurons; MSNs) and various populations of striatal interneurons (Bolam et al., 2000; Tepper et al., 2010), information from the striatum is then sent to the GPe or GPi, and SNr through a direct or an indirect route (Fig. 1.1). This systematic way of processing allows for segregated and functionally compartmentalized information to be sent to their respective targets in the thalamus and brainstem. Thalamic output projections are then sent to the cerebral cortex or back to the striatum, through a series of functionally segregated basal ganglia-thalamocortical and basal ganglia-thalamostriatal circuits as seen in Fig. 1.1 (Galvan and Wichmann, 2008; Smith et al., 2004; Wichmann and DeLong, 2003).

1.2.2 Basal Ganglia-Thalamocortical network

1.2.2.1 Direct and Indirect Pathways

The direct and indirect pathway model has been at the forefront of basal ganglia research since the early 1990's. These pathways are the two major tracts through which information flows in the basal ganglia circuitry (Fig. 1.1). Since its introduction, this model is always under constant revision and updates based on new research of the basal ganglia circuitry. The current rate model of the basal ganglia is one of the few models that depict the normal and abnormal physiology of

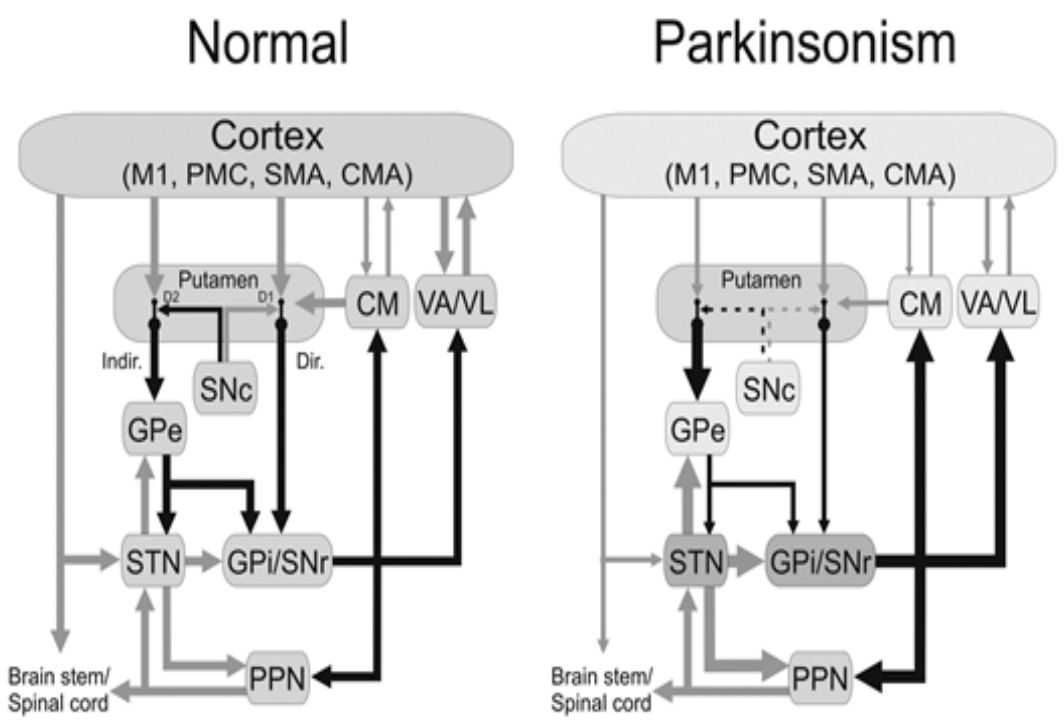

Figure 1.1. **Simplified classical view of the basal ganglia-thalamocortical circuitry under normal conditions (left) and rate changes in parkinsonism (right).**

Inhibitory connections are black, and excitatory connections are gray. The change in line widths', i.e. thick or thin arrows indicates either a decrease or increase in activity, and dotted lines indicate a nearly complete loss. CM, centromedian nucleus of thalamus; VA/VL, ventral anterior and ventral lateral nucleus of thalamus; PPN, pedunculopontine nucleus. Figure from (Galvan and Wichmann, 2008; Wichmann and DeLong, 2003).

basal ganglia in the parkinsonian state. The nigrostriatal projection is the primary modulator of information flow through the direct and indirect pathways (Fig. 1.1). The direct pathway consists of the monosynaptic connection between the striatum and the two basal ganglia output nuclei, GPi and SNr. On the other hand, the indirect pathway involves a more complex relay system, which involves multiple synaptic connections that link the striatum to the GPi/SNr indirectly via the GPe and STN. Both pathways ultimately transmit information to the cortex.

The GABAergic striatal projection neurons that give origin to the direct or indirect pathway (Shink and Smith, 1995) can be distinguished based on differential neuropeptide and dopamine receptor subtype expression. The direct pathway neurons contain substance P and D1 dopamine

receptors, whereas the indirect pathway cells express enkephalin and D2 dopamine receptors. In addition to their differential expression of neuropeptides and dopamine receptors, studies have shown other differences in the physiology and morphology of direct and indirect pathway MSNs in mice. Overall, indirect pathway MSNs are more responsive to cortical inputs than direct pathway MSNs, despite their similarities in morphology and electrophysiological properties (Berretta et al., 1997). In general, D1-containing MSNs tend to be less excitable than D2-containing MSNs (Gertler et al., 2008), maybe because of the larger dendritic arbor of D1-containing MSNs over D2-containing MSNs. The direct and indirect pathway MSNs have been shown to interact with each other via neighboring axon collaterals in the striatum (Taverna et al., 2008). In mice, connections from D2- to D1-containing MSNs are more common than D1- to D2-positive neurons (Taverna et al., 2008). Despite evidence for segregation of D1 and D2 dopamine receptors in different populations of MSNs, there is a small population of striatal MSNs that co-express D1 and D2 dopamine receptors (Surmeier et al., 1996; Taverna et al., 2008). In addition, there is significant overlap in the projection of many direct pathway MSNs that sends axon collaterals not only to the EPN (GPi) and SNr but also to the GP (GPe) in rodents and monkeys (Kawaguchi et al., 1990; Parent et al., 1995; Parent et al., 2000; Wilson and Phelan, 1982; Wu et al., 2000).

Projections from STN neurons collateralize and terminate in multiple structures. In addition to GPi and SNr, STN efferents are also known to project to the striatum, the substantia nigra pars compacta, the pedunculopontine nucleus, the nucleus reticularis tegmenti pontis (NRTP), several basal pontine nuclei, the thalamus, and send reciprocal projections to the GPe (Bolam et al., 2000; Bostan et al., 2010; Bostan and Strick, 2010; Giolli et al., 2001; Lanciego et al., 2004; Rico et al., 2010). In primates, this STN projection to the GPi and GPe is highly topographic and functionally organized. This topography is extended to the modality of certain neurons such that, neurons that exhibit similar functional modality tend to remain connected through segregated loops (Shink et

al., 1996). In addition to the striatum, cortical information can also affect the basal ganglia system via another point of entry, the STN. This particular pathway where the STN receives cortical information directly is known as the "hyperdirect pathway"(Carpenter et al., 1981).

In most circuit level organizations of the basal ganglia, the GPe is seen as a homogeneous structure reciprocally linked with the STN (Albin et al., 1989; Mink, 1996; Nambu et al., 2002; Redgrave et al., 1999; Wichmann and DeLong, 1996). However, this was likely to be an oversimplification because electrophysiological studies achieved in the primate GPe have revealed the existence of at least two major groups of GPe neurons based on their firing rates and patterns (DeLong, 1971). In the rodent GP, specific populations of neurons were found to have diverse intrinsic membrane properties (Kita and Kitai, 1991; Nambu and Llinaś, 1994) and different somatodendritic and axonal structure (Kita, 2007). Recent rodent studies have revealed the existence of a dichotomous functional organization of the GP, such that two major GABAergic projection cell types have been identified, the "prototypic" and "arkypallidal" neurons (Abdi et al., 2015; Mallet et al., 2012). Prototypic GP neurons fire tonically at high rates in vivo, often express parvalbumin, and always innervate STN (Mallet et al., 2012). On the other hand, arkypallidal neurons fire in phase to STN neurons (unlike prototypic neurons that fire antiphase to STN neurons), are devoid of parvalbumin, express neuropeptide pre-proenkephalin, and innervate only the striatum (Mallet et al., 2012). As a result, in both diseased and normal conditions, there is no longer a single population of GPe cells, but two populations that can influence the entire basal ganglia network at a cellular level (Abdi et al., 2015; Mallet et al., 2012).

Disruption of the activity of the direct and indirect pathways influences the functionality of the basal ganglia network. In Parkinson's disease (PD), the loss of dopamine in the striatum results in increased activity of the indirect pathway and decreased output from direct MSNs. As a result of this loss of dopamine in the striatum, the functioning of the basal ganglia system becomes

abnormal. This dysfunction of the direct and indirect pathway has opposing effects on the network and thereby causes an increased GABAergic outflow to the thalamus that could potentially reduce cortical excitation and therefore decrease motor behaviors (Fig. 1.1).

1.3 Thalamus: functional compartmentalization, cellular composition, and connections

The thalamic targets of basal ganglia outflow from the GPi and SNr are the ventral motor thalamic nuclei and caudal intralaminar nuclei, the two thalamic nuclei that are the focus of the research presented in this thesis. In the following account, I will review the anatomy of the mammalian thalamus, with a special emphasis on the cellular composition and synaptic organization of these nuclear groups.

1.3.1 Thalamic compartmentalization and nomenclature

1.3.1.1 Anatomical Organization of Thalamus

The thalamus is primarily known as a relay nucleus, transmitting information from the basal ganglia to the cortex and brainstem. In general, the thalamus is subdivided into major nuclear groups based on their location. The dorsal portion of the diencephalon, caudal part of the forebrain, contains three major parts: the epithalamus, the dorsal thalamus (known as the motor thalamus), and the ventral thalamus. The epithalamus is a part of the dorsal forebrain including the pineal gland, the habenular nuclei, the stria medullaris, and the associated paraventricular nuclei. The two other thalamic groups, ie the dorsal and ventral thalamus, comprises many subnuclei that receive inputs from several brain structures and transmit afferent signals to specific areas of the cerebral cortex, except for the RTN which projects only to other thalamic nuclei and brainstem (Jones, 2002a; Jones, 2007).

The dorsal thalamus is subdivided into several core thalamic nuclear groups: the anterior, medial, lateral, and posterior nuclear groups. This division is created by a band of myelinated fibers known as the internal medullary lamina of the thalamus. The anterior nuclear group, which is separated by a myelinated capsule, consists of two nuclei, the principal anterior and anterodorsal

thalamic nuclei, which receive strong inputs from the hippocampal formation by way of the fornix. On a functional level, the anterior group of the thalamus regulates emotional behavior and memory mechanisms and is in part responsible for information that involves the limbic system. In humans, the mediodorsal nucleus of the medial nuclear group is the most developed. Anatomically, the medial nuclear group is located medial to the internal medullary lamina. The mediodorsal nucleus is a major relay center for cognitive information to the prefrontal cortex and influences affective behavior, decision making, as well as judgment and memory. Following the medial nuclear group is the lateral nuclear group. The lateral nuclear group of the thalamus is subdivided into two main nuclear groups, dorsal and ventral. The lateral nuclear group, also known as the dorsal-tier thalamic nuclei, is located dorsal to the ventral nuclear group and includes three major nuclei: the pulvinar, the lateral posterior nucleus, located at an intermediate level, and the lateral dorsal nucleus, the most rostral component of this nuclear mass (Jones, 2007; Smith and Sidibe, 2003). In particular, the lateral dorsal nucleus receives inputs from the hippocampus and the mammillary bodies and projects to the cingulate gyrus. It is functionally different from nuclei of the anterior group, but also part of the limbic thalamus. The pulvinar is referred to as a relay station between subcortical visual areas and their respective association cortices in the temporal, parietal, and occipital lobes (Jones, 2007). The pulvinar has a primary role in speech and pain mechanisms as well as selective visual attention. Unlike the dorsal nuclear subgroup, the ventral nuclear subgroup of the lateral nuclear group belongs to the modality-specific thalamic nuclei and is divided into three separate nuclei: the ventral anterior, ventral lateral, and ventral posterior nuclei. All of the nuclei in this group have reciprocal relationships with specific cortical areas. Specifically, the ventral anterior group, the most rostral of the ventral nuclear group, receives inputs from the GPi, the SNr, and premotor and prefrontal cortices (Jones, 2007). Efferent connections from the ventral anterior nucleus are sent to premotor cortices and to areas of the prefrontal cortex, including the frontal eye fields. As a result the ventral anterior nucleus becomes influential in the regulation of movement when motor information is relayed to

these cortical areas. The ventral lateral nucleus in the ventral nuclear subgroup is located caudal to the ventral anterior nucleus and plays a role in motor integration. Afferent connections to the ventral lateral nucleus arise from the deep cerebellar nuclei, the GPi, and the primary motor cortex (that display reciprocal connections). Fibers from the ventral lateral nucleus then project to the primary motor cortex, as well as the premotor and supplementary motor cortices (Jones, 2007). The ventral lateral nucleus is known to relay information via the cerebellum, basal ganglia and cerebral cortex. Together, the ventral anterior and ventral lateral thalamic groups are known to make up the motor thalamus. Lastly, the ventral posterior nucleus, located in the caudal part of the thalamus, is made up of two parts: the ventral posterior medial nucleus (VPm) and the ventral posterior lateral (VPl) nucleus; both of which receive input from the primary somatosensory cortex as well as other tracts (Jones, 2007). Often referred to as the ventrobasal complex, efferent projections from both nuclei are sent to the somatosensory cortex. Unlike the dorsal thalamus, the ventral thalamus comprise the reticular nucleus, ventral lateral geniculate nucleus, the zona incerta, and the fields of Forel (Jones, 2007). The reticular nucleus, positioned between the external medullary lamina and the internal capsule, surrounds the entire extent of the dorsal thalamus and, unlike all other thalamic nuclei, does not provide inputs to the cortex, but instead innervates other thalamic nuclei and the brainstem, and receives input from the cerebral cortex and other thalamic nuclei (Jones, 2007). As a result, this nucleus plays a role in integrating and gating activities of thalamic nuclei. Another thalamic nuclear group, enclosed within the boundaries of the internal medullary lamina in the caudal thalamus, comprises the intralaminar nuclei. These nuclei, which are often considered as nonspecific or diffusely projecting nuclei, are divided into two main groups: the rostral group, which contains the paracentral, centrolateral, and centromedial nuclei, and the caudal group that includes the centromedian and parafascicular nuclei (Jones, 2007; Smith and Sidibe, 2003). Afferent connections to the intralaminar nuclei come from the reticular formation of the brainstem, the cerebellum, the spinothalamic tract, the GPi, the cerebral cortex, as well as the vestibular nuclei and periaqueductal gray matter (Kaufman

and Rosenquist, 1985a). The intralaminar nuclei sends projections to a wide range of cortical areas including: all visual cortical areas except area 17, the frontal eye fields, anterior cingulate gyrus, suprasylvian fringe of the auditory cortex, insular cortex, parietal areas 5 and 7, and to the striatum (Jones and Leavitt, 1974; Kaufman and Rosenquist, 1985b; Royce and Mourey, 1985). The thalamostriatal projection from the centromedian (CM) and parafascicular (Pf) nuclei is topographically organized, such that the CM nucleus projects to the putamen and the Pf projects to the caudate nucleus (Jones, 2007). Largely, the intralaminar nuclei receive inputs from several motor and sensory sources and project diffusely to the cortex and are involved in motor control mechanisms. The midline thalamic nuclei are more or less distinct cell clusters along the medial portion of the thalamus. These nuclei are smaller and more poorly developed in humans and monkeys than in rodents. Consisting of multiple cell groups, they are located along the medial border of the thalamus close to the third ventricle. Subnuclei of this group include the paraventral, central, and reunion nuclei which receive inputs from the hypothalamus, brainstem nuclei, amygdala, and parahippocampal gyrus, and send projections to the limbic cortex and ventral striatum (Jones, 2007; Smith and Sidibe, 2003). The midline nuclei tend to have an influential role in emotion, memory, and autonomic function.

Overall, most thalamic nuclei can be classified based on shared features of fiber connectivity and function. Thalamic nuclei are classified as either modality-specific nuclei, multimodal-association nuclei, or nonspecific and reticular, diffusely projecting nuclei (Smith and Sidibe, 2003). In most species, specific motor or sensory thalamic nuclei are a part of the modality-specific group and have distinct connections with precise cortical areas that reflect the same modality and undergo degeneration when there is a lesion of the specific cortical area they project to (Jones, 2007). On the other hand, the multimodal-association nuclei (such as the pulvinar and mediodorsal nuclei) receive inputs mainly from the RTN and project widespread to association areas of the cortex in the frontal, parietal, and temporal lobes. Unlike modality-specific nuclei, the multimodal-

associative nuclei do not receive inputs form one dominant subcortical structure, but are rather innervated by many different afferent inputs (Smith and Sidibe, 2003). Consistent with such a pattern of innervation, the functions of association nuclei are not precise and modality-specific, but are related to higher cognitive functions such as language, learning, and sensorimotor processing (Smith and Sidibe, 2003). Lastly, diffusely projecting nuclei are characterized by widespread cortical projections and innervate the striatum and include the intralaminar, midline, and reticular thalamic nuclei (Jones, 2007).

1.3.1.2 Motor Thalamus

The motor thalamus encompasses the basal ganglia-receiving thalamus and the cerebellar-receiving component of the thalamus, both of which impact motor output. The motor thalamus projects widely to specific frontal motor cortices. As mentioned above, the motor thalamus is divided into several compartments. In rodents, though less defined in primates, the ventral medial (VM) nucleus receives afferent connections from SNr and associative areas of the cortex (Bodor et al., 2008; Lanciego et al., 1998; Sakai et al., 1998). Major inputs to the ventral anterior (VA) nucleus are from SNr and premotor areas of the cortex, and minor inputs are from GPi and associative areas of the cortex. The VA and ventral lateral (VL) nuclei are the main targets of basal ganglia and cerebellar inputs to the thalamus. These two nuclear groups are divided into various subnuclei based on cytologic criteria. The parvocellular part of the VA nucleus (VApc) receives inputs from the GPi and premotor cortex, and to a lesser extent, from the cerebellum, whereas the posterior ventrolateral nucleus (VLp) is the main target of ascending cerebellar afferents as shown in cats and primates (Ilinsky et al., 1982; Ilinsky and Kultas-Ilinsky, 1984; Ilinsky, 1990; Ilinsky et al., 1993; Ilinsky et al., 1997; Kultas-Ilinsky et al., 1997). Although some regions receive inputs from basal ganglia and cerebellum, these two afferents are largely segregated in the primate thalamus and exhibit more of an overlap in rodents (Ilinsky et al., 1982; Ilinsky and Kultas-Ilinsky, 1984; Ilinsky, 1990; Ilinsky et al., 1993; Kultas-Ilinsky et al., 1983).

Because of these close relationships with motor-related subcortical regions, the VApc nucleus is often termed as the motor thalamic nucleus. In contrast with the long-held belief that basal ganglia outflow was conveyed exclusively to premotor (PM) and supplementary motor (SMA) cortical areas, it is now established that a substantial contingent of information from the basal ganglia is sent to the primary motor cortex (M1) (McFarland and Haber, 2002; Rouiller et al., 1998; Rouiller and Welker, 2000).

1.3.1.3 Caudal Intralaminar Thalamus

The intralaminar nuclei comprise two major groups, namely the anterior and posterior intralaminar nuclei. As previously mentioned, the two main nuclei that are recognized in the anterior group are the paracentral and the centrolateral, whereas the posterior group comprises the CM and Pf nuclei. The main projection site of the caudal intralaminar nuclei is the striatum, whereas rostral nuclei innervate preferentially the cerebral cortex with significant axon collateralization to the striatum. The organization and function of the thalamostriatal system and its place in the functional circuitry of the basal ganglia are discussed in section 1.3.7.2.

In primates, the CM is composed of projection neurons and interneurons. The projection neurons in the CM are mostly medium-sized (< 35-40μm in diameter in the cat and primate), with multiple perikarya, few primary dendrites, and frequent somatic spines, whereas interneurons are smaller (Balercia et al., 1996; Jones, 2007; Tseng and Royce, 1986). The morphology of CM/Pf neurons are unique in that they have a different morphology compared to other thalamic nuclei. There are four types of axonal boutons in the CM, the first being terminals that are small-to-medium-size and contain small round vesicles (SR) and form asymmetric contacts (Balercia et al., 1996; Jones, 2007; Tsumori et al., 2002). These boutons are typically identified as corticothalamic terminals. Next, are heterogeneous medium-sized terminals that form asymmetric synapses and contain large round vesicles (Balercia et al., 1996; Jones, 2007; Tsumori et al., 2002). These terminals are similar to the large round (LR) terminals which originate from the

cortex (Jones, 2007). Thirdly, there are heterogeneous small-to-medium-size GABAergic boutons (Balercia et al., 1996; Jones, 2007; Tsumori et al., 2002). Often these terminals contain pleomorphic vesicles, form multiple symmetric synapses, and are usually considered as pallidothalamic and RTN terminals. The last type of terminals in the primate CM is presynaptic profiles that express the neurotransmitter GABA and receive afferent synaptic inputs. These are considered as vesicle-containing dendrites of interneurons (Balercia et al., 1996; Jones, 2007; Tsumori et al., 2002). In the monkey CM, complex synaptic arrangements referred to as a synaptic triad are often found. These presynaptic elements are comprised of serial synapses and synaptic triads with LR and SR boutons that display synaptic contact with projection neuron dendrites and somata (Balercia et al., 1996). Similar to the ventral motor thalamus, classical glomeruli are found less frequently in CM/Pf nuclei. LR and SR boutons have also been known to establish synapses on dendrites of interneurons (Balercia et al., 1996). Compared to other previously studied motor-related thalamic nuclei, differences in synaptic coverage between proximal and distal projection neuron dendrites tend to be less pronounced, and the density of synapses formed by interneurons on projection neuron dendrites are lower (Balercia et al., 1996; Kultas-Ilinsky and Ilinsky, 1990; Kultas-Ilinsky and Ilinsky, 1991).

1.3.2 Motor Thalamic neurons

The mammalian motor thalamus encompasses three major cell types: (1) large glutamatergic relay cells, which project their axons to the cerebral cortex or the striatum; (2) the small GABAergic interneurons, which are abundant in primates, but largely absent in rodents, have their axons and synaptic connections confined within the nuclei in which they lie (Smith et al., 1987); and (3) the GABAergic reticular neurons, which have their perikarya confined within the limits of the reticular nucleus and send their axons to the dorsal thalamus as seen in Figure 1.2 (Ilinsky et al., 1999; Jones and Yang, 1985; Pinault et al., 1995).

1.3.2.1 Relay Cells: Glutamatergic thalamocortical neurons

In the ventral motor thalamus, relay cells have a bushy appearance, containing a relatively symmetrical dendritic field with occasional dendritic appendages or protrusions. Overall, relay cells have larger somata than those of interneurons, but they exhibit a broad range of sizes. For instance, the perikarya of relay cells area in the ventral lateral nucleus of monkeys range from 70 μm^2 to more than 400 μm^2 and tend to have a long total dendritic length (Shi and Apkarian, 1995). The majority of dendrites on VL projection neurons are smooth (Shi and Apkarian, 1995). On the other hand, thalamocortical cells in the CM and other intralaminar nuclei are morphologically different. They tend to have a medium-sized multipolar soma and display two types of primary dendrites: sparsely branching (straight and smooth) and densely branching (curvy and possessing spines).

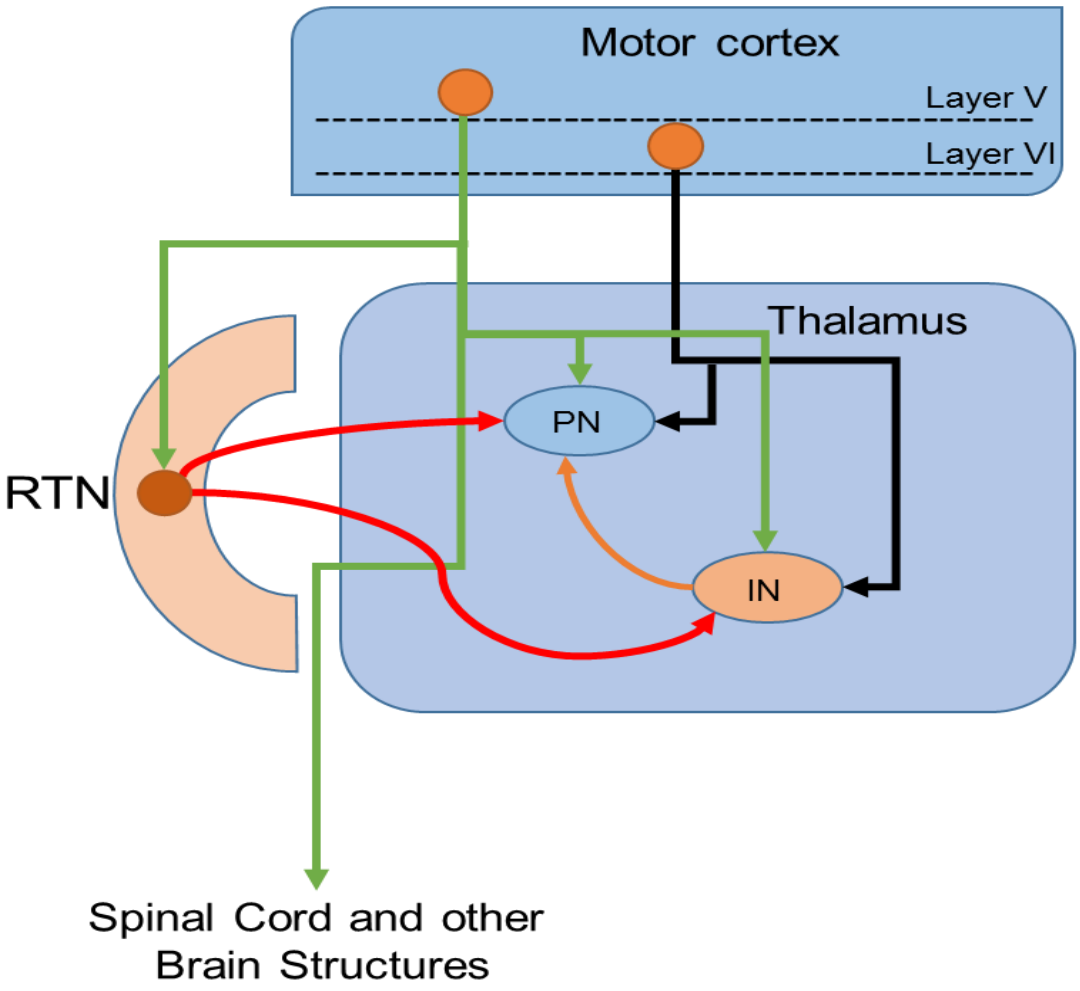

Figure 1.2. **A schematic of cell types in the ventral motor thalamus.**

Cell types in the thalamus consist of thalamocortical neurons, interneurons, and reticular thalamic (RTN neurons). Both VApc and CM receive the same cellular input and motor input from layer V and VI. Abbreviations: RTN, reticular thalamic nucleus; IN, interneuron; PN, projection neuron; VApc, parvocellular part of anterior ventral thalamic nucleus; CM, centromedian thalamic nucleus. Red and orange represent GABAergic connections; green and black correspond to excitatory connections.

1.3.2.2 GABAergic Interneurons

The neuronal makeup of various nuclei is different in rodents when compared to monkeys. In primates, one of the key sources of inhibitory information in the thalamus comes from GABAergic interneurons. The GABAergic interneurons, which are found in all thalamic nuclei in primates, are much smaller than relay cells (diameter generally < 10 μm) (Jones and Yang, 1985).

In general, their somata are less than 10 μm in diameter, with a few short dendrites that give off numerous lengthy processes that end in terminal boutons and form dendro-dendritic synapses (Jones and Yang, 1985). In primates, interneurons form approximately 30% of the total neuronal population in all thalamic nuclei, except in intralaminar nuclei, where they are slightly less abundant and account for about 15% to 20% of neurons (Smith et al., 1987). However, the dorsal thalamic nuclei in rodents, except the lateral geniculate nucleus, are practically devoid of GABAergic interneurons. Hence, rodents have a unique thalamus in which processing of extrinsic information and thalamocortical outflow are under the sole influence of GABAergic inputs from the reticular nucleus and basal ganglia.

GABAergic interneurons give rise to pre-synaptic dendrites that form single symmetric synapses with small distal dendrites of thalamocortical neurons (see Fig. 1.3). These pre-synaptic dendrites are often contacted by putative excitatory boutons, which provide an additional structural criterion to differentiate them from GABAergic terminals (Jones, 2007). Despite their high prevalence in the primate thalamus, the anatomy and synaptic integration of GABAergic interneurons in the microcircuitry of the motor thalamus is largely unknown. However, when present, they add to the complexity of the intrathalamic GABAergic network via a dense meshwork of dendro-dendritic synapses with thalamocortical neurons as shown in Fig. 1.3 (Casale and McCormick, 2011; Deschênes et al., 1982b; Deschênes and Hu, 1990; Deschênes et al., 1998; Ilinsky and Kultas-Ilinsky, 1990; Ilinsky et al., 1999; Jones and Powell, 1969; Jones, 2001; Jones, 2002b; Kultas-Ilinsky and Ilinsky, 1991; Kultas-Ilinsky et al., 2011). In many thalamic nuclei, they are also key components of synaptic glomeruli and triads, two fundamental forms of synaptic aggregations that likely contribute to the high level of synchronization and oscillation in the mammalian thalamus (see Fig. 1.3) (Sherman and Guillery, 2002; Sherman and Guillery, 2011; Shindo et al., 1995; Shink et al., 1996).

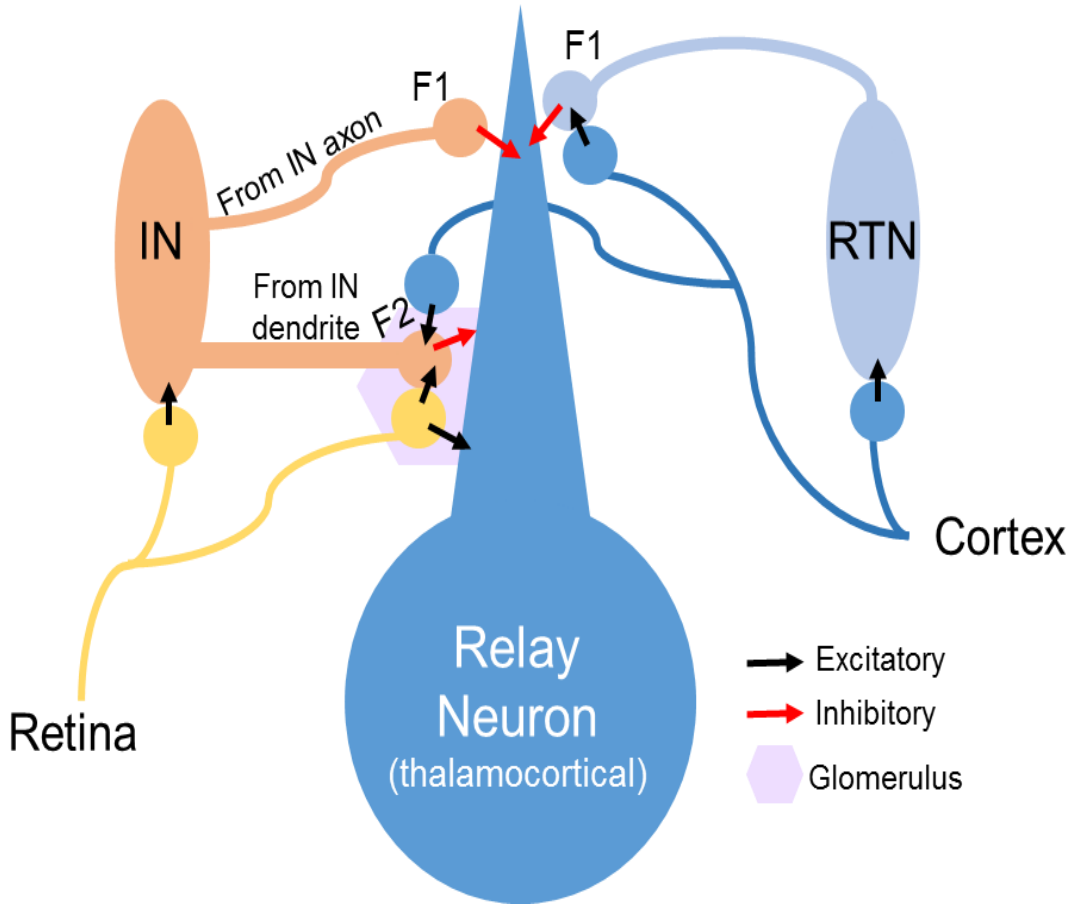

Figure 1.3. **A simplified schematic of a triad and synaptic glomerulus in a cat/rodent lateral geniculate nucleus.**

Shown are the various inhibitory and excitatory synaptic contacts (arrows). Here, the F2 terminal is part of a conventional triad, involving three synapses (from the retinal terminal to the F2 terminal, from the retinal terminal to an appendage of the relay cell dendrite, and from the F2 terminal to the same appendage). Neurons of the RTN receive input from the cerebral cortex and dorsal thalamus via axosomatic and axodendritic contacts (Liu and Jones, 1999; Ohara and Lieberman, 1985; Ohara, 1988). Abbreviations: F1 and F2, 'flattened vesicle' synaptic terminals; IN, GABAergic interneuron; RTN, reticular thalamic nucleus. Adapted from (Cox, 2014; Govindaiah and Cox, 2006).

1.3.2.3 Reticular Thalamic Nucleus Neurons

RTN is a thin layer of GABAergic neurons that partially surrounds the dorsal thalamus (Jones, 2007), and its neurons innervate thalamocortical neurons (Pinault, 2004). Terminals from

reticular thalamic nucleus (RTN) neurons in the motor thalamus form single symmetric synapses, usually with no more than one postsynaptic target (Ilinsky et al., 1999).

The cells of the reticular nucleus are relatively large, with soma diameters ranging from 25 to 50 μm in monkeys and humans (Jones and Yang, 1985). Although it has long been considered as a homogeneous nucleus, single-cell filling studies have revealed a significant neuronal heterogeneity in the RTN. Three types of reticular neurons have been identified in rats based on three-dimensional reconstruction of their dendritic tree: (1) cells with dorso-ventral dendritic arbors (as seen in Fig. 1.3), (2) cells with rostro-caudal dendritic arborization and (3) cells with dendrites that arborize in all directions (Smith and Sidibe, 2003). The axons of reticular neurons have short collaterals within the nuclei, and in some species, the dendritic branches form dendro-dendritic synapses. Structural and morphometric analyses of the axonal projections from juxtacellularly-stained reticular neurons in rats revealed complex and variable patterns of distribution within dorsal thalamic nuclei (Pinault and Deschênes, 1998). Based on their pattern of connectivity, thalamocortical and reticular neurons form open- and closed-loop connections, which likely represent mechanisms for lateral and feedback inhibitions, respectively (Kimura et al., 2007; Kimura, 2014; Pinault and Deschênes, 1998; Willis et al., 2015). Although the main neurotransmitter found in RTN neurons is GABA, other chemicals found in reticular neurons include calcium binding proteins (parvalbumin and calretinin), somatostatin, thyrotropin-releasing hormone, vasoactive intestinal peptide, neuropeptide Y, and prolactin-releasing peptide (Arai et al., 1994; Bendotti et al., 1990; Burgunder and Young, 1992; Clemence and Mitrofanis, 1992; Graybiel and Elde, 1983; Jones, 2007; Pinault, 2004; Smith, 2008).

1.3.3 Ventral Motor Thalamus: afferent connections

1.3.3.1 Corticothalamic system

The main thalamic nuclei that receive cortical projections from the motor cortices are the dorsal thalamic nuclei, the cerebellar-receiving thalamic nuclei and the VApc. The dorsal thalamic

nuclei and the cerebral cortex are reciprocally linked through thalamo-corticothalamic loops, characterized by the tight topography between thalamocortical inputs to a specific and restricted cortical sector, which, in turn, provides a significant feedback projection to the same thalamic region that contributed the cortical innervation (Galvan et al., 2014b; Jones, 2007). Thalamic nuclei are also involved in open feedback loops that facilitate integration of information coding preparatory and performance aspects of movement. Information is first relayed from limbic areas to non-motor thalamic nuclei (such as the mediodorsal nucleus), then to the associative cortex, then to the motor cortex via the motor thalamus (Bosch-Bouju et al., 2013; Haber and Calzavara, 2009; McFarland and Haber, 2002). This open feedback loop that involves the basal ganglia, cerebellum, motor thalamus, and cortex ensures that motivational and proprioceptive aspects of the movement are incorporated into the highly integrated motor program that develops in the motor thalamus (Bosch-Bouju et al., 2013). The motor thalamus receives afferents from layers V and VI of the primary motor cortex (M1), supplementary motor area, and premotor cortex (PM) (McFarland and Haber, 2002; Rouiller et al., 1998; Rouiller and Welker, 2000). Overall, the corticothalamic system provides a massive and widespread innervation of the thalamus. In the primate thalamus, corticothalamic terminals form synapses with both glutamatergic projection neurons and GABAergic interneurons. Cortical inputs to thalamic projection cells are separated into ‘driver’ and ‘modulatory’ inputs (Abbott and Chance, 2005; Rovó et al., 2012). In high order associative thalamic nuclei, excitatory driver inputs arise from cortical layer V innervating proximal dendrites of thalamocortical neurons. These inputs are fast-conducting collaterals of long-range corticobulbar and corticospinal axons that do not project to the reticular nucleus (Jahanshahi et al., 1995; Rascol et al., 1994) and give rise to large boutons with multiple synapses onto thalamic targets. They are spontaneously active, show task-related activity, and have sensory receptive fields (Lefaucheur, 2005). In contrast, layer VI efferents provide axon collaterals to the RTN as they enter the motor thalamus (Deschenes et al., 1994; Kakei et al., 2001; Rouiller and Welker, 2000). Corticothalamic terminals from layer VI neurons tend to be abundant, small and

form synapses preferentially with distal dendrites of thalamic cells across the whole thalamus (Kakei et al., 2001; Rouiller and Welker, 2000; Sirota et al., 2005). Unlike layer V corticothalamic terminals that are considered as “drivers”, layer VI terminals are seen as “modulators” of thalamic activity (Rovó et al., 2012; Sherman, 2012). Overall, individual basal ganglia terminals form multiple synapses with the proximal dendrites of relay cells (Bodor et al., 2008). It has been suggested that the morphology of SNr terminals (and likely GPi terminals) allow these boutons to maintain synaptic inhibition, without depression, at high presynaptic firing rate (Bodor et al., 2008; Wanaverbecq et al., 2008). The lack of large “driver-like” glutamatergic terminals coupled with the presence of multisynaptic GABAergic terminals on the proximal dendrites of relay cells in the basal ganglia-receiving motor thalamus strongly suggest that the integration and process of information that flows through these nuclei differ from that in other thalamic nuclei that receive prominent extrinsic driver-like glutamatergic inputs (such as the mediodorsal thalamic nucleus) (Kuroda and Price, 1991). Dysfunction of the strong GABAergic influences on the basal ganglia-receiving motor thalamus may contribute to the relay of aberrant basal ganglia output to the neocortex via the thalamus in Parkinson's disease. Significant knowledge has been gained in regards to the cellular and synaptic organization of the corticothalamic system in the rodent sensory thalamus; such is not the case for the primate motor thalamus. To address this knowledge gap, part of this thesis aims at quantifying and assessing the morphology and synaptic connectivity of corticothalamic terminals in the monkey motor thalamus.

1.3.3.2 Pallidothalamic system

Pallidal projections to the VApc are functionally topographic, use GABA as transmitter, and terminate in a patch-like pattern, like most inputs to the VA/VL complex. The pallidothalamic projection travels via the ansa lenticularis and lenticular fasciculus to terminate in a topographic fashion in the VApc (Parent and Hazrati, 1995b; Percheron et al., 1996). Terminals from the GPi

also have collaterals that project to the CM. According to recent anatomical data, pallidothalamic fibers originating in the caudal portion of the GPi, including the motor territory, travel predominantly medially through the lenticular fasciculus en route to the thalamus, while fibers running below the ventral border of the pallidum in the ansa lenticularis originates mostly from cells located in the rostral half of GPi (Baron et al., 2001). The high level of calbindin D 28K expression in the basal ganglia-receiving regions of the VA/VL complex provides clear landmarks between GPi and cerebellar termination sites (Percheron et al., 1996). About 10-20% of pallidothalamic neurons in the monkey GPi project to the contralateral VApc (Hazrati and Parent, 1991).

The functional organization of pallidothalamic neurons is highly dependent on their source of striatal innervation. For instance, neurons in the ventroposterior two-thirds of GPi receive sensorimotor striatal inputs, dorsal third GPi neurons receive associative afferents from the caudate nucleus, and anteromedial GPi neurons receive predominately limbic inputs from the ventral striatum. This pattern of organization led to the concept of functionally segregated cortico-striato-pallido-thalamo-cortical loops throughout the basal ganglia circuitry (Alexander et al., 1986). Efferent projections from the sensorimotor GPi remain largely segregated from the associative and limbic projections at the level of the thalamus. In squirrel monkeys, the associative, limbic and sensorimotor inputs are segregated in different subnuclei of the ventral motor thalamus (Sidibe et al., 1997).

According to the classical model of the basal ganglia (Fig. 1.1), VApc neurons are considered as silent at rest, probably due to tonic inhibition from basal ganglia output nuclei. This inhibition is relieved once striatal neurons are activated and phasically inhibit GPi neurons. The activity of thalamocortical neurons, as a result, becomes highly dependent on changes in GPi output. This basic model of tonic inhibition /disinhibition of thalamic cells by BG output is partly true, but

likely more complex, and becomes dysfunctional in diseased states because of changes in pattern of GPi activity.

1.3.4 CM/Pf: afferent connections

The CM/Pf are the main targets of basal ganglia projections from GPi and SNr, which largely arise from collaterals of the basal ganglia outputs to the VApc (Jones, 2007). Projections from brainstem cholinergic and monoaminergic inputs in the pedunculopontine nucleus, raphe nuclei, and locus coeruleus have also been established (Jones, 2007). Notably, projections from the pedunculopontine nucleus are mainly directed toward Pf and display a high degree of chemical heterogeneity (Jones, 2007; Smith and Sidibe, 2003). The reticular formation (RF) also provides massive inputs to anterior and posterior intralaminar nuclei. By virtue of these strong associations with the RF, the intralaminar nuclei are traditionally seen as part of the reticular activating system that regulates the mechanisms of cortical arousal and attention (Smith and Sidibe, 2003). Other functions of intralaminar nuclei include the regulation of tolerance to pain and motor control mediated by spinothalamic and basal ganglia afferents, respectively.

In the CM/Pf complex, pallidal axons arising from the sensorimotor GPi terminate exclusively in CM where they form synapses with thalamostriatal neurons projecting back to the sensorimotor territory of the striatum. In contrast, associative inputs from the GPi terminate massively in the dorsolateral extension of PF (PFdl), which does not project back to the caudate nucleus, but rather innervates preferentially the pre-commissural region of the putamen. Finally, the limbic GPi innervates selectively the rostrodorsal part of PF which, in turn, projects back to the nucleus accumbens. Therefore, it appears that the CM/Pf complex is part of closed and open functional loops with the striatopallidal complex (Sidibe et al., 2002; Smith et al., 2004; Smith et al., 2009). These anatomical studies and many others provide clear evidence that the basal ganglia outflow from the GPi reaches cortical areas that extend far beyond motor-related cortices, but also involve cognitive and associative regions of the prefrontal cortex (Akkal et al., 2007; Alexander et al.,

1986; Middleton and Strick, 1994; Middleton and Strick, 1996; Middleton and Strick, 2002). Cross-talks between these different channels are likely mediated by cortico-cortical connections. Recent single cell filling studies have identified two major types of projection neurons in the monkey GPi; the type I neurons project to the ventral motor nuclei with collaterals to the pedunculopontine nucleus and/or the CM/Pf, while the type II neurons, located along the border of GPi, project to the lateral habenula with rare collaterals to the anterior thalamic nuclei (Parent et al., 2001).

1.3.5 RTN: afferent connections

RTN neurons receive inputs from branches of thalamocortical axons that are in route to the cortex as well as branches from corticothalamic axons going to the thalamus (Pinault, 2004). The RTN also receives prominent and functionally important cholinergic and monoaminergic brainstem inputs (Ohara and Lieberman, 1985; Ohara, 1988). Projections from RTN to thalamic nuclei are highly specific and topographic. Inputs from RTN neurons terminate primarily on distal dendrites of thalamic cells (Ilinsky et al., 1999). Unlike in the sensory thalamic nuclei where RTN neurons target preferentially dendrites of thalamocortical cells, some authors have reported that the majority of RTN terminals form synapses with interneurons in the primate motor thalamus (Ilinsky et al., 1999). RTN neurons are responsible for regulating the activity of thalamic neurons by activating GABA-A or GABA-B receptors, depending on the firing mode of RTN cells (Crunelli and Leresche, 1991; Kim et al., 1997; McCormick and Bal, 1994).

1.3.6 Ventral Motor Thalamus: efferent connections

1.3.6.1 Thalamocortical system

The output structures of the basal ganglia influence cortical activity through GABAergic inhibitory synapses with relay neurons in the VApc. In the main sensory nuclei, giant excitatory terminals, known as drivers originate from nuclei that transmit sensory inputs from the periphery. For example in the lateral geniculate nucleus, driver inputs are from ganglion cells in the retina,

while in VP, driver inputs are from primary somatosensory brainstem afferents that travel from gracile and cuneiform nuclei through the medial lemniscus. In contrast, large driver like inputs from layer V of the motor cortex are mainly found in higher order associative and sensory nuclei, not in primary sensory relay nuclei (Jones, 2007). Very few, if any, driver-like excitatory terminals contact thalamocortical neurons in basal ganglia-receiving region of the VApc which receive its main inputs from the GPi, the premotor cortex and the RTN (Rovó et al., 2012). Unlike the basal ganglia-receiving region of the VApc, the synaptic organization of the cerebellar-receiving thalamic territory is more closely similar to that of the sensory thalamus, primarily due the driver-like glutamatergic inputs from the deep cerebellar nuclei (Bosch-Bouju et al., 2013; Rovó et al., 2012). GPi projections are ipsilateral, use GABA as neurotransmitter, and terminate on the proximal part of thalamocortical neurons and presynaptic dendrites, whereas cerebellar inputs are glutamatergic and arise predominantly from the contralateral dentate nucleus (Jones, 2007). The historic perception of the pallidothalamic efferent projection was that pallidothalamic outflow to the cerebral cortex was restricted to supplementary and premotor cortices, while information along the cerebellothalamic tract was solely directed to the primary motor cortex (Schell and Strick, 1984; Strick, 1985); it has now been shown that information from both the pallidum and cerebellum gains access to all motor-related cortices through thalamocortical cells (Sakai et al., 1999; Sakai et al., 2000; Sakai et al., 2002; Tokuno et al., 1992). However, the sources of GPi or cerebellar projections to specific motor cortical areas are quantitatively different and largely segregated. In particular, the GPi outflow to various thalamic regions that project the supplementary and pre-supplementary motor is quite massive, more so than the dentate nucleus innervation to these respective areas (Akkal et al., 2007). The opposite is true for thalamic nuclei that are connected to M1, whereas they receive stronger inputs from the dentate nucleus than from the basal ganglia.

In the basal ganglia-thalamocortical network, there is a diverse topographical organization of afferent connections from the GPi and SNr to the cortex by way of the thalamus. The dorsal GPi/ SNr sends axonal projections to dorsal thalamic nuclei (specifically, the dorsal ventral lateral (VLd) thalamic nuclei, medial dorsal thalamic nuclei and the ventral anterior thalamic nuclei) that project mainly to associative and cognitive cortical areas. On the other hand, limbic-related information originates from the rostromedial part of GPi that projects to the Pf nucleus, the VLd, VA, and ventral medial nucleus. On the other hand, sensorimotor information that originates from the ventrolateral region of the GPi is sent to the VApc and CM (Haber et al., 1990; Parent and Hazrati, 1995a). Based on previous studies, it appears that the topographical organization of the thalamocortical system is partly conserved across species. Unlike the thalamocortical systems in primates, the organization of the motor thalamocortical projections in rats is more parsed out. In rodents, the ventral medial thalamic nucleus (VM) is the main thalamic target of basal ganglia outflow from the SNr and entopeduncular nucleus (EPN; the GPi analogue in rodents). The VM in rodents innervates both the lateral agranular (AGl-homologue of primary motor cortex in primates) and the medial agranular (AGm, homologue of pre-motor cortices in primates) cortex, (Akintunde and Buxton, 1992; Barth et al., 1990; Leichnetz and Gonzalo-Ruiz, 1987; Leichnetz et al., 1987; Neafsey et al., 1986a; Neafsey et al., 1986b; Passingham et al., 1988; Reep et al., 1990; Uylings and van Eden, 1990). Unlike thalamocortical projections from VApc in primates, which terminate in deep layer V/VI and more superficial layers II/III, the VM projections are confined to layer I of most of the neocortex (Cicirata et al., 1986; Herkenham, 1979; Herkenham, 1980; Rieck and Carey, 1985). As a result, the VM influences widespread motor areas as well as sensory areas. Although there is slight overlap between the ending zones of VM, VA/VL, and the most lateral part of MD in the rodent AGm, it seems that via their thalamic targets, the entopeduncular nucleus (EPN) can reach primary motor cortex and premotor areas (AGI and AGm, respectively), (Cicirata et al., 1986; Donoghue and Parham, 1983; Jones and Leavitt, 1974; Reep et al., 1984; Reep et al., 1990; Uylings and van Eden, 1990), whereas the SNR can reach

predominantly AGm as well as extensive areas of the pre frontal cortex (Cicirata et al., 1986; Fabri and Burton, 1991; Groenewegen, 1988; Herkenham, 1979; Kosar et al., 1986; Krettek and Price, 1977; Reep et al., 1984; Reep et al., 1990; Uylings and van Eden, 1990). Despite the widespread overlap in the rat AGm, it appears that the thalamic targets of EPN and SNR innervate different cortical areas, such that the EPN projects largely to motor and premotor areas and the SNR to associative PFC areas (in primates, this connection might extend to the limbic/autonomic PFC areas) (Goldman-Rakic and Selemon, 1990; Hikosaka, 1991; Parent, 1990).

Irrespective of the known relationship of a topographically segregated basal ganglia-thalamocortical organization, there is a still a lack of understanding of the thalamocortical system. It is imperative that new viewpoints into the organization of the thalamo-cortical projection system are taken of utmost importance as it might enhance our understanding of the different patterns of organization of the intrinsic basal ganglia circuitry.

1.3.7 CM/Pf: efferent connections

1.3.7.1 Thalamocortical system

In cats and primates, the CM-Pf complex projects in a topographic manner to specific regions of the motor and premotor cortices or to the striatum (Royce and Mourey, 1985; Sadikot et al., 1992a). In cats, these fibers distribute primarily to cortical layers I and III; however, the projection to layer I is more extensive (Royce and Mourey, 1985). The CM neurons that extend to the cerebral cortex arborize predominantly in motor and premotor areas, whereas Pf neurons innervate chiefly prefrontal areas. Unlike the cat, cortical innervation from both nuclei is more abundant in layers V and VI than in layer I in primates (Parent and Parent, 2005). Relying on data mainly obtained in non-primates, the cortical projections of intralaminar nuclei are organized as follows: anterior intralaminar nuclei project mainly to various functional areas in the prefrontal, cingulate, parietal, temporal, prepiriform, and entorhinal cortices as well as the hippocampus; the

CM is reciprocally connected with motor and somatosensory cortical regions, and the Pf projects to prefrontal, premotor, and cingulate cortices (Jones, 2007; Royce and Mourey, 1985). The subcortical projection from the CM-Pf complex terminates within the caudate nucleus, putamen, globus pallidum, subthalamic nucleus, zona incerta, fields of Forel, hypothalamus, thalamic reticular nucleus, and rostral intralaminar nuclei (Jones, 2007). Furthermore, the projections from these intralaminar nuclei to various cortical regions are less massive than thalamic inputs to the striatum.

1.3.7.2 Thalamostriatal system

The caudal intralaminar nuclei, CM and Pf, are the main sources of the thalamostriatal projection in primates and non-primates (Castle et al., 2005; Cowan and Powell, 1956; Lacey et al., 2007; McFarland and Haber, 2000; McFarland and Haber, 2001; McHaffie et al., 2005; Parent and De Bellefeuille, 1983; Parent and Parent, 2005; Raju et al., 2006; Smith and Parent, 1986; Smith et al., 2004; Smith et al., 2009). The CM projects preferentially to the post-commissural putamen (the sensorimotor striatal territory), whereas the Pf innervates the pre-commissural putamen, the caudate nucleus, and nucleus accumbens (the associative and limbic striatal regions, respectively) (Sadikot et al., 1992a). Other relay and associative thalamic nuclei also contribute significantly to the thalamostriatal projections in primates and non-primates.

Based on differential neurochemical expression as well as specific afferent and efferent connections, sub-areas called the patch (or striosome) and matrix compartments have been identified within the dorsal and ventral striatum (predominantly the caudate nucleus, anterior putamen, and core of the accumbens) in primate and non-primate species (Gerfen, 1984; Gerfen et al., 1987a; Gerfen et al., 1987b; Graybiel and Ragsdale, 1978; Graybiel et al., 1981; Johnston et al., 1990; Jongen-Rělo et al., 1993; Martin et al., 1991; Meredith et al., 1993; Meredith et al., 1996; Sadikot et al., 1992a; Voorn et al., 1989; Zahm and Brog, 1992). Some anatomical evidence suggests that thalamic inputs from CM preferentially target a subpopulation of striatal

projection neurons that innervate preferentially the internal globus pallidum (GPi), so-called direct striatofugal neurons, although a significant contingent of this projection also innervates indirect pathway neurons (Lanciego et al., 2004; Parent et al., 1995). In turn, the CM and Pf are main targets of basal ganglia outputs from GPi and SNr. As described in the previous section, these projections are massive and display a high level of functional specificity (see section 1.3.1.3).

1.4 Parkinson's disease

The second most common neurodegenerative disease, with 50,000 new diagnoses each year in the United States, is Parkinson's disease (PD). The neurological disorder Parkinson's disease is named after James Parkinson and was first described in 1817. James Parkinson described many of the motor hallmarks of the disease, which include resting tremor, muscle rigidity, akinesia, bradykinesia, hunched posture, and shuffling gait (Parkinson, 1817). Not only are motor symptoms associated with this disease, but there are also numerous non-motor symptoms, including depression, cognitive impairment, inflammation, dementia, hallucinations, and sleep disturbances.

The pathological hallmarks of PD are the loss of the nigrostriatal dopaminergic neurons and the presence of intraneuronal cytoplasmic inclusions known as "Lewy Bodies". Loss of nigrostriatal dopamine (DA) in PD is thought to increase the basal ganglia inhibitory output from the thalamus that stems from the GPi and SNr. Ultimately, this increased inhibition results in reduced activity of thalamocortical projections, leading to decreased cortical and motor activity (Fig.1). However, the functional and potential morphological impact of the increased BG outflow to the thalamus remains speculative. Although the primary system affected is the dopaminergic system, neurodegeneration in PD has been shown to extend beyond the dopaminergic system, affecting the serotonergic, cholinergic, and noradrenergic systems as well (Bohr et al., 2005; Jellinger, 1991; Pahapill and Lozano, 2000; Scatton et al., 1983).

Unfortunately, we are still unaware of the pathophysiology and cause of human PD, although there is insight that both genetic and environmental factors might have an influential role into the source of PD. Various genetic mutations have been identified that can cause familial, heritable forms of PD (Rochet, 2012; Rochet et al., 2012), however; these only account for a fraction of all PD cases. As of today, there is no cure for PD. Current studies are ongoing to look for potential early biomarkers and neuroprotective measures. Presently, symptomatic treatments, such as dopamine agonist, like levodopa, that alleviate parkinsonian motor symptoms are used to treat the motor symptoms of PD (Smith et al., 2012).

1.4.1 MPTP (1-methyl-4-phenyl-1,2,3,6-tetrahydropyridine) model of Parkinson's disease

1.4.1.1 The MPTP-treated monkey model of Parkinson's disease

The current gold-standard animal model of PD involves the use of a neurotoxin referred to as MPTP. The MPTP-treated monkey model of PD is the primary non-human primate representation used to mimic the motor symptoms of PD. MPTP-treated monkeys display very similar motor symptoms that are common amongst human PD patients, possess analogous brain anatomy and physiology, show some of the PD non-motor symptoms (McDowell and Chesselet, 2012), undergo comparable cellular damage in the midbrain, and respond to antiparkinsonian drugs in a very parallel manner, including the progressive development of motor side-effects. Furthermore, the functional alterations such as changes in firing rates and patterns, increased oscillations, and aberrant neuronal synchrony, have been observed in MPTP-treated parkinsonian monkeys (Leblois et al., 2007; Meissner et al., 2005; Nini et al., 1995; Raz et al., 2000; Wichmann and DeLong, 2003). Additional mice PD models that involve MPTP are used to induce midbrain dopaminergic neurodegeneration, but these animals do not fully display the behavioral symptoms seen in PD patients (Bové and Perier, 2012).

Fortunately, one of the highlights of MPTP is its ability to enter the system trans-cutaneously or through inhalation of vapors, and cause a gradual degeneration of dopaminergic neurons (Przedborski et al., 2001). The MPTP monkey model overall depicts how the body responds to a loss of dopamine. On the other hand, the slow progression of PD over several years is not mimicked in this model, as is the case for all neurotoxin-based models of PD. However, to induce slow neuronal death and generate a monkey model that displays a slowly progressive development of parkinsonian motor symptoms, MPTP can be administered at low doses over long periods of time (3-5 months). The sections below go into depth about the discovery and mechanism of action of MPTP.

1.4.1.1.1 The discovery of MPTP

Synthesized in the 1940s, MPTP was commonly used as a chemical intermediate in the creation of other molecules (Dauer and Przedborski, 2003). Originally, MPTP did not appear to be toxic, it wasn't until several years later that people learned of the toxicity of this compound through an unfortunate situation. In the late 1970s, the synthesis of meperidine (Demerol) analog was altered by a chemistry graduate student. By altering this substance, toxic MPTP was produced. Following injection of this contaminated chemical, the student developed severe parkinsonism. To help with the PD motor symptoms, the graduate student was later treated with levodopa. This situation sparked an investigation of the student's lab, where they found MPTP, along with several other chemicals to be present. Although, MPTP was found in the lab, no direct link between MPTP and parkinsonism was determined. Eighteen months later the student passed away from a drug overdose and an autopsy showed that he had damage to the dopaminergic cells of the substantia nigra (Davis et al., 1979).

In 1982, a chemist interfered with the synthesis of a meperidine analog and distributed the product to young drug users as a strain of heroin; it was during this period that the full potential of MPTP was discovered. Following this situation, an outbreak of cases of rapid-onset advanced

Parkinson's disease in young drug users was observed in several hospitals. Further investigation of the patients' leftover drugs revealed the presence of MPTP. Following these series of events, administration of MPTP to monkeys was shown to give rise to the behavioral motor symptoms that are often seen in human parkinsonism. Around this same time, MPTP was later shown to induce death of the same midbrain dopaminergic neurons that die in PD (Langston et al., 1984). Altogether, the gold-standard MPTP-treated nonhuman primate model of PD was developed and became a standard for investigating Parkinson's disease in non-human primates. Ultimately, the development of MPTP administration has led to great developments in the process of understanding Parkinson's disease.

1.4.1.1.2 Mechanism of action of MPTP

The lipophilic properties of non-toxic MPTP allow MPTP to cross the blood-brain barrier after systemic administration. Once in the brain, the chemical MPTP is converted into its active (toxic) metabolite 1-methyl-4-phenylpyridinium (MPP+) in astrocytes by monoamine oxidase B within non-dopaminergic cells (Dauer and Przedborski, 2003). Since MPP+ has an affinity for the dopamine transporter, it is then selectively taken up into dopaminergic terminals in the striatum. From that point, MPP+ then interferes with complex I of the electron transport chain inside of mitochondria, one of the mechanisms of cellular death. In addition to the effect it has on the dopaminergic system, slow MPTP intoxication has also been shown to cause damage to the other monoaminergic systems, including serotonergic and noradrenergic cells (Ansah et al., 2011; Masilamoni et al., 2011; Nayyar et al., 2009), as seen in PD (Jellinger, 1991; Scatton et al., 1983).

1.4.2 Pathophysiology of Parkinson's disease and the involvement of the thalamus

1.4.2.1 BG-thalamocortical network in Parkinson's disease

In patients with PD, degeneration of the nigrostriatal dopaminergic projection alters the level of activity in "direct" vs. "indirect" striatal MSNs, due to their differential expression of dopamine receptors. Direct pathway neurons (contains D1), which are normally excited by dopamine,

decrease their activity, whereas the indirect pathway D2-contining neurons, normally inhibited by dopamine, displays an increased activity in PD (see Fig. 1.1 (Wichmann and DeLong, 2003)). Increased striatal GABAergic outflow to the GPe reduces inhibitory pallidal influences on the STN thereby increasing glutamatergic drive to the output nuclei. As a result, this increased glutamatergic drive from the STN leads to an overactive inhibitory basal ganglia outflow to thalamocortical neurons, reducing motor cortex activity and inhibiting voluntary movements. In particular, studies in MPTP-treated (parkinsonian) monkeys have suggested that metabolic activity is increased in the basal ganglia motor thalamus in the parkinsonian state (Mitchell et al., 1989; Rolland et al., 2007), likely reflecting increased activity of basal ganglia projections to the thalamus. Consistent with this, electrophysiologic studies in such animals showed a decrease in neuronal firing rate in these nuclei (Kammermeier et al., 2014; Ni et al., 2000; Schneider and Rothblat, 1996; Vitek et al., 1994; Voloshin et al., 1994), although other studies found no change in firing rates (Pessiglione et al., 2005) or an increase in firing rates (Bosch-Bouju et al., 2014).

The direct and indirect "rate model" of the basal ganglia circuitry in Parkinson's disease depicted in Fig. 1.1 is useful in understanding PD pathophysiology. However, because of its simplistic nature, this model does not take into account all abnormal features of the basal ganglia-thalamocortical circuits found in PD, and cannot explain the motor symptoms (or the lack of) seen after lesion of specific parts of the circuit. Furthermore, previous studies have shown that lesions of the thalamus or GPe in normal animals do not cause parkinsonism (Canavan et al., 1989; Soares et al., 2004). Currently, additional alterations in basal ganglia neuronal activity, such as firing pattern, has been show to play an important role in parkinsonian pathophysiology (Galvan and Wichmann, 2008; Wichmann and DeLong, 1993; Wichmann and DeLong, 2003).

The synaptic circuitry of the basal ganglia may also be influenced by various morphological and ultrastructural fluctuations as a result of parkinsonism. Previous studies observed pruning and morphological changes of corticostriatal and corticosubthalamic terminals in non-human

primates, as well as in rodent models, of parkinsonism (Chu et al., 2017; Day et al., 2006; Deutch, 2006; Ingham et al., 1998; Mathai and Smith, 2011; Mathai et al., 2015; Raju et al., 2008; Villalba et al., 2009; Villalba and Smith, 2010; Villalba and Smith, 2011; Villalba et al., 2015). In addition, several studies have observed that the VApc and CM appear to be differentially affected by parkinsonism-associated pathology. While the total number of basal ganglia motor thalamic neurons is not significantly changed in PD (Halliday et al., 2005), as much as 40-50% neuronal loss has been shown in the CM/Pf of PD patients (Halliday et al., 2005; Henderson et al., 2000a; Henderson et al., 2000b) and MPTP-treated monkeys (Villalba et al., 2014).

1.4.2.2 Firing abnormalities in Parkinson's disease

In addition to alterations in firing rates among various nuclei, there is the presence of abnormal firing patterns in basal ganglia activity in Parkinson's disease. Previous studies have described abnormal oscillations in neuronal firing in the STN, GPi, and SNr in animal models, as well as in PD patients (Brown, 2007). In addition, recordings of spontaneously firing thalamic cells in MPTP-treated monkeys (Guehl et al., 2003; Pessiglione et al., 2005) and in patients with PD showed an increased incidence of irregular firing or burst discharges in the basal ganglia motor thalamus (BGMT) (Guehl et al., 2003; Kammermeier et al., 2014; Kaneoke and Vitek, 1995; Magnin et al., 2000; Molnar et al., 2005; Vitek et al., 1994; Zirh et al., 1998).

Another abnormal feature of the basal ganglia activity observed in Parkinson's disease is increased neuronal synchrony. As described above, the basal ganglia circuitry is organized in functionally segregated loops; neurons within close proximity of each other often fire independently and aids in the maintenance of this segregation at the cellular level. Conversely in parkinsonian conditions, the system undergoes synchronized neuronal firing across many neurons, thereby interfering in the typical flow of information and affecting the functionally segregated neuronal activity (Hammond et al., 2007). Bursting often occurs in the context of pathological oscillatory activity (Buzsaki et al., 1990; Guehl et al., 2003; Magnin et al., 2000;

Ohye et al., 1970; Raeva et al., 1999; Zirh et al., 1998). Coherent theta-band oscillations that engages both thalamus and cortex have been identified in studies that combined recordings of thalamic field potentials with those of cortical EEG in humans (Sarnthein and Jeanmonod, 2007). Pathological oscillatory bursting in other frequency ranges in the thalamus has also been described, perhaps resulting from oscillatory activity in basal ganglia output (Gatev et al., 2006; Kammermeier et al., 2014). Overall, increased burst firing have been described in the parkinsonian basal ganglia model in the pallidum and STN (Bergman et al., 1994; Soares et al., 2004; Wichmann et al., 1999). Moreover, several studies have shown that when dopamine is lost in PD patients and animal models, the frequency and length of bursts are increased (Hutchison et al., 1994; Magnin et al., 2000; Wichmann and Soares, 2006). Thus, the neuronal activity in various nodes of the basal ganglia-thalamocortical circuitry is severely hampered in the parkinsonian state. However, the underlying substrates of these complex changes remain largely unknown. One of the main goals of the work presented in this thesis is to directly address this issue through a detailed assessment of the changes in the synaptic microcircuitry of GABAergic and glutamatergic networks in the BGMT of parkinsonian monkeys.

1.5 Goals of Thesis

According to the direct and indirect pathway model of the basal ganglia, loss of nigrostriatal dopamine in PD is thought to increase basal ganglia inhibition of thalamus from the GPi and the SNr, resulting in reduced activity of thalamocortical projections, which may then lead to decreased cortical activity and motoric slowing (Fig.1.1). However, as discussed above, the lack of information about the pathophysiology of the functional relationships between the basal ganglia, cortex and thalamus in PD makes the prediction of the model highly speculative. There is evidence suggesting that the pallidothalamic system undergoes electrophysiological and metabolic changes in animal models of PD and in PD patients (Anderson et al., 2003; Eidelberg et al., 1997; Freeman et al., 2001; Guehl et al., 2003; Magnin et al., 2000; Mitchell et al., 1989;

Molnar et al., 2005; Nini et al., 1995; Vitek et al., 2012). Although the plasticity of GABAergic synapses in the BG-thalamocortical network remains poorly understood (Barroso-Chinea et al., 2008; Villalba and Smith, 2011), studies in rodent models of PD have suggested that GABAergic synapses from the globus pallidum (GPe in primates) onto STN neurons (Fan et al., 2012) display structural plasticity that may contribute to parkinsonism-related changes in GABAergic inhibition of the STN. Knowing that GPi and GPe GABAergic terminals display common ultrastructural and functional features, altered activity of the basal ganglia-receiving thalamic nuclei may be associated with ultrastructural changes in the microcircuitry of pallidal GABAergic synapses in MPTP-treated parkinsonian monkeys. Furthermore, in light of evidence for significant plastic changes in the prevalence and morphology of glutamatergic cortical inputs to the striatum and the STN in the parkinsonian state, we hypothesize that similar changes may be found in the corticothalamic glutamatergic system.

Here, we aim to elucidate the morphological and ultrastructural plasticity that may underlie abnormal communication between the basal ganglia and the thalamus in parkinsonism. My thesis project is part of joint efforts between the Smith and Wichmann labs to better understand the pathophysiology of the thalamus and its relationships with the basal ganglia and cerebral cortex in Parkinson's disease. The specific series of experiments presented in my thesis aim at elucidating plasticity in the synaptic organization of GABAergic and glutamatergic terminals and morphology of terminals in the VApc and CM thalamic nuclei in MPTP-treated parkinsonian monkeys. The following specific aims are proposed:

1.5.1 Specific Aim 1

To assess potential changes in the abundance and pattern of synaptic connectivity of the different populations of GABAergic and glutamatergic terminals in the VApc and CM of normal and MPTP-treated monkeys.

1.5.2 Specific Aim 2

To compare the morphology and number of GABAergic synapses formed by single GPi terminals in the VApc, and to determine changes in their ultrastructural features in parkinsonian monkeys using a three-dimensional EM reconstruction approach.

To achieve these goals, a series of high resolution electron microscopic approaches, tract tracing methods and immunocytochemical techniques were used in control and MPTP-treated parkinsonian monkeys.

Chapter 2 : Structural Plasticity of GABAergic and Glutamatergic Networks in the Motor Thalamus of MPTP-treated Parkinsonian Monkeys

Contains excerpts from:

Swain AJ, Galvan A, Wichmann T, and Smith Y. 2018. Structural Plasticity of GABAergic and Glutamatergic Networks in the Motor Thalamus of MPTP-treated Parkinsonian Monkeys. Brain Structure Function (Submitted).

2.1 Introduction

In the primate thalamus, VApc and CM are the main targets of inhibitory (GABAergic) inputs from the GPi, the primary motor output nucleus of the basal ganglia (Parent et al., 1983; Parent et al., 2001; Parent and Parent, 2004). The VApc is the main source of thalamic inputs to the supplementary motor area and premotor cortex, while the CM gives rise to a massive innervation of the sensorimotor striatum (Akkal et al., 2007; Inase et al., 1996; McFarland and Haber, 2000; McFarland and Haber, 2001; Sadikot et al., 1992b; Sakai et al., 1999; Sakai et al., 2000; Schell and Strick, 1984; Shindo et al., 1995; Sidibé and Smith, 1996; Smith and Parent, 1986; Smith et al., 2014a; Tokuno et al., 1992). In addition to massive GABAergic inputs from the GPi, the neurons of the VApc and CM receive prominent glutamatergic inputs from the cerebral cortex as well as GABAergic afferents from the reticular thalamic nucleus and GABAergic interneurons. The latter neuronal types accounts for 15-30% of the total neuronal population of VApc and CM in primates (Ilinsky and Kultas-Ilinsky, 1990; Jones, 2007; Smith et al., 1987). Despite their high prevalence in the primate thalamus, the anatomy and synaptic integration of GABAergic interneurons in the microcircuitry of the motor thalamus is largely unknown.

In traditional models of the pathophysiology of Parkinson's disease, the loss of nigrostriatal dopamine increases the activity of the inhibitory basal ganglia output projections to the ventral motor thalamus, leading to reduced activity of thalamocortical projections (Albin et al., 1989; DeLong, 1990). Recent studies have identified altered activity (including firing rate changes, bursting, oscillatory firing properties, and altered somatosensory responses) of thalamic cells in the VApc of animal models of PD and in PD patients (Aymerich et al., 2006; Bosch-Bouju et al., 2014; Chen et al., 2010; Guehl et al., 2003; Hirsch et al., 2000; Kammermeier et al., 2016; Kaneoke and Vitek, 1995; Lanciego et al., 2009; Magnin et al., 2000; Mitchell et al., 1989; Molnar et al., 2005; Ni et al., 2000; Orieux et al., 2000; Pessiglione et al., 2005; Raeva et al.,

1999; Rolland et al., 2007; Sarnthein and Jeanmonod, 2007; Schneider and Rothblat, 1996; Vitek et al., 1994; Zirh et al., 1998).

In the basal ganglia, the parkinsonian state is associated with characteristic morphologic and ultrastructural changes. Thus, in the striatum and subthalamic nucleus (STN), the dopamine-depleted state is accompanied by substantial remodeling of specific synaptic microcircuits. In particular, significant changes in the number and ultrastructural features of cortical terminals, associated with robust alterations in electrophysiological and plastic properties of corticostriatal and corticosubthalamic synapses have been reported in rodent and primate models of PD (Chu et al., 2017; Day et al., 2006; Deutch, 2006; Ingham et al., 1998; Mathai and Smith, 2011; Mathai et al., 2015; Raju et al., 2008; Smith et al., 2014b; Villalba et al., 2009; Villalba and Smith, 2010; Villalba and Smith, 2011; Villalba et al., 2015). In the STN of dopamine-depleted mice, there is a significant increase in the number of synapses formed by individual GABAergic terminals from the external segment of the globus pallidum (GPe), accompanied with increased synaptic strength of pallidosubthalamic synapses (Chu et al., 2017; Fan et al., 2012).

The possibility that similar structural alterations also occur in glutamatergic and GABAergic thalamic microcircuits in the parkinsonian state has not been examined. The objective of the present study was to compare the relative prevalence, pattern of synaptic connectivity and ultrastructural features of glutamatergic and GABAergic inputs to thalamocortical neurons and interneurons in the VApc and CM in control and MPTP-treated parkinsonian monkeys. Having such knowledge is critical to a deeper understanding of changes in thalamocortical and corticothalamic interactions in PD.

2.2 Materials and methods

2.2.1 Animals

Twenty-two rhesus macaque monkeys (Macaca mulatta) (12 males, 10 females; 2.5-17 years old; Table 2.1) obtained from the Yerkes National Primate Research Center colony) were used in

these studies. All animals were housed in temperature-controlled rooms and exposed to a 12-hour light cycle. The animals were fed twice daily with monkey chow supplemented with fruits and vegetables and received ad lib water. All animal procedures were approved by the Institutional Animal Care and Use Committee (IACUC) of Emory University, and were performed according to the Guide for the Care and Use of Laboratory Animals and the U.S. Public Health Service Policy on the Humane Care and Use of Laboratory Animals. See Table 2.1 for more details on animals. The surgery, perfusion, assessment, and treatment of these animals were performed by various members in the Smith and Wichmann lab.

2.2.2 MPTP treatment and assessment of Parkinsonism

Ten animals were rendered parkinsonian in the course of these studies. These animals received weekly MPTP injections (0.2-0.8 mg/kg i.m.; cumulative doses: 2.8–26.79 mg/kg; Natland International, Morrisville, NC or Sigma, St. Louis, MO), until they reached comparable states of stable, moderate parkinsonism. As described in previous studies (Bogenpohl et al., 2012; Devergnas et al., 2014; Galvan et al., 2010; Kliem et al., 2009; Masilamoni et al., 2010; Masilamoni et al., 2011; Wichmann et al., 2001; Wichmann and Soares, 2006), we assessed the severity of parkinsonism weekly for 15-min periods in an observation cage that was equipped with infrared beams, allowing us to measure their body movements as infrared beam break events. In addition, we used a parkinsonism rating scale to quantify impairments in 10 aspects of motor function (speed of movement, incidence and severity of “freezing” episodes, extremity posture, trunk posture, presence and severity of tremor, amount of arm movements, amount of leg movements, finger dexterity, home cage activity, and balance). Each item was scored on a 0–3 scale (maximal score, 30). The final parkinsonian motor scores ranged between 4.5-16, corresponding to mild and moderately severe parkinsonism. The severity of the parkinsonian motor signs had to be stable for a period of at least 6 weeks after the last MPTP injection before the monkeys were considered parkinsonian for this study. We have used the same protocol in

many previous studies (Bogenpohl et al., 2013; Devergnas et al., 2016; Galvan et al., 2014a; Hadipour-Niktarash et al., 2012; Masilamoni et al., 2010; Masilamoni et al., 2011; Masilamoni and Smith, 2017; Mathai et al., 2015; Villalba et al., 2014).

Table 2.1 Animal Summary

Monkey #	Age at time of sacrifice	Sex	Control/ MPTP	Modified PRS score	Delay between last dose of MPTP and sacrifice	Cumulative dose of MPTP (mg/kg)
MR 165	3.5 years	Male	Control	----------	----------	----------
MR 249	3 years	Male	Control	----------	----------	----------
MR 252	3 years	Female	Control	----------	----------	----------
MR 186	3.5 years	Male	Control	----------	----------	----------
MR 194	4.75 years	Female	Control	----------	----------	----------
MR 271	3 years	Male	Control	----------	----------	----------
MR 209	14 years	Female	Control	----------	----------	----------
MR 231	9 years	Female	Control	----------	----------	----------
MR 232	13 years	Female	Control	----------	----------	----------
MR 255	3.9 years	Male	Control	----------	----------	----------
MR 259	2.6 years	Male	Control	----------	----------	----------
MR 272	3 years	Male	Control	----------	----------	----------
MR 244	17 years	Female	MPTP	12/30	~11 years	17.5 mg/kg
MR 246	10 years	Female	MPTP	13.5/30	~ 4 years	7.1 mg/kg
MR 245	14 years	Female	MPTP	10/30	~8 years	4.15 mg/kg
MR 240	4 years	Male	MPTP	7/30	~4 months	18.15 mg/kg
MR 269	5 years	Male	MPTP	16/30	~1 year and 8 months	8.2 mg/kg
MR 205	12 years	Female	MPTP	14/30	~5 years	26.79 mg/kg
MR 247	15 years	Female	MPTP	14/30	~2 years	9.5 mg/kg
MR 250	9 years	Male	MPTP	10/30	~2 years	10.9 mg/kg
MR 218	4 years	Male	MPTP	5/30	~1 year	2.8 mg/kg
MR 222	5 years	Male	MPTP	4.5/30	~6 months	13.25 mg/kg

2.2.3 Anterograde labeling of pallidothalamic terminals

In 2 control and 2 MPTP-treated monkeys, pallidothalamic terminals were labeled anterogradely with viral vector injections in the GPi. A total of 2-8 µl of AAV5-hSyn-ChR2-EYFP or AAV5-hSyn-Arch3-EYFP was delivered in the GPi. In the control monkeys, the injections were made under isoflurane anesthesia with the animal fixed in a stereotaxic frame using aseptic surgical procedures. Pre-operative MRI scans of these monkeys were performed to help define the stereotaxic coordinates. Small holes were drilled in the skull and a Hamilton microsyringe was used to inject the viral vector at a single site in the ventrolateral part of GPi. To deliver the viral vector solution, the plunger of the syringe was pressed manually at an approximate rate of 1 µl/5 min. After completion, the syringe was left in place for 10 min before withdrawing. At the end of the surgery, the skin was sutured and the animals were treated with analgesics. The animals were allowed to survive for at least six months after injection.

In the MPTP-treated monkeys, the viral vector solutions were delivered in the GPi using extracellular recordings as a guide to delineate the borders of the neighboring nuclei using procedures previously described from our laboratory (Galvan et al., 2010; Kliem et al., 2007). Preparatory to the injections, recording chambers were stereotactically directed at the pallidum on either side of the brain, placed at an angle of 40° from the vertical in the coronal plane. The chambers were then affixed to the skull with dental acrylic, along with metal holders for head stabilization. Metal screws were used to anchor the acrylic to the bone.

During sessions conducted 2 to 3 weeks' post-surgery, electrophysiological mapping served to outline the borders of GPe and GPi. GPi cells were identified based on the depth of the electrode (at least 2 mm ventral to the first GPe unit), the presence of 'border' cells between GPe and GPi (DeLong, 1971), and the presence of neurons that fired at high frequency, characteristic for GPi cells (DeLong, 1971; Galvan et al., 2005; Galvan et al., 2011). The subsequent injections were done using a probe in which the injection tubing was combined with a recording microelectrode

(Kliem and Wichmann, 2004). Extracellular recordings were conducted while lowering the injection system to help to define the final location of the injections in the GPi (Galvan et al., 2010; Kliem et al., 2007). A microsyringe connected to a pump was used to deliver the viral vector solutions at a rate of 0.1 to 0.2 µl/min. At the end of the injection, the injectrode was left in place for 10 min before withdrawing. These animals were allowed to survive for 1.5-7 months (during which the animals were used in other experiments).

All animals with virus injections were eventually perfusion-fixed as described below, and their brains prepared to allow immunohistochemical localization of the tag protein, enhanced yellow fluorescent protein (EYFP; see below).

2.2.4 Tissue collection

At the completion of the study, the animals were euthanized with pentobarbital (100 mg/kg, iv), and transcardially perfused with a Ringer's solution and a mixture of paraformaldehyde (4%) and glutaraldehyde (0.1%). The brains were removed from the skull, post-fixed in 4% paraformaldehyde, and cut in serial sections (60 µm) with a vibratome. The sections were stored at -20^{o}C in antifreeze until further histological processing.

2.2.5 Immunohistochemistry

2.2.5.1 Tissue processing for microscopy

Tissue processed for immunohistochemistry was prepared for light or electron microscopy (LM and EM, respectively). The tissue was pre-treated with 1% sodium borohydride in phosphate buffer solution for 20 min prior to immunohistochemistry processing. The sections were subsequently thoroughly washed in phosphate-buffered saline (PBS). Sections used for LM were incubated with antibodies as described below, while sections prepared for EM were placed in a cryoprotectant solution (phosphate buffer [PB], 0.05 M, pH 7.4, containing 25% sucrose and 10% glycerol) for 20 min, frozen at −80°C for 20 min, thawed, and returned to a graded series of

cryoprotectant solution (100%, 70%, 50%, 30%) diluted in PBS. They were then washed in PBS before further processed.

The sections were pre-incubated in a solution containing 10% normal goat or horse serum (depending on the source of the primary antibody) and 1% bovine serum albumin (BSA) in PBS for 1 hour. For LM, 3% Triton-X-100 was used in addition to normal serum (NS) and BSA throughout the immunohistochemical reactions. Sections were then incubated with the respective primary antibodies for 48 hours at 4°C (for antibody dilutions, see Table 2) in a solution containing 1.0% NS and 1.0% BSA in PBS. Next, the sections were rinsed in PBS and transferred for 1.5 hours to a solution containing the secondary biotinylated antibody (dilution, 1:200). After rinsing with PBS, the sections were put in a solution containing 1% avidin-biotin-peroxidase complex (Vector Laboratories, Burlingame, CA USA). The tissue was then washed in PBS and Tris buffer (0.05 M pH 7.6) before being transferred into a solution containing 0.01M imidazole, 0.005% hydrogen peroxide, and 0.025% 3,3′-diaminobenzidine tetrahydrochloride (DAB; Sigma, St. Louis, MO) in Tris (0.05 M pH 7.6) for 10 min. The DAB reaction was terminated with several rinses of the sections in PBS. Sections prepared for LM were then mounted on gelatin-coated slides and prepared for observation.

Some sections were further processed for EM observations without the use of Triton. These sections were transferred to PB (0.1 M, pH 7.4) for 10 min and exposed to 1% osmium tetroxide for 20 min. They were then rinsed with PB and dehydrated in an increasing gradient of ethanol. Uranyl acetate (1%) was added to the 70% alcohol step in the gradient to increase contrast. The sections were subsequently treated with propylene oxide before being embedded in epoxy resin (Durcupan, ACM; Fluka, Buchs, Switzerland) for 12 hours, mounted on microscope slides, and placed in a 60°C oven for 48 hours (Villalba and Smith, 2011). Blocks of tissue (1 mm^2) from the VApc and CM (2-4 blocks per animal) were then taken out from the slides and glued on top of resin blocks with cyanoacrylate glue. These blocks were trimmed and cut serially into 60-nm

ultrathin serial sections with an ultramicrotome (Ultra-cut T2; Leica, Germany) and collected on single-slot Pioloform-coated copper grids. To limit our observations to tissue with similar antibody penetration, the EM analyses were restricted to ultrathin sections from the most superficial sections of blocks. Prior to being placed in the electron microscope, grids were stained with lead citrate for 5 minutes and then placed in aqueous solution for 5 minutes.

In control experiments, sections were processed as described above, but without primary antibodies (as a control for the specificity of binding of the secondary antibodies). The resulting sections were completely devoid of immunostaining following the incubations.

2.2.5.2 Striatal tyrosine hydroxylase (TH) immunostaining

To verify denervation of the nigro-striatal pathway by MPTP intoxication, sections at the level of the striatum and the substantia nigra from MPTP-treated monkeys were stained with mouse anti-TH antibody (Table 2.2), as described in our previous studies (Bogenpohl et al., 2013; Devergnas et al., 2016; Galvan et al., 2014a; Hadipour-Niktarash et al., 2012; Masilamoni et al., 2010; Masilamoni et al., 2011; Masilamoni and Smith, 2017; Mathai et al., 2015). Sections were prepared with the TH antibody as previously mentioned in section 2.2.5.1.

2.2.5.3 Post-embedding GABA immunostaining

To differentiate GABAergic from non-GABAergic terminals in VApc and CM, post-embedding immunogold labeling for GABA was carried out on thalamic tissue of control and parkinsonian monkeys, as described previously (Charara et al., 2005). Sections that were prepared for post-embedding EM immunolabeling underwent EM processing (osmium and tissue dehydration, as described above), were cut out and glued onto resin blocks, cut into ultrathin sections (60nm) and placed on gold slot grids. The sections were then incubated for 10 min on drops of Tris-buffered saline containing 0.01% Triton X-100 (TBS-T 0.01%; pH 7.6). Following pre-incubation, the grids were incubated overnight at room temperature with a well-characterized specific polyclonal GABA antiserum (Table 2.2), diluted in a solution of TBS-T 0.01%. After many washes in TBS-

T (pH 7.6) and TBS (0.05M pH 8.2), the grids were then incubated for 90 min with 15 nm gold-conjugated secondary antibodies (1:50; Cedarlane Lab), diluted in TBS (pH 8.2). Grids were subsequently washed in TBS (pH 8.2) and ultrapure water for 5 min. They were then incubated in a 2% aqueous solution of uranyl acetate for 90 min, and in distilled water for 5 min. The grids were subsequently stained with lead citrate.

2.2.5.4 vGAT and GAD67 immunoperoxidase labeling

For LM analysis of changes in the intensity of immunostaining of markers for GABA terminals and cell bodies in the VApc and CM, every twelfth section (4-7 sections per animal) was stained for vGAT or GAD67 (Fig 2.1 a-d, f-k). At the level of CM, adjacent sections were immunostained for calbindin (Cb) D28K to help delineate the external border of the nucleus with the assistance of a rhesus monkey brain atlas (Lanciego and Vázquez, 2012).

2.2.5.5 GFP immunoperoxidase labeling

In the 4 monkeys that received viral vector injections in the GPi (see above), the viral vector injection sites and the resulting anterograde labeling in the VApc and CM were localized using a specific GFP antibody (Table 2.2) and the immunoperoxidase ABC method. Note that this antibody also labels EYFP, the tag protein used in these experiments. The tissue was processed to localize labeling at the LM or EM levels, as described above. For EM observations, one block of tissue/animal at the level of the VApc and CM that contained dense anterograde labeling was taken out from slides and cut in ultrathin sections. These sections were used to study the pattern of synaptic connectivity and morphology of GPi terminals, as described below (see section 2.2.6).

2.2.5.6 vGluT1 immunostaining

A specific vGluT1 antibody (Table 2.2) was used to identify corticothalamic terminals in VApc and CM. The EM immunoperoxidase procedure to localize vGluT1 was the same as described above.

Table 2.2 Antibody Information

Antigen	Immunizing species	Vendor (Primary)	Antibodies dilution used	Secondary antibodies dilution used	Vendor (Secondary)	Purpose
vesicular GABA Transporter (vGAT)	Mouse	R&D Systems, catalog no. MAB6847	1:5,000	Horse anti Mouse 1:200 (biotinylated)	Vector, catalog no. BA2000	Light Microscopy
Glutamic Acid Decarboxylase 67 (GAD67)	Mouse	Millipore, catalog no. MAB5406	1:5,000	Horse anti Mouse 1:200 (biotinylated)	Vector, catalog no. BA2000	Light Microscopy
Calbindin D28k (Cb)	Goat	R&D Systems, catalog no. AF3320	1:1,000	Horse anti Goat 1:200 (biotinylated)	Vector, catalog no. BA9500	Light Microscopy
GFP	Rabbit	Life Tech, catalog no. A11122	1:5,000	Goat anti Rabbit 1:200 (biotinylated)	Vector, catalog no. BA9400	Pre-Embedding Electron Microscopy
vesicular Glutamate Transporter 1 (vGluT1)	Guinea Pig	Millipore, catalog no. AB5905	1:5,000	Goat anti Guinea Pig 1:200 (biotinylated)	Vector, catalog no. BA7000	Pre-Embedding Electron Microscopy
GABA	Rabbit	Sigma. catalog no. A2052	1:1,000	Goat anti Rabbit (BBI) 1:50 (gold)	BBI, catalog no. EMAR-15	Post-Embedding Electron Microscopy
Tyrosine hydroxylase (TH)	Mouse	Millipore, catalog no. MAB318	1:1,000	Horse anti Mouse 1:200 (biotinylated)	Vector, catalog no. BA2000	Light Microscopy

2.2.6 Analysis of material

2.2.6.1 Striatal TH immunostaining intensity measurements

The tissue was examined with a Leica DMRB light microscope (Leica Microsystems, Inc., Bannockburn, IL) and images were taken with a CCD camera (Leica DC 500; Leica IM50 software). For low magnification images, slides were scanned at 20× using a ScanScope CS scanning system (Aperio Technologies, Vista, CA). Digital representations of the slides were

saved and analyzed using ImageScope software (Aperio Technologies). Using the ImageScope viewer software (Aperio), 0.7x magnification digital images of the stained tissue slides containing the caudate nucleus, putamen, or substantia nigra were randomly selected and imported into ImageJ (NIH) (Schneider et al., 2012) for optical density measurements (Villalba and Smith, 2011; Villalba et al., 2014; Villalba et al., 2015). The images were converted into 16-bit grayscale format and inverted. Measurements of the intensity of labeling were obtained in two sections at the striatal and nigral levels from two groups of animals (control and MPTP-treated). In each section, the intensity of TH-staining was measured in four representative areas in each structure. To control for background staining, the optical density measurement in the internal capsule (for caudate and putamen) and cerebral peduncle (for SNc) was subtracted from the measurements. The resulting values were averaged in the MPTP-treated animals, and compared with similar data obtained in controls to determine the percent of TH immunostaining loss in the striatum (caudate nucleus + putamen) and the substantia nigra in the MPTP-treated cases (Fig. 2.1g).

2.2.6.2 Density of vGAT and GAD67-staining

Based on LM images of vGAT and GAD67-stained sections, the NIH Image J software was used to determine average densitometry values of vGAT and GAD67 immunolabeling intensity in the VApc and CM of control or MPTP-treated monkeys. The measured values were background-corrected by subtracting densitometry measurements from the internal capsule. To control for variability in the intensity of immunostaining between animals and runs of immunostaining, the densitometry measurement values in VApc and CM were then expressed relative to the intensity of immunostaining in the medial geniculate nucleus (MGN) or the ventral posteromedial nucleus (VPM), two thalamic nuclei with no known involvement in the pathophysiology of parkinsonism. We averaged densitometry measurements from regions of interest that covered approximately 85-90% of the total surface of the VApc, CM, MGN, or VPM. The ratios of VApc/MGN or CM/VPM average intensity measurements from 4-7 sections per animal were calculated for each

animal, followed by statistical comparisons (t-test or Mann-Whitney test, as appropriate) of the mean VApc/MGN and CM/VPM ratios between control and parkinsonian monkeys.

2.2.6.3 Density of GABAergic and glutamatergic terminals

GABA-immunostained ultrathin sections of VApc and CM tissue from control and parkinsonian animals were examined in the EM. We collected >100 randomly chosen micrographs at 40,000X, from at least two blocks of tissue per animal from 4-5 control and 3 MPTP-treated animals in both the VApc and CM. The total number of micrographs analyzed in these experiments accounted for 1770 mm^2 and 2743 μm^2 of VApc in control and MPTP-treated monkeys, respectively, and 1770 μm^2 of CM in both control and MPTP-treated animals. Using these micrographs, we distinguished different types of terminals in the thalamus based on their GABA expression and ultrastructural features, and determined their relative density (as terminals/μm^2; see Results section). Some micrographs that were used in this analysis were overlaid with gold particles indicative of GABA immunoreactivity (as described above). We arbitrarily considered that an ultrastructural element was positive for GABA if it contained more than two times the average density of gold particles than the background labeling, defined as the average density of gold particles over putative glutamatergic terminals that formed asymmetric axo-spinous synapses in the same ultrathin section as the one containing the GABA-immunoreactive terminals. The density of terminals was compared between control and parkinsonian animals by One Way ANOVA; Holm-Sidak post-hoc testing for normally distributed data, and Dunn's Method post-hoc testing for data not normally distributed.

2.2.6.4 Size of glutamatergic terminals

EM sections of vGluT1-stained material were used to compare the average cross-sectional area of corticothalamic terminals between control and MPTP-treated monkeys. The cross-sectional area of at least 30 vGluT1-labeled terminals in the VApc and CM of 3 control and 3 MPTP-treated monkeys was used. EM sections were selected and imported into ImageJ. The average cross-

sectional areas of vGluT1-positive terminals for each animal were calculated and the means were averaged amongst their respective group and compared between control and parkinsonian monkeys with t-tests.

2.2.6.5 Pattern of synaptic connectivity of GABAergic and glutamatergic terminals

The post-synaptic targets of terminals were identified as cell bodies, large, medium or small dendrites (>1.0, 0.5-1.0 and <0.5 μm in diameter, respectively), based on their ultrastructural features and cross-sectional diameters (Peters et al., 1991). Dendrites of projection neurons were separated from dendrites of interneurons based on the presence of dendritic vesicles, which are exclusively found in interneurons (Hámori et al., 1974; Jones, 2002a; Jones, 2007; Sherman and Friedlander, 1988; Sherman, 2004). The analysis included dendrites of projection neurons from at least 2 blocks per animal from 4-6 control and 3-5 MPTP-treated animals. The proportions of terminals in contact with each target were compared between control and parkinsonian animals for each pre-synaptic element by One Way ANOVA for normally distributed data, and Kruskal-Wallis analyses for data not normally distributed.

2.2.6.6 Relative prevalence of dendritic profiles

We compared the relative density of large, medium and small dendrites in the VApc and CM between control and MPTP-treated monkeys. To do so, 25 randomly scanned electron micrographs of VApc and CM neuropil (25,000X) were analyzed in each animal. Dendrites were categorized by their cross-sectional diameter, as described above. The percentages of the different sizes of dendrites from each block of tissue were averaged for each animal. From there, the relative proportion of small-, medium- or large-sized dendrites in the VApc and CM was determined in control and parkinsonian monkeys.

2.2.6.7 Proportion of vGluT1-labeled terminals and of anterogradely labeled GPi terminals in contact with GABAergic interneurons

The post-synaptic targets of 184 vGluT1-immunoreactive and 516 GFP-labeled GPi terminals were categorized as dendrites of projection neurons (no synaptic vesicle) or interneurons (with synaptic vesicles). The proportion of immunolabeled terminals in contact with each post-synaptic structure was determined and compared between control and parkinsonian monkeys. We collected data from 3-5 blocks per animal (vGluT1-labeled: 3 control and 3 MPTP-treated animals; labeled GPi terminals: 2 control and 2 MPTP-treated animals). Because of the low number of animals that could be used in this analysis, no statistics was performed on the data collected from GFP-labeled GPi terminals. Mann-Whitney Rank Sum test was used to determine significance between average number of vGluT1-labeled terminals that come in contact with projection neurons and interneurons in control and parkinsonian monkeys.

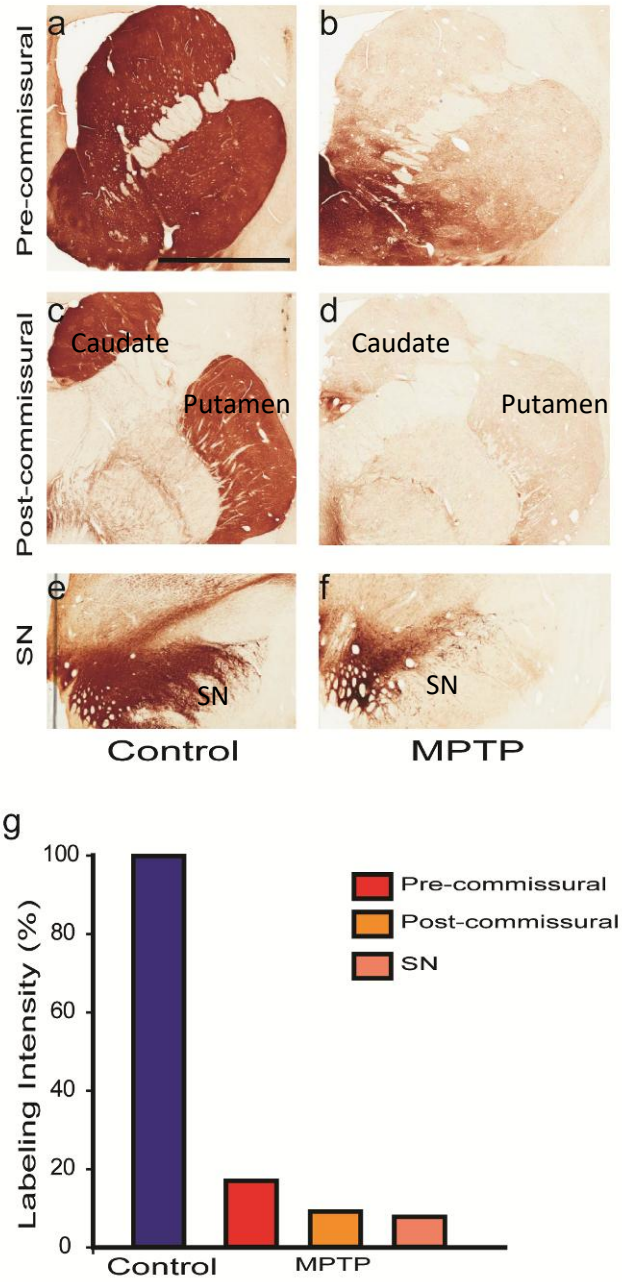

***Figure 2.1*. Tyrosine hydroxylase immunoreactivity (TH-IR) in the striatum and substantia nigra (SN).**

(a-f) Coronal sections at the level of the pre-commissural striatum (a-b), post-commissural striatum (c-d) and SN (e-f) to illustrate TH-IR in control (a, c, e) and MPTP-treated monkeys (b, d, f). (g) The normalized intensity of TH-IR in the control of the pre- and post- commissural striatum and SN. Data is expressed as % reduction from control for each structure. The data in g for the pre and post-commissural areas are based on an averaged of the labeling intensity in both the caudate nucleus and putamen. CD caudate nucleus, Pu putamen. Scale bars in a (applies to b-f) and corresponds to 4 mm.

2.3 Results

2.3.1 Nigrostriatal dopamine denervation in MPTP-treated monkeys

The depletion of the striatal dopaminergic innervation in the MPTP-treated animals was determined by assessing the decrease in the extent of TH immunoreactivity (TH-IR) in representative coronal sections of the pre-commissural, commissural, and post commissural striatum in one control and one MPTP-treated monkey (Fig. 2.1). All of the parkinsonian animals had decreased levels of TH-IR throughout the striatum (Fig. 2.1b, d, f). The quantification of the intensity of TH immunostaining in the pre- and post-commissural striatal levels showed an 83-91% lower level in MPTP-treated monkeys than in controls (Fig. 2.1g). In the SN, a >90% lower level of TH-IR was observed in the MPTP-treated monkeys compared to controls (Fig. 2.1g). These results are consistent with previous findings from our laboratory using the same animal model (Villalba et al., 2014).

2.3.2 GAD67 and vGAT Immunolabeling in VApc and CM

Thalamic tissue from six control and four MPTP-treated monkeys was immunostained for vGAT and GAD67 (Fig.2.21a-d, f, h, i, k), and the density of these markers expressed as ratios to that found in neighboring MGN and VPM areas, as described in Methods. The boundaries of VApc and CM were determined using adjacent sections that were immunolabeled for calbindin D28K (Fig. 2.2g, i). We found that the VApc/MGN ratios for vGAT and GAD67 staining did not significantly differ between the MPTP-treated and control groups (Fig. 2.2e; $p = 0.091$, $p = 0.484$, respectively; t-test). Likewise, no significant difference was found in the CM/VPM ratios for vGAT and GAD67 staining between the two animal groups (Fig. 2.2l; $p = 0.429$, $p = 0.067$, respectively; t-test and Mann-Whitney Rank Sum test).

2.3.3 Types of GABAergic and glutamatergic terminals in VApc and CM

At the EM level, 3 types of axon terminals were identified in VApc and CM based on ultrastructural features reported in previous electron microscopic studies of the mammalian motor

thalamus (Jones, 2007), and additional tract-tracing and immunohistochemical data presented in this study (Figs 2.3,2.4): (1) terminals forming asymmetric synapses ('As'-type terminals; Fig. 2.4a, c), which putatively originate from the cerebral cortex, (2) terminals forming single symmetric synapses ('S1'-type terminals; Fig. 2.4a-c), likely representing GABAergic inputs from the thalamic reticular nucleus (RTN) or GABAergic interneurons, and (3) terminals forming multiple symmetric synapses ('S2'-type terminals; Fig. 2.3a-c), which originate from GABAergic neurons in GPi.

To further confirm that GPi was the source of S2 terminals, AAV5-eYFP was injected into the GPi (see Fig. 2.5) of 2 control (MR271 and MR272) and 2 MPTP-treated monkeys (MR240 and MR269), and the morphology of 82 anterogradely labeled terminals was examined in the EM. As expected, anterogradely labeled GPi terminals were large (1.0-3.0 mm in diameter) (Ilinsky et al., 1997; Kultas-Ilinsky et al., 1983; Kultas-Ilinsky et al., 1997; Shink et al., 1997), densely filled with mitochondria, and formed multiple axo-dendritic synapses onto dendrites in VApc (Fig. 2.3a) and CM (Fig. 2.3c). To demonstrate the GABAergic nature of S1 and S2 terminals, ultrathin sections of VApc and CM from 3-4 control and 4-5 MPTP-treated monkeys were processed for post-embedding GABA immunolabeling. In this material, both S1 and S2 terminals were overlaid with a large number of gold particles, while As terminals were devoid of staining (Fig. 2.4). All terminals categorized as S1 or S2 were overlaid with a density of gold particles that was at least twice as large as that over As glutamatergic terminals in the same ultrathin sections.

Examples of the three categories of terminals forming axo-dendritic synapses in VApc and CM are shown in fig. 2.3 and 2.4. In figure 2.4A, the GABA-positive S1 terminal is in contact with a vesicle-filled dendrite of a putative GABAergic interneuron in the VApc of a control monkey (Fig. 2.4a). These data provide strong evidence that three major types of terminals in VApc and CM can be differentiated by their ultrastructural features in control and MPTP-treated parkinsonian monkeys.

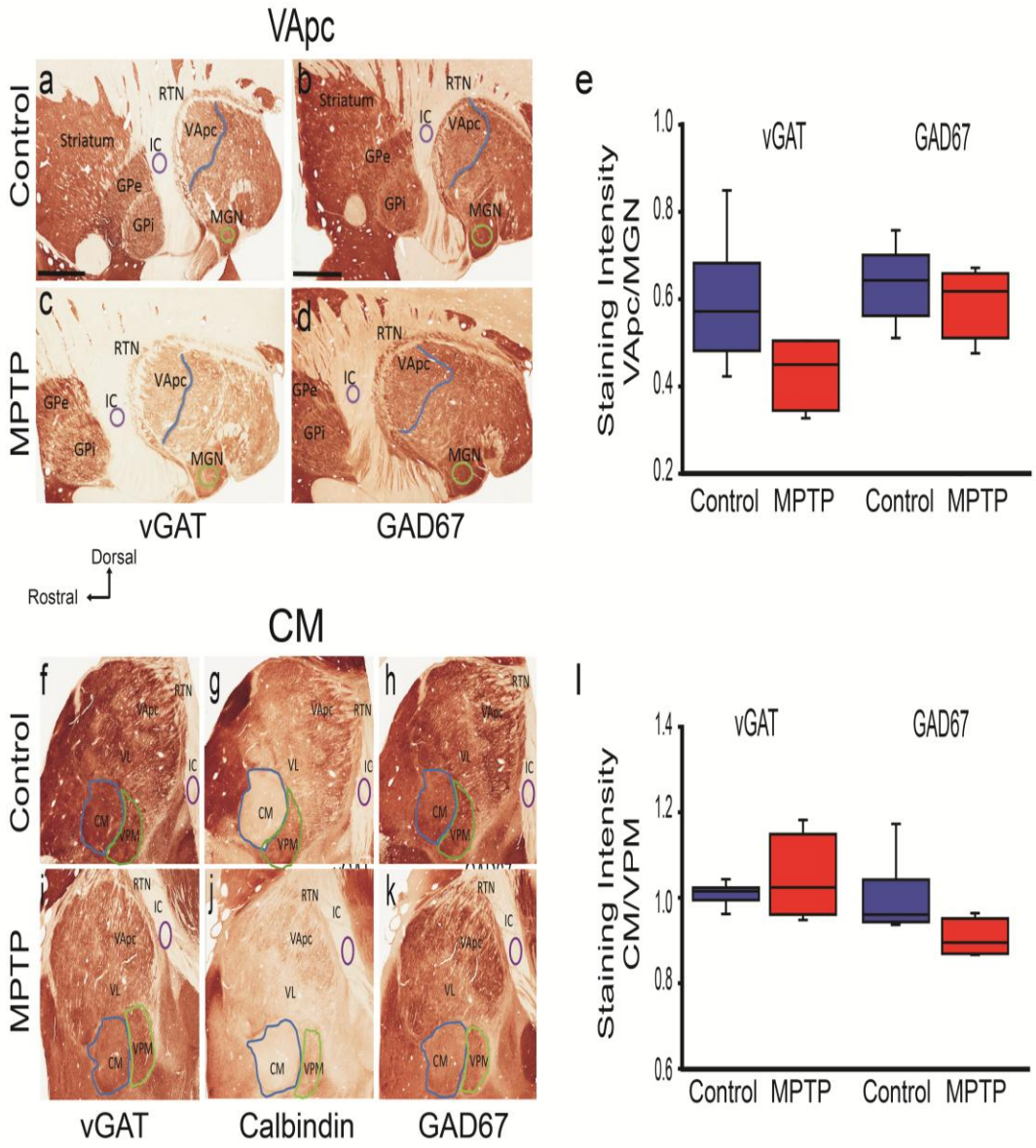

Figure 2.2. **Vesicular GABA Transporter (vGAT) and glutamic acid decarboxylase 67 (GAD67) immunoreactivity (IR) in the ventral anterior parvocellular part (VApc) and centromedian (CM) thalamic nuclei.**

Sagittal sections of the VApc (a-d) and CM (f-k) in control and MPTP-treated animals processed for vGAT-IR, GAD67-IR, and calbindin. Intensity of vGAT-IR and GAD-67 IR in the VApc and CM of control and MPTP-treated monkeys, expressed as ratio of staining intensity (e) VApc/medial geniculate nucleus (MGN) or (l) CM/ventral posteromedial nucleus (VPM). *GPe*, *GPi* Globus pallidum external, internal (respectively), *RTN* reticular thalamic nucleus, *IC* internal capsule, *VL* ventral lateral thalamic nucleus. Data are expressed as mean± SEM. *Scale bars* in a, b (applies to c, d, f-k) and corresponds to 4mm.

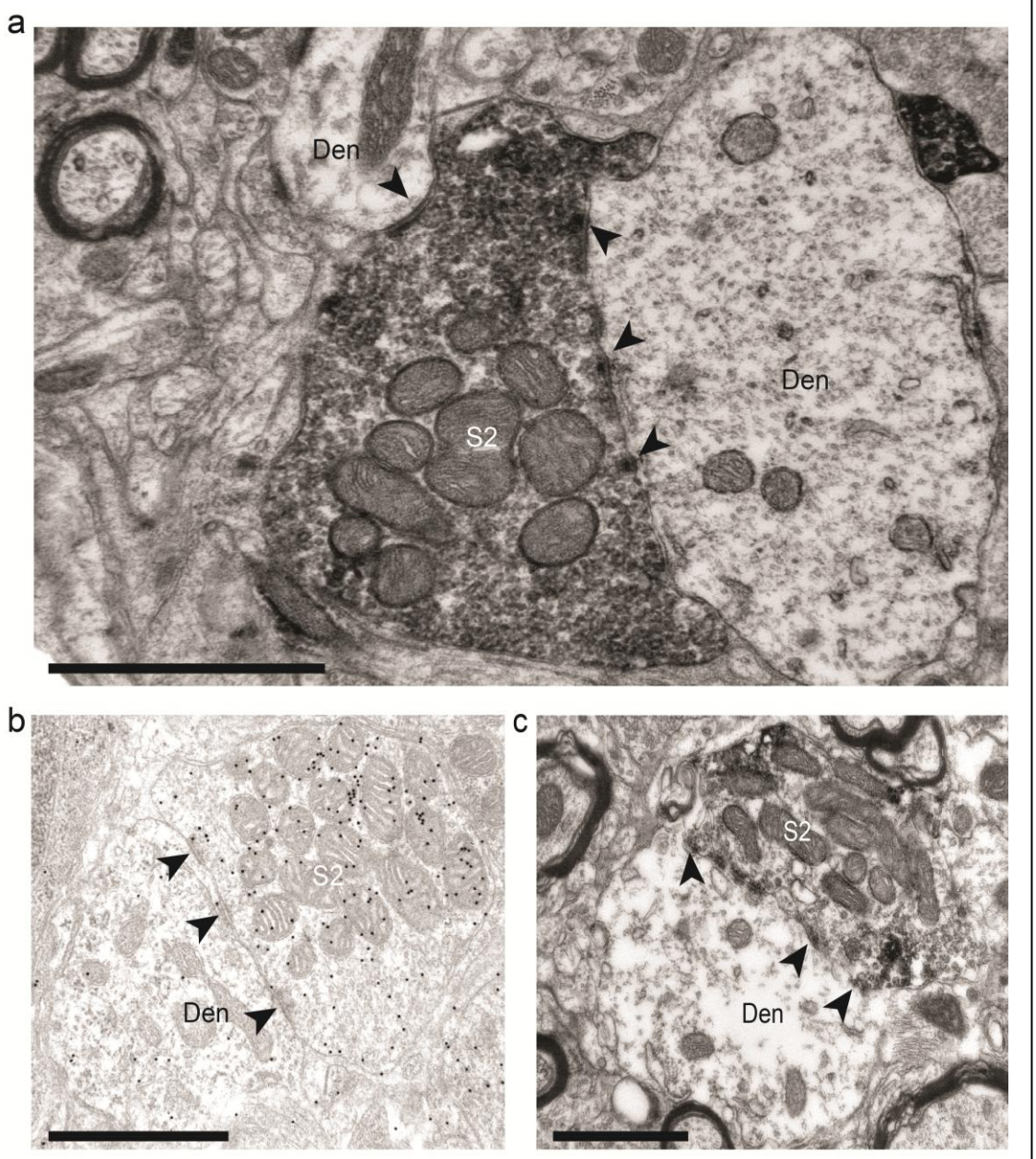

Figure 2.3. **S2-type terminals in the VApc and CM in Normal and MPTP-treated monkeys.**

(a, c) Electron micrograph of a EYFP-containing GPi (S2-type) terminal forming multiple synapses (arrowheads) onto a dendrite in the (a) VApc of a MPTP-treated monkey and (c) CM of a normal animal. (b) Electron micrograph of a S2-like GABA-labeled terminal forming multiple synapses onto a dendrite in the VApc of a normal monkey. In a and c, the GFP was revealed with immunoperoxidase (dense deposits), in b, GABA was revealed with immunogold particles (small black dots). Black arrowheads = individual synapses. *Scale bars* correspond to 1 micron.

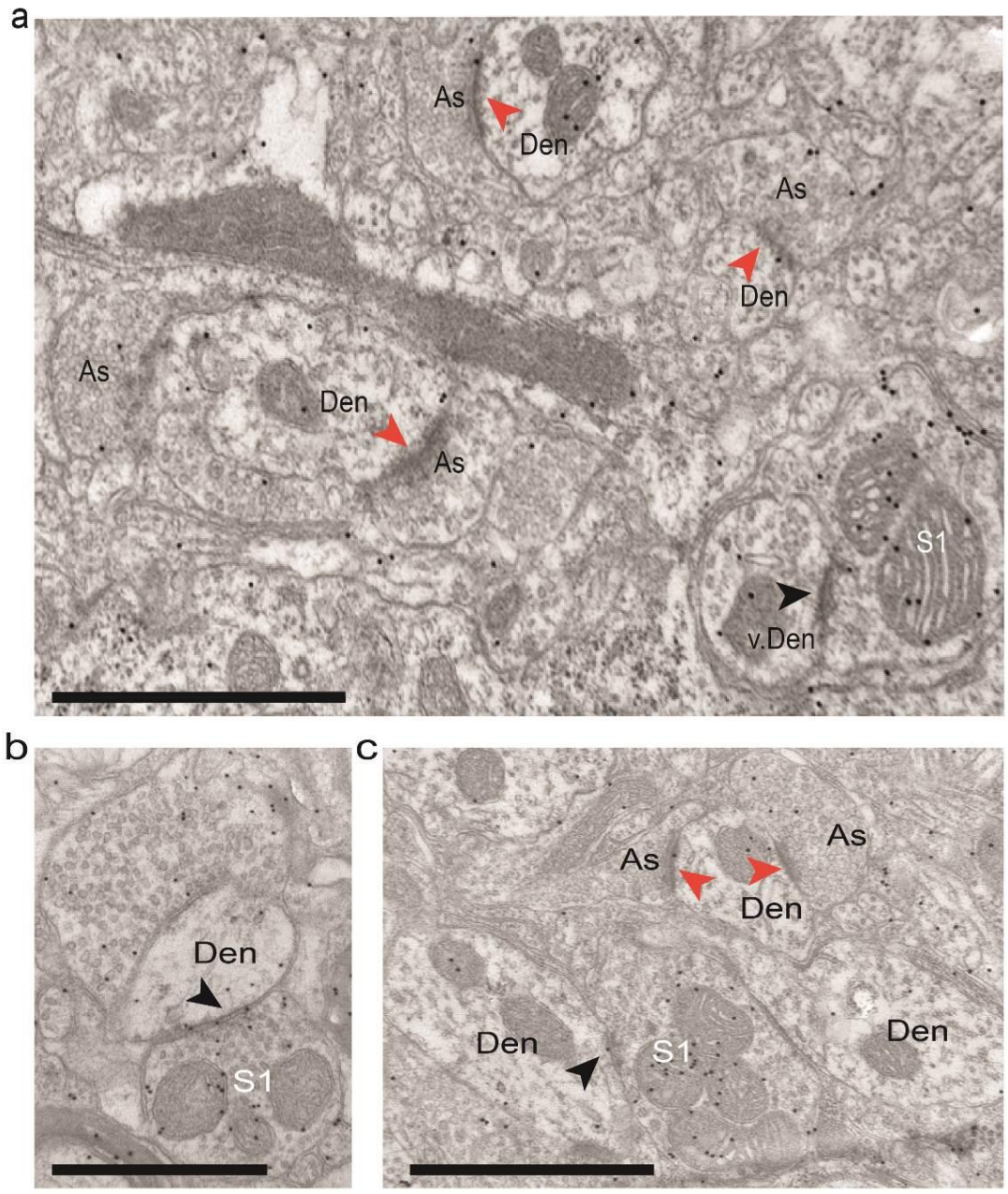

Figure 2.4. **S1 and As-type terminals in the VApc and CM in Normal and MPTP-treated monkeys.**

(a) Post-embedding immunogold GABA labeling that shows GABA-negative As-type terminals in contact with distal dendrites (Den) and a GABA-positive S1 terminal in contact with a vesicle-filled interneuron's dendrite (v. Den) in the VApc of a control monkey. (b) S1-type terminal in the CM of an MPTP-treated monkey in contact with a medium dendrite. (c) GABA-positive S1-type terminal in the VApc of a normal monkey in contact with a medium dendrite. *Scale bars* correspond to 1 micron.

2.3.4 Relative prevalence and preferred post-synaptic targets of GABAergic and glutamatergic terminals in the VApc and CM

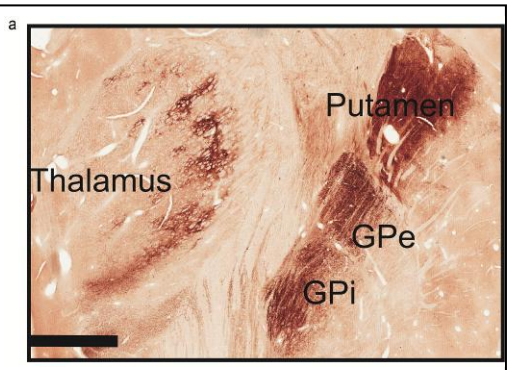

Figure 2.5. **Injection site of AAV5-hsyn-ChR2-eYFP into the GPi of a MPTP-treated monkey.**

Anterograde labeling of GPi terminals in the thalamus. *Scale bar* = 2mm.

To compare the relative abundance of As, S1 and S2 terminals in the thalamus of parkinsonian monkeys with that found in untreated animals, the density of each group of terminals was quantified in the VApc and CM of 5 control and 3 parkinsonian monkeys. Overall, the density of As terminals was significantly higher than that of S1 and S2 terminals in VApc of control and parkinsonian monkeys (Fig 2.6a; Control: $p<0.001$ for comparisons between the densities of As and S1 terminals, and of As and S2 terminals; MPTP: As vs S1: $p = 0.020$; As vs S2: $p = 0.004$; One Way ANOVA with Holm-Sidak post-hoc testing), and significantly higher than that of S2 terminals in CM of control monkeys (Fig. 2.7a; $p = 0.019$, One Way ANOVA with Dunn's Method). There was no significant group difference for S1 and S2 terminal densities between control and parkinsonian animals in both thalamic nuclei. However, compared to controls, the prevalence of As-type terminals was significantly lower in the VApc, but not in the CM, of the parkinsonian monkeys (Fig. 2.6a; $p<0.001$, One Way ANOVA with post-hoc Holm-Sidak testing).

To assess possible differences of the pattern of synaptic connectivity of As, S1 and S2 terminals between control and parkinsonian animals, the post-synaptic targets contacted by the three terminal sub-types were categorized as cell bodies, large (>1.0 µm in diameter), medium (0.5-1.0 µm in diameter) or small (<0.5 µm in diameter) dendrites. The percentages of specific terminals in contact with each post-synaptic element was averaged and compared between control and parkinsonian animals with ANOVA. This analysis revealed no significant difference in the

pattern of synaptic connectivity of As, S1, and S2 terminals in the VApc and CM between control and parkinsonian monkeys (Figs. 2.6b-d, 2.7b-d).

In both VApc and CM of control and parkinsonian monkeys, S2 terminals preferentially targeted large- and medium-sized dendrites, whereas As terminals were mainly located on medium dendrites of thalamic cells (Figs. 2.6b-d, 2.7b-d). To determine whether this pattern of synaptic connections was random, and merely reflected the neuropil dendritic composition of the two thalamic nuclei, the average relative density of each dendrite type (i.e., small, medium, large) was assessed in the VApc and CM of 2 control and 2 parkinsonian monkeys. The relative abundance of each category of dendrites was closely similar between VApc and CM, and not significantly different between control and parkinsonian monkeys (Figs. 2.8a, c). In both thalamic nuclei and both conditions, small- (~50-63% of all dendrites) and medium (~28-43%) sized dendrites accounted for most dendritic profiles, while large-sized dendrites (~7-16%) were less common (Figs. 2.8a, c). To determine if the three types of terminals preferentially targeted a specific subset of dendrites, we calculated the ratio between the percent of each terminal subtype in contact with a specific population of dendrites over the average percentage of small-, medium- or large-sized dendrites in the VApc and CM of control (Fig. 2.8b, d) and MPTP-treated (Fig. 6b, d) monkeys. This analysis showed that S2 and As terminals were largely segregated on the proximal and distal dendrites of VApc and CM neurons, respectively, in both control and parkinsonian monkeys (Fig. 2.8b, d), while S1 terminals were more homogeneously distributed along the somatodendritic domain of thalamic cells in each nucleus. In addition to this general pattern of synaptic connectivity, we found that in the VApc, very few S1 terminals contacted large-sized dendrites in the normal state, while the prevalence of such relationships was higher in parkinsonian animals (Fig. 2.8b). In the CM of MPTP-treated monkeys, synaptic contacts between S2 terminals and large-sized dendrites were uncommon (Fig. 2.8d).

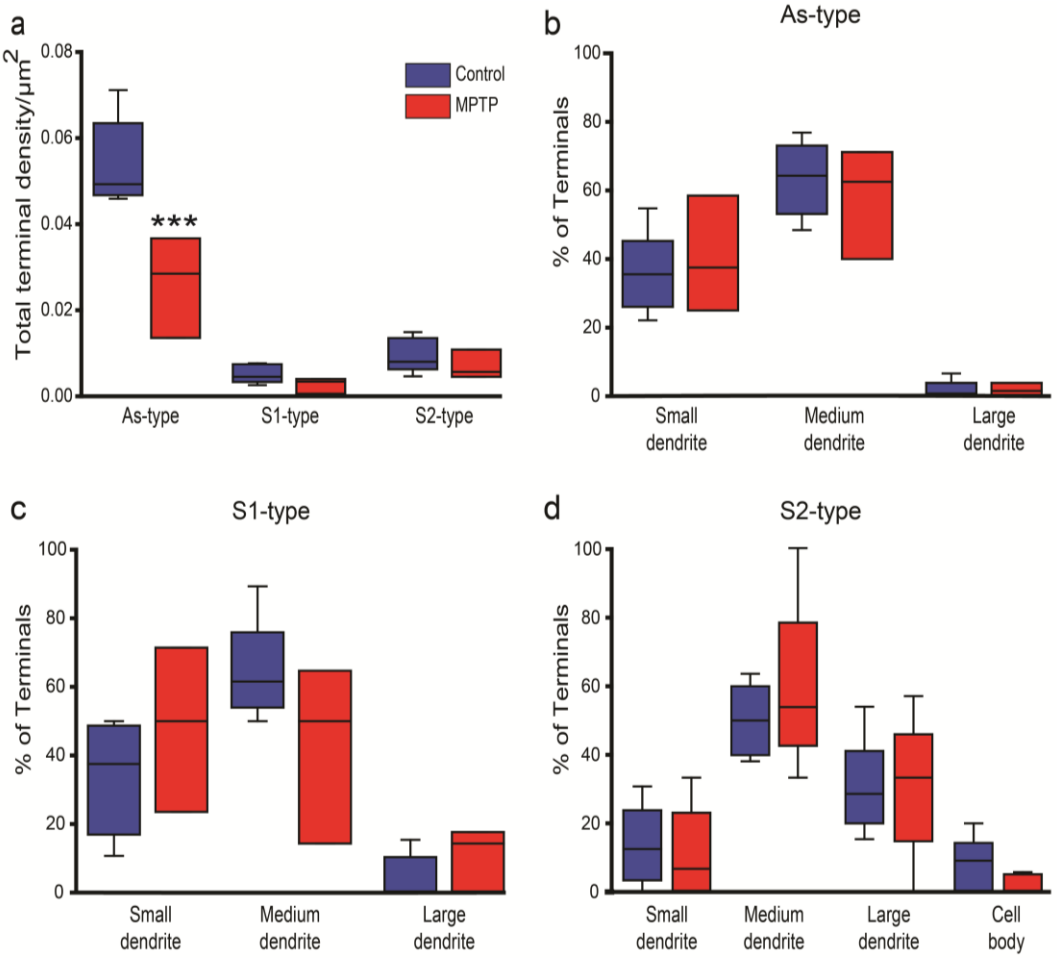

Figure 2.6. **Relative prevalence and post-synaptic targets of GABAergic and glutamatergic terminals in the VApc.**

(a)Total density of each terminal sub-type in the VApc of control (n = 5) and parkinsonian (n = 3) monkeys. (b-d) Percentage of each terminal subtype in synaptic contact with dendritic profiles of different sizes in control (n = 5-6) and parkinsonian (n = 3-5) monkeys. Lines inside boxes indicate medians, top and bottom of boxes indicate 1st and 3rd quartile respectively, and whiskers indicate minimum and maximum data points. (Significant decrease in As-type terminals *** = $p<0.001$. S1-type terminals; $p=0.851$, S2- type terminals; $p= 0.941$, One-Way ANOVA (Holm-Sidak)).

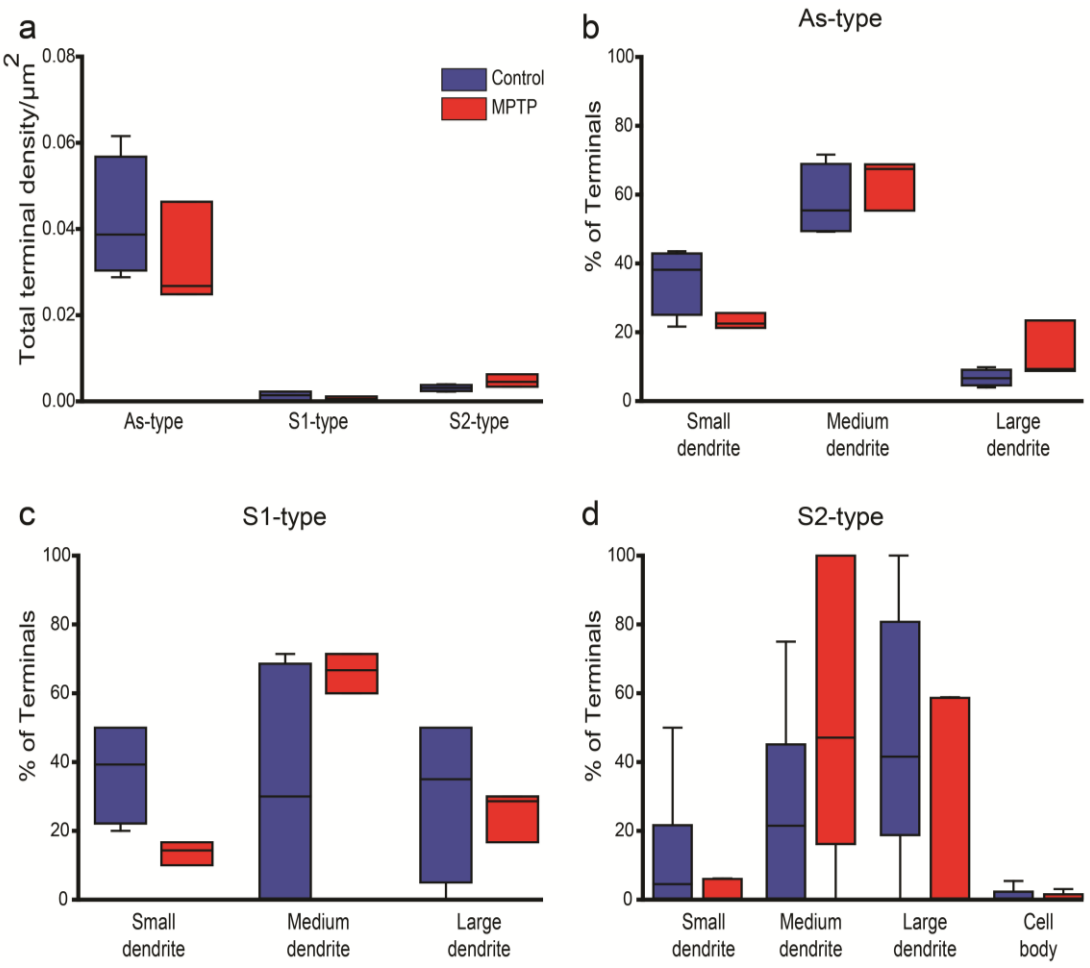

Figure 2.7. **Relative prevalence and post-synaptic targets of GABAergic and glutamatergic terminals in the CM.**

(a) Total density of each terminal sub-type in the CM of control (n = 4) and parkinsonian (n=3) monkeys. (b-d) Percentage of each terminal subtype forming synaptic contact with dendritic profiles of different sizes in control (n=4-6) and parkinsonian (n=3-5) monkeys. Lines inside boxes indicate medians, top and bottom of boxes indicate 1st and 3rd quartile respectively, and whiskers indicate minimum and maximum data points. Significant difference in As-type terminals and S2-type terminals in control conditions $p=0.019 < 0.05$, Dunn's Method One Way Analysis of Variance on Ranks.

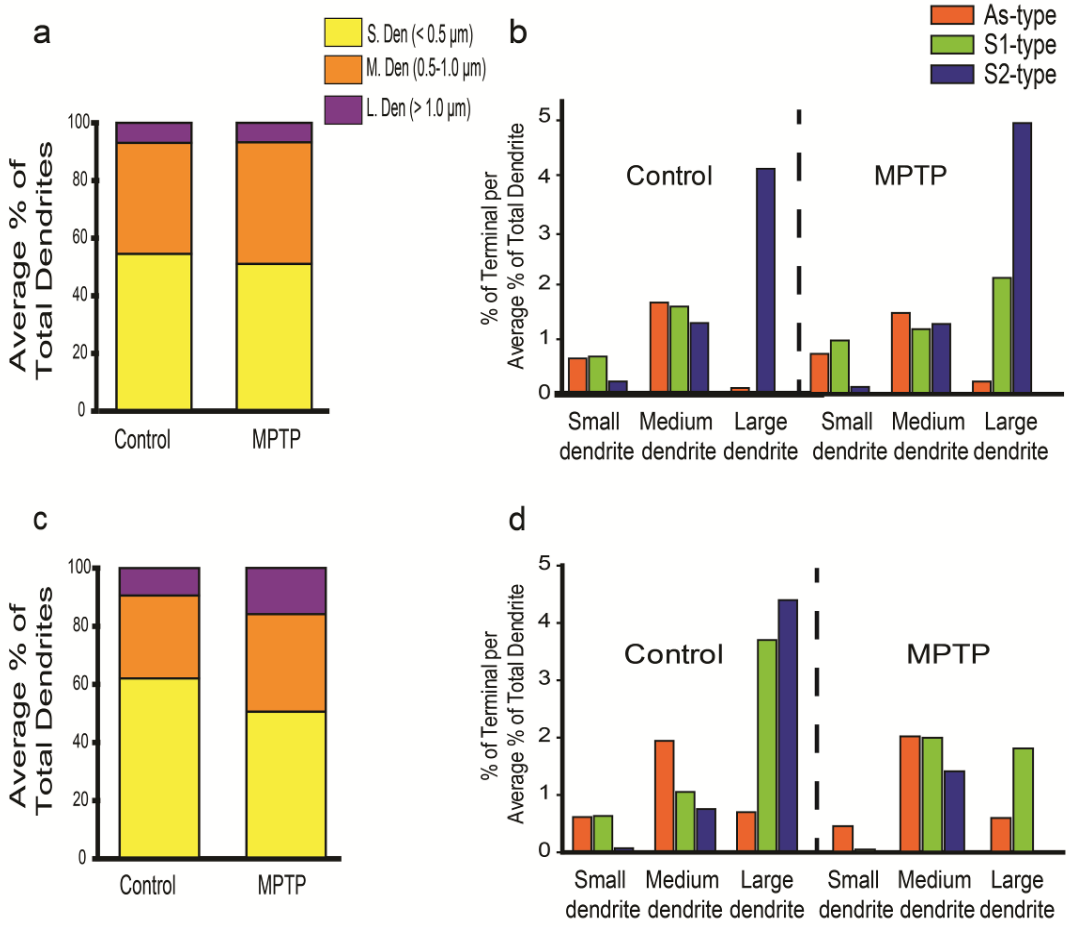

Figure 2.8. Preferential post-synaptic target of all terminal subtypes in the VApc and CM.

(a, c) Average percentages of small, medium, and large dendrites in the VApc (a) and CM (c). (b, d) Ratio between the percent of terminal subtypes in contact with dendrites of different sizes and the relative proportion of small-, medium- or large-sized dendrites in the VApc (b) and CM (d) of control and MPTP-treated monkeys.

2.3.5 Size of glutamatergic and GABAergic terminals in the VApc and CM of MPTP-treated monkeys

We measured the cross-sectional area of vGluT1-positive (i.e. As, corticothalamic) and anterogradely labeled GPi terminals (i.e. S2, pallidothalamic) in the VApc and CM of control and parkinsonian monkeys. We examined 181 (VApc: 87, CM: 94) and 257 (VApc: 179, CM: 78) vGluT1- positive terminals in 3 control and 3 parkinsonian animals, respectively. This analysis revealed a significant increase in the average cross-sectional area of individual vGluT1-positive terminals in the CM of MPTP-treated monkeys (Fig. 2.9a; VApc, $p = 0.053$; CM $p<0.001$,

student's t test). In addition, 436 (VApc: 295, CM: 141) and 300 (VApc: 244, CM: 56) anterogradely labeled GPi terminals were examined in 2 control and 2 parkinsonian animals, respectively. Although a slight increase in the cross-sectional area of pallidal GABAergic terminals was found in the CM of parkinsonian monkeys, it did not reach significance (see figure 2.10).

2.3.6 Corticothalamic and pallidothalamic synapses onto putative interneuron dendrites

We quantified the proportion of vGluT1-immunoreactive terminals and anterogradely labeled terminals from GPi in contact with interneurons in VApc and CM of controls and parkinsonian monkeys. Dendrites of interneurons were differentiated from those of thalamocortical cells by their content of synaptic vesicles (Fig. 2.11a). Examples of direct synaptic contacts between the two types of thalamic afferent terminals and interneurons are shown in Figures 2.11 and 2.12. In some instances, the pre-synaptic terminals that contacted the interneuron dendrites also formed synapses with neighboring dendrites of thalamocortical cells (Fig. 2.11a). The quantitative analysis of the synaptic connectivity of 184 vGluT1-positive and 516 GPi terminals revealed that the proportion of pallidothalamic (S2) terminals in contact with GABAergic interneurons in both thalamic nuclei of MPTP-treated parkinsonian monkeys was larger than in the control animals (Fig. 2.12d, e). There was no significance between control and parkinsonian animals in the average percentage of vGluT1-labeled terminals that came in contact with projection neurons and interneurons (Fig. 2.11: VApc: projection neurons: $p = 0.400$ and interneurons: $p = 0.400$; CM: projection neurons: $p = 0.700$ and interneurons: $p = 0.100$; Mann-Whitney Rank Sum Test).

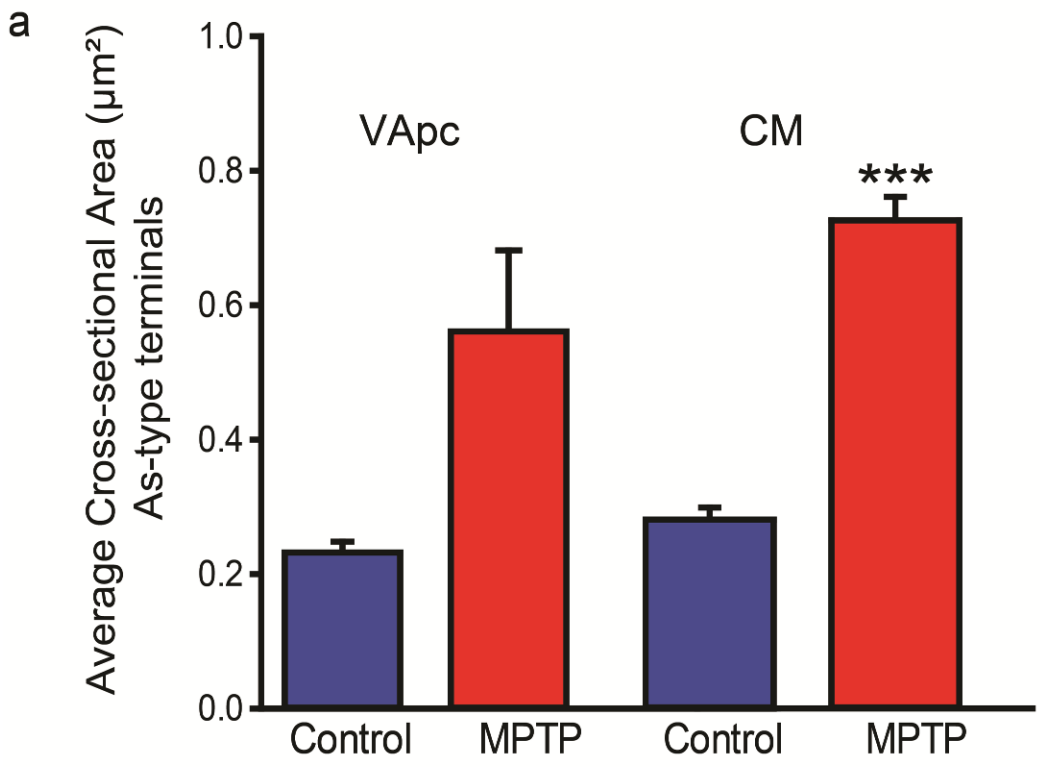

Figure 2.9. The cross sectional area of As-type terminals is enlarged in MPTP-treated monkeys.

(a) vGluT1-positive terminals were analyzed in control (N=3) and parkinsonian (N=3) monkeys in the VApc (Control, n = 87 terminals; MPTP, n = 179 terminals), with an average area of 0.232 µm² in control and 0.563 µm² in MPTP animals, and CM (Control, n = 94 terminals; MPTP, n = 78 terminals), with an average area of 0.281 µm² in control and 0.727 µm² in MPTP animals. Data are expressed as mean± SEM. (Statistical difference was found using a Student T-test in the CM, ***p<0.001).

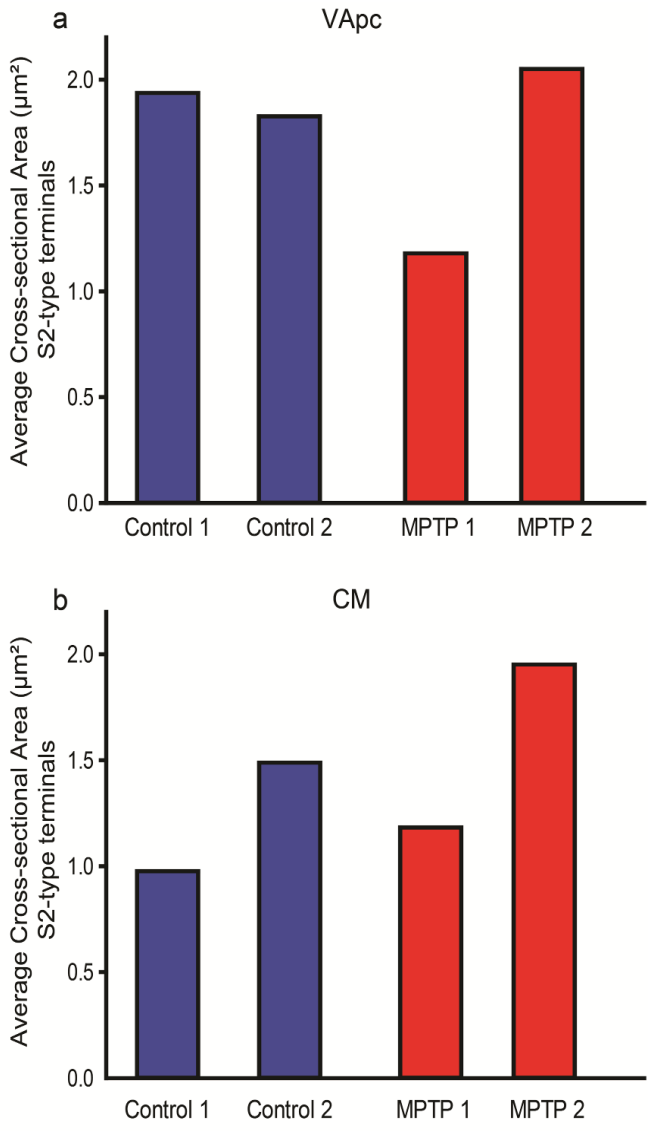

Figure 2.10. **The cross sectional area of S2-type terminals in control and MPTP-treated monkeys.**

(a) GFP-labeled terminals were analyzed in control (N=2) and parkinsonian (N=2) monkeys in the VApc (Control, n = 295 terminals; MPTP, n = 244 terminals) and CM (Control, n = 141 terminals; MPTP, n = 56 terminals).

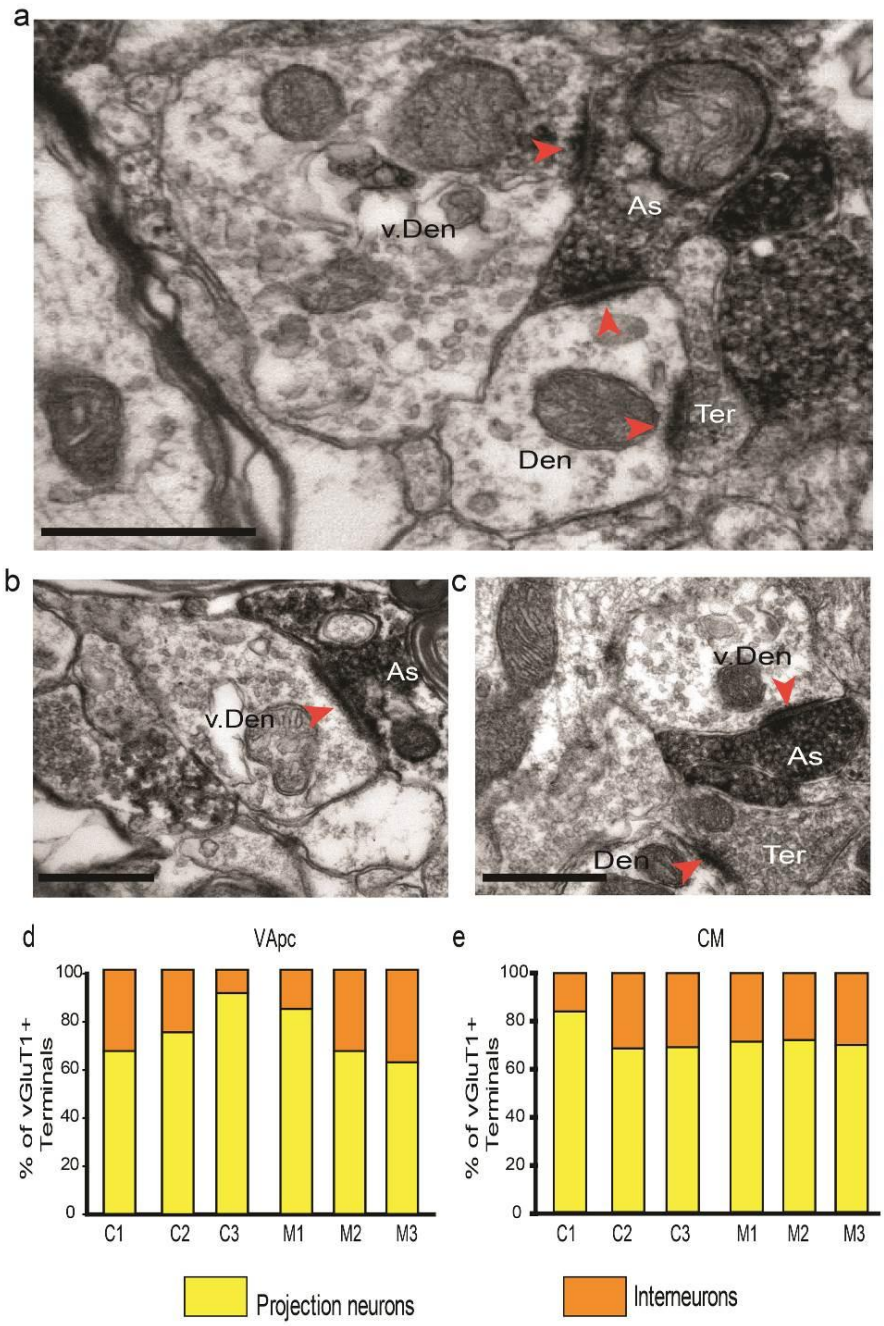

Figure 2.11. **vGluT1-Labeled As-type (putative corticothalamic) terminals form synaptic contacts with vesicle-filled putative interneuron dendrites.**

(a-c) vGluT1-Iabeled terminal (As) making synaptic contact (red arrowheads) with a vesicle-filled interneuron's dendrite (v. Den) and a projection neuron (Den) in the VApc of a MPTP-treated monkey. An unlabeled bouton in asymmetric contact with the same dendrite is also shown (Ter). (d-e) Proportion of vGluT1-Iabeled terminals in the VApc (d) and the CM (e) in contact with dendrites of projection neurons and interneurons in individual control (C1-C3) and parkinsonian (M1-M3) monkeys. *Scale bars* correspond to 500 nm.

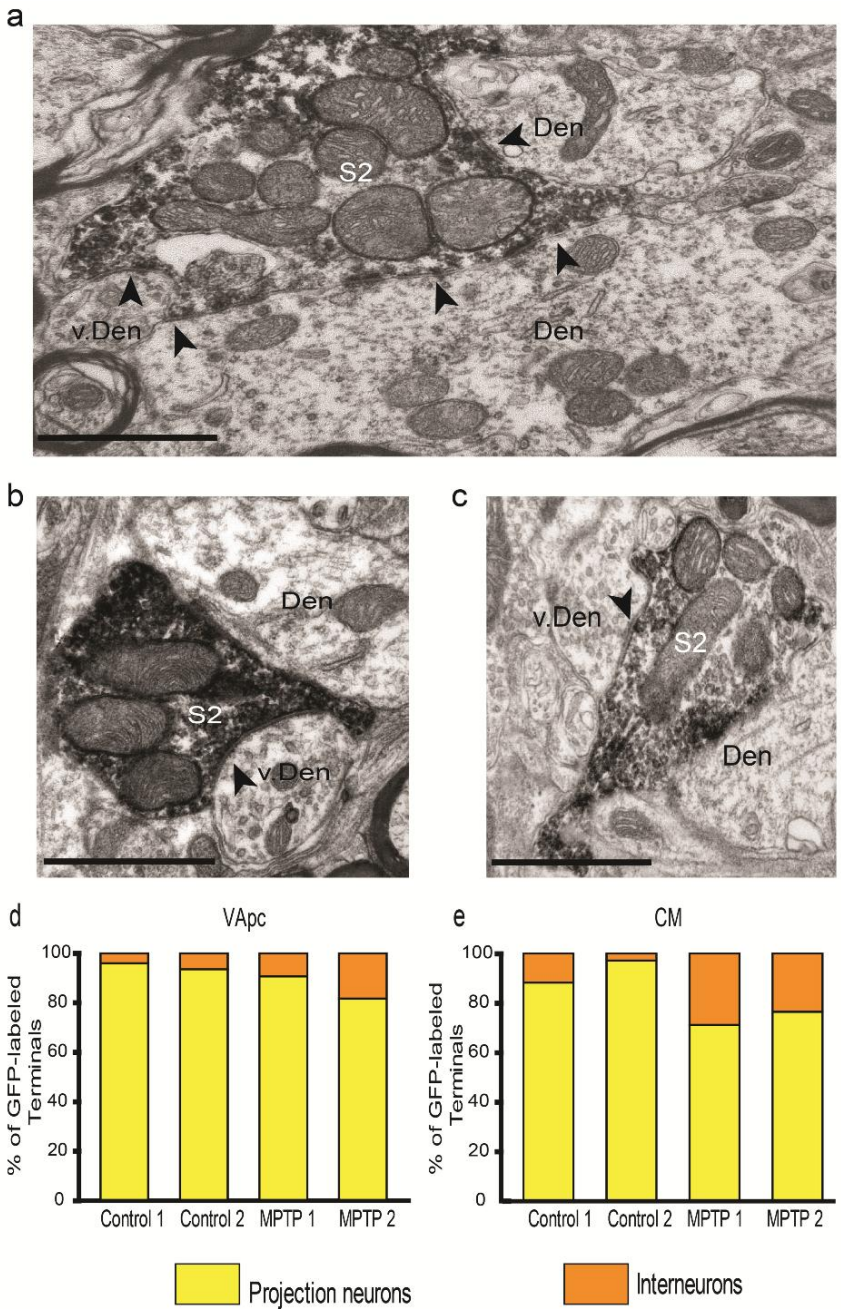

Figure 2.12. **S2-type terminals form dual synaptic contacts with dendrites of projection neurons and vesicle-filled putative interneuron dendrites.**

(a-c) GFP-Iabeled terminal (S2) making synaptic contact (black arrowheads) with a vesicle-filled interneuron's dendrite (v. Den) and a projection neuron (Den) in CM (a-b) of a normal monkey and in the VApc (c) of a MPTP-treated monkey. (d-e) Proportion of GFP-Iabeled (pallidothalamic-S2) terminals in the VApc (d) and the CM (e) in contact with dendrites of projection neurons or interneurons in control and parkinsonian monkeys. *Scale bars* correspond to 1µm.

2.4 Discussion

We compared the relative prevalence, pattern of synaptic connectivity and ultrastructural features of the main glutamatergic and GABAergic inputs to the two thalamic-recipient nuclei of basal ganglia efferents, the VApc and CM, between control and MPTP-treated parkinsonian monkeys. Three main observations were made: 1) the prevalence and overall pattern of synaptic connectivity of GABAergic terminals in VApc or CM was the same in the control and parkinsonian animals, 2) the prevalence of vGluT1-positive, putatively corticothalamic (i.e. As), terminals was significantly reduced in the VApc of parkinsonian animals and 3) the cross-sectional area of the remaining vGluT1-immunoreactive terminals in the VApc of parkinsonian monkeys was significantly increased. Our findings also suggest that a larger proportion of pallidal terminals were in contact with dendrites of GABAergic interneurons in parkinsonian monkeys than in controls. The pruning and morphological changes of corticothalamic terminals seen in parkinsonian monkeys are reminiscent of previous findings from our group and others about corticostriatal and corticosubthalamic terminals in MPTP-treated monkeys, and in 6-hydroxydopamine-treated rodents (Chu et al., 2017; Day et al., 2006; Deutch, 2006; Ingham et al., 1998; Mathai and Smith, 2011; Mathai et al., 2015; Raju et al., 2008; Villalba et al., 2009; Villalba and Smith, 2010; Villalba and Smith, 2011; Villalba et al., 2015). The increase in the prevalence of pallidal terminals in contact with thalamic GABAergic interneurons suggests a possible reorganization of thalamic GABAergic microcircuits in the parkinsonian state.

2.4.1 Synaptic Organization of VApc and CM in Control vs. Parkinsonian Monkeys

The pattern of synaptic organization of the VApc and CM in normal monkeys is consistent with previous findings in rats, cats and monkeys (Bodor et al., 2008; Grofová and Rinvik, 1974; Ilinsky et al., 1999; Jones, 2007; Kultas-Ilinsky et al., 1983; Rovó et al., 2012; Sidibe et al., 1997; Smith et al., 1987). Similarly, the categorization of thalamic terminals in VApc and CM into three main groups (As,S1,S2) based on their chemical content (GABA vs. non-GABA), pattern of

synaptic connections and ultrastructural features is also similar to previous observations (Bodor et al., 2008; Ilinsky et al., 1997; Ilinsky et al., 1999; Jones, 2007; Kultas-Ilinsky and Ilinsky, 1990; Kultas-Ilinsky et al., 1997; Sherman, 2004; Smith et al., 1987; Wanaverbecq et al., 2008). Although the exact source(s) of these terminals was not determined in the present study (except for showing that at least some S2 terminals belong to projections from GPi), data from previous tracing experiments published by our group and others suggest that most S1 terminals originate from the RTN, while the bulk of As terminals arise from the cerebral cortex (Jones, 2007; Kultas-Ilinsky et al., 1990; Smith et al., 1987). It is noteworthy that the VApc and CM receive other brainstem inputs (serotonergic, noradrenergic, dopaminergic, cholinergic) that were not considered in this study (Jones, 2007). The fact that many of these terminals do not form conventional synapses and do not display GABA or vGluT1 immunoreactivity (Jones, 2007), reduces the likelihood that they contribute substantially to the three main groups of terminals categorized in the present study.

Consistent with the previous literature (Balercia et al., 1996; Deschênes et al., 1998; Kakei et al., 2001; Kuo and Carpenter, 1973; Liu and Jones, 1999; Rouiller and Welker, 2000; Steriade, 2001; Wörgötter et al., 2002; Zhang and Jones, 2004), our data demonstrate that putative corticothalamic boutons (i.e., As terminals) are 4-6 times more abundant than GABAergic terminals from GPi and RTN in the VApc and CM. Based on their small size, general morphology and monosynaptic interactions with their postsynaptic targets, As terminals in VApc and CM are likely to be ‘modulatory’ (Bodor et al., 2008; Deschenes et al., 1994; Galvan et al., 2016a; Rovó et al., 2012; Sherman, 2005). The significantly lower density of corticothalamic terminals in the VApc (but not in the CM) in parkinsonian monkeys suggests that this system may undergo homeostatic (or maladaptive) plasticity and/or degeneration in the parkinsonian state (see below).

The general pattern of synaptic connections of As, S1 and S2 terminals with thalamocortical cells in the normal VApc and CM is consistent with previous reports. We found that corticothalamic (As) and RTN/interneuron (S1) terminals mainly target distal dendrites, while GPi terminals innervate preferentially the proximal dendrites and cell body of thalamocortical neurons (Grofová and Rinvik, 1974; Ilinsky and Kultas-Ilinsky, 1990; Jones, 2007; Kultas-Ilinsky et al., 1983; Sherman, 2004; Shink et al., 1997; Smith et al., 1987). Our findings did not reveal differences in these patterns of connectivity between control and parkinsonian animals. However, in the absence of detailed three-dimensional reconstructions, we cannot rule out the possibility of subtle changes of innervation.

The lack of differences in the prevalence and pattern of synaptic connections of GABAergic pallidothalamic synapses between the normal and parkinsonian animals does not exclude the possibility that the strength and functional properties of these synapses is affected in the parkinsonian state. Thus, the strength of the pallidothalamic system may be dynamically regulated by changes in the number, size, and proximity of synapses formed by individual pallidothalamic terminals, as previously described for other multisynaptic terminals (Bodor et al., 2008; Rovó et al., 2012; Wanaverbecq et al., 2008). Most importantly, such structural changes have also been described for pallidosubthalamic terminals in 6-OHDA-treated mice (Fan et al., 2012). Changes in the expression or the subunit composition of GABA receptors, mechanisms of GABA release and/or expression of GABA transporters must also be considered as mechanisms that may affect the pallidothalamic system in the parkinsonian state (and was not specifically examined in this study).

2.4.2 GABAergic innervation of CM in the parkinsonian state

The number of CM neurons is significantly decreased in PD patients and chronically MPTP-treated parkinsonian monkeys, compared to controls (Halliday et al., 2005; Halliday, 2009; Henderson et al., 2000a; Henderson et al., 2000b; Villalba et al., 2014). Surprisingly, despite the

loss of CM neurons, the density of GABAergic terminals targeting such neurons was the same in normal and parkinsonian monkeys. This suggests that the GABAergic GPi and RTN terminals may preferentially target sub-populations of CM neurons that do not degenerate in the parkinsonian state. Findings from Halliday and colleagues suggest that non-parvalbumin (PV)-expressing neurons are particularly vulnerable in the CM of PD patients. Future studies that compare the innervation of PV- and non-PV-containing CM neurons by GABAergic afferents in normal and parkinsonian monkeys are obviously warranted. While the prevalence and pattern of synaptic connectivity of GABAergic terminals did not differ between the MPTP-treated and control monkeys, the proportion of single GPi terminals in contact with interneurons in the CM of MPTP-treated monkeys tended to be higher than that found in controls. These findings are discussed in more detail in another section.

2.4.3 Plastic remodeling of the corticothalamic projection to VApc and CM in the parkinsonian state

Our findings demonstrate a lower prevalence of glutamatergic terminals in VApc, and a larger volume of these boutons in VApc and CM of parkinsonian monkeys, as compared to normal animals. These observations suggest that the corticothalamic system undergoes significant synaptic remodeling in the parkinsonian state.

In primates and rodents, corticothalamic glutamatergic terminals originate from pyramidal neurons in cortical layers V and VI. Although the physiological properties and morphology of these two populations of terminals have not been fully characterized in the motor thalamus, rodent data have provided strong evidence that these two groups of terminals are anatomically and functionally different in high order sensory nuclei. Corticothalamic projections from layer V pyramidal neurons are fast-conducting collaterals of long-range corticofugal axons that do not project to RTN (Jahanshahi et al., 1995; Rascol et al., 1994). In the pulvinar and medial dorsal nucleus, corticothalamic terminals of layer V neurons are relatively sparse, large, and form

multiple asymmetric synapses with proximal dendrites and cell bodies of thalamocortical neurons and GABAergic interneurons (Callaway and Wiser, 1996; Deschenes et al., 1994; Paré and Smith, 1996; Rovó et al., 2012; Sherman and Guillery, 2001; Sherman, 2005; Stepniewska et al., 2007). In contrast, corticothalamic terminals of layer VI neurons are abundant, small, and form synapses preferentially with distal dendrites of thalamic cells across the whole thalamus (Kakei et al., 2001; Rouiller and Welker, 2000; Rovó et al., 2012; Sirota et al., 2005). Electrophysiological studies have also demonstrated significant differences in the strength and functional properties of layer V and layer VI corticothalamic terminals in rodents, cats, and non-human primates (Deschenes et al., 1994; Kakei et al., 2001; Na et al., 1997; Rovó et al., 2012). Based on their high synaptic strength, layer V corticothalamic terminals are considered as potential "drivers" of high order thalamic nuclei, while layer VI terminals are seen as "modulators" of thalamic activity (Rovó et al., 2012; Sherman, 2012).

The basal ganglia-receiving nuclei of the primate motor thalamus receive inputs from layer V neurons in the primary motor cortex, the supplementary motor area, and the premotor cortex (McFarland and Haber, 2002; Rascol et al., 1992; Rouiller et al., 1998; Rouiller and Welker, 2000), but are devoid of large multisynaptic "driver-like" glutamatergic terminals (Goldberg et al., 2013; Jones, 2007; Percheron, 1997; Rovó et al., 2012). Data from our study using vGluT1 as a general marker of all corticothalamic terminals are consistent with these previous observations: none of the vGluT1-positive terminals in VApc and CM displayed the ultrastructural features of driver-like glutamatergic terminals in control and parkinsonian monkeys. Future studies using tracing and physiologic methods that allow differentiating layer V from layer VI corticothalamic projections to the VApc and CM of control and parkinsonian monkeys are needed to further examine the specific properties of these cortical inputs in the motor thalamus.

As stated above, we found that the abundance of vGluT1-containing cortical terminals in the VApc was significantly lower in parkinsonian monkeys than in untreated animals. This difference

may be due to degeneration of corticothalamic neurons in motor cortices, specific loss of corticothalamic terminals in contact with thalamocortical cells, or from the loss of thalamic neurons that receive cortical afferents. However, in contrast to the cell loss known to occur in CM, there is no neuronal loss in the VApc in parkinsonian humans and MPTP-treated monkeys (Halliday et al., 2005; Halliday, 2009; Henderson et al., 2000a; Villalba et al., 2014). The maintained abundance of vGluT1-positive terminals in the CM in MPTP-treated animals, despite the neuronal loss that occurs in this nucleus, could indicate sprouting of new terminals from the remaining cortical axons and/or may indicate that the cell loss affects a subpopulation of CM cells that are not strongly innervated by the degenerated cortical afferents. Upregulation of vGluT1 expression per terminal or an increased size of remaining vGluT1 terminals, as shown for vGluT1 terminals in the striatum may also explain some of these paradoxical findings. If the vGluT1 terminals increase in size, then there is a higher chance of these terminals being more visible through single ultrathin sections; 3D EM reconstruction can be used to sort this out.

2.4.4 Plasticity of Cortical and Pallidal Inputs to Putative GABAergic Interneurons in MPTP-treated Parkinsonian Monkeys

Up to 30% of all neurons in the primate VApc and CM are GABAergic interneurons (Ilinsky and Kultas-Ilinsky, 1990; Jones, 2007; Smith et al., 1987). In contrast, motor thalamic nuclei in rodents are practically devoid of GABAergic interneurons (Gabbott et al., 1986a; Gabbott et al., 1986b; Ohara et al., 1983). Limited data is available on the functional integration of the interneurons in the GABAergic microcircuitry of VApc and CM in primates (Ilinsky and Kultas-Ilinsky, 1990; Ilinsky et al., 1997; Ilinsky et al., 1999; Kultas-Ilinsky and Ilinsky, 1990; Kultas-Ilinsky and Ilinsky, 1991; Kultas-Ilinsky et al., 1997).

Because of the lack of a technical approach to selectively interrogate thalamic GABAergic interneurons in the primate brain, their physiologic responses and processing functions remain enigmatic. For instance, there is a tendency for the proportion of single GPi terminals in contact

with interneurons in the CM and VApc to be larger in parkinsonian monkeys than in normal animals. It is possible that the plastic reorganization of pallidal inputs to interneurons is a compensatory mechanism that counterbalances the increased inhibitory influences of GPi inputs onto thalamocortical cells. This change in synaptic organization could also alter other aspects of firing patterns in the thalamus (such as the level of synchrony between neighboring cells).

One caveat of these experiments is the fact that dendrites of GABAergic interneurons were recognized solely on the basis of the presence of synaptic vesicles. Although this ultrastructural feature is recognized as a unique characteristic of these interneurons (Jones, 2007), we cannot rule out that some of the dendritic profiles without synaptic vesicles in the present material also belong to interneurons. Thus, the proportion of interneuron dendrites in contact with As, S1, and S2 terminals reported in the present study is likely to be an underestimate.

Chapter 3 : Ultrastructural Features of Single Pallidothalamic Terminals in Control and Parkinsonian Monkeys visualized using 3D Electron Microscopic Reconstruction Approaches

Contains excerpts from:

Swain AJ, Kelley H, and Smith Y. Ultrastructural Features of Single Pallidothalamic Terminals in Control and Parkinsonian Monkeys using 3D Electron Microscopic Reconstruction Approaches. Brain Structure Function (In preparation).

3.1 Introduction

In the primate thalamus, the VApc is one of the main thalamic targets of inhibitory (GABAergic) inputs from the GPi, the primary motor output nucleus of the basal ganglia (Parent et al., 1983; Parent et al., 2001; Parent and Parent, 2004). In traditional models of the pathophysiology of Parkinson's disease, loss of nigrostriatal dopamine increases the activity of the inhibitory basal ganglia output projections to the ventral motor thalamus, which, in turn, results in reduced activity of thalamocortical projections (Albin et al., 1989; DeLong, 1990). Despite conflicting evidence, some recent studies have directly identified altered activity (including firing rate changes, bursting, and oscillatory firing properties) of thalamic cells in VApc and CM in animal models of PD and in PD patients (Aymerich et al., 2006; Bosch-Bouju et al., 2014; Chen et al., 2010; Guehl et al., 2003; Hirsch et al., 2000; Kammermeier et al., 2016; Kaneoke and Vitek, 1995; Lanciego et al., 2009; Magnin et al., 2000; Mitchell et al., 1989; Molnar et al., 2005; Ni et al., 2000; Orieux et al., 2000; Pessiglione et al., 2005; Raeva et al., 1999; Rolland et al., 2007; Sarnthein and Jeanmonod, 2007; Schneider and Rothblat, 1996; Vitek et al., 1994; Zirh et al., 1998).

In the basal ganglia, the altered neuronal activity in the parkinsonian state is associated with characteristic morphologic and ultrastructural changes. Thus, in the striatum and subthalamic nucleus, the dopamine-depleted state is accompanied by substantial remodeling of specific synaptic microcircuits. In particular, significant changes in the number and ultrastructural features of cortical terminals, associated with robust alterations in electrophysiological and plastic properties of corticostriatal and corticosubthalamic synapses have been reported in rodent and primate models of PD (Chu et al., 2017; Day et al., 2006; Deutch, 2006; Ingham et al., 1998; Mathai and Smith, 2011; Mathai et al., 2015; Raju et al., 2008; Smith et al., 2014b; Villalba et al., 2009; Villalba and Smith, 2010; Villalba and Smith, 2011; Villalba et al., 2015). In the STN of dopamine-depleted mice, there is a significant increase in the number of synapses formed by

individual GPe GABAergic terminals accompanied with increased synaptic strength of pallidosubthalamic synapses (Chu et al., 2017; Fan et al., 2012).

The possibility of structural alterations in the glutamatergic and GABAergic thalamic microcircuits that regulate thalamocortical outflow in the parkinsonian state has not been examined. Data from the previous chapter did not reveal major changes in the prevalence and overall pattern of synaptic connections of GPi terminals in the VApc of parkinsonian monkeys. However, this study did not examine whether GPi terminals undergo morphological changes (i.e. changes in volume, number and size of synapses etc.) in parkinsonian animals. The GPi is known to give rise to GABAergic terminals in the thalamus that displays a multi-synaptic morphology. This multi-synaptic morphology is also common to GABAergic synapses of GPe terminals in the STN (Fan et al., 2012; Ilinsky et al., 1997; Kultas-Ilinsky et al., 1983). Multi-synaptic arrangements have also been documented for SNr GABAergic terminals in the rat thalamus (Bodor et al., 2008). This synaptic pattern creates favorable conditions for inter-synaptic spillover of GABA among the multiple synapses of single terminals, which may enable tonic inhibition even under conditions of high presynaptic firing rates (Bodor et al., 2008; DiGregorio et al., 2002; Wanaverbecq et al., 2008). Although the plasticity of GABAergic GPi synapses in the thalamus has not been examined, studies in rodent models of PD have suggested that GABAergic synapses from the globus pallidus (GPe in primates) onto STN neurons display structural plasticity in the number of synapses that may contribute to parkinsonism-related changes in GABAergic inhibition of the STN (Fan et al., 2012). An understanding of the plasticity of the morphological features of pallidothalamic terminals, such as number of synapses, size of synapses and volume of pallidal terminals, will aid in understanding the impact of altered GPi outflow onto thalamocortical neurons in parkinsonism.

Here, high resolution 3D electron microscopic (EM) reconstructions is used to examine the morphology of individual GPi terminals, and determine whether there is a change in the overall

number and size of pallidal GABAergic synapses formed by single GPi boutons in the VApc of parkinsonian monkeys.

3.2 Materials and methods

3.2.1 Animals

Two adult rhesus monkeys, MR271 and MR240 (animal details are listed in table 1) were used in this study. The monkeys were raised in the breeding colony of the Yerkes National Primate Research Center. The animal's diet, housing, euthanasia and fixation procedures were conducted as described in section 2.2.1. All animal procedures were approved by the Institutional Animal Care and Use Committee (IACUC) of Emory University, and were performed according to the Guide for the Care and Use of Laboratory Animals and the U.S. Public Health Service Policy on the Humane Care and Use of Laboratory Animals.

3.2.2 MPTP treatment and assessment

One animal, MR 240, was rendered parkinsonian following chronic administration of MPTP as described in section 2.2.2. This animal was gradually rendered mildly parkinsonian by repeated exposure to MPTP, following a protocol that we have used in many previous studies (Bogenpohl et al., 2013; Devergnas et al., 2016; Galvan et al., 2014a; Hadipour-Niktarash et al., 2012; Masilamoni et al., 2010; Masilamoni et al., 2011; Masilamoni and Smith, 2017; Mathai et al., 2015; Villalba et al., 2014). The degree of parkinsonism of this monkey was done the same way as described in section 2.2.2. The extent of MPTP-induced nigrostriatal denervation was assessed from post-mortem tissue using TH immunocytochemistry (see Fig. 2.1 and methods from previous papers) (Bogenpohl et al., 2013; Devergnas et al., 2016; Galvan et al., 2014a; Hadipour-Niktarash et al., 2012; Masilamoni et al., 2010; Masilamoni et al., 2011; Masilamoni and Smith, 2017; Mathai et al., 2015).

3.2.3 Anterograde labeling of pallidothalamic terminals

Animals received injections in the GPi of AAV5-hSyn-ChR2-EYFP to help identify pallidothalamic terminals in VApc. Labeled pallidothalamic terminals from these injections and unlabeled putative GPi terminals forming multiple symmetric synapses, were used for 3D EM reconstruction. Animals that received an anterograde viral vector in the GPi were used in the previous experiments in Chapter 2. The injection of this viral vector is described in detail in section 2.2.3.

3.2.4 Immunohistochemistry

3.2.4.1 GFP immunoperoxidase labeling

The immunoperoxidase labeling method using a Green Fluorescent Protein (GFP) antibody, which identifies pallidothalamic terminals that were labeled anterogradely with the viral vector, is described in detail in section 2.2.4.4.

3.2.5 Ultrathin serial sectioning electron microscopy analysis and 3D reconstruction

Coronal sections in the VApc from the two monkeys described above underwent immunostaining for GFP. Sections were processed for electron microscopy (stopping at DAB revelation) as described in section 2.2.4.1. Sections that had the maximum amount of GFP immunostaining were packaged into a vial that contained a phosphate buffer solution and sent to Renovo Inc (Cleveland, OH, USA) for further EM processing (osmium fixation, dehydration and resin embedding) (similar to what was described in section 2.2.5.1). After embedding, small regions of interest in the VApc that contained large amount of GFP-labeled GPi terminals were taken out from slides and used for 3D reconstruction utilizing a serial block-face scanning electron microscopy (SBF/SEM) method. SBF/SEM is used to generate large volumes of high resolution images from small samples that can be used to create 3D models. With SEM, a scanning electron microscope is used to scan serial images of single block of tissue that is placed on an ultramicrotome. Similar to transmission electron microscopy (TEM), the tissue undergoes a

similar EM processing. Once the tissue section is placed on the ultramicrotome, black-scattered electrons are used to help detect the tissue that has been embedded in resin. After the images are collected, the ultramicrotome cuts thin sections from the face of the block to remove the scanned section and then raise the tissue sample back to the focal plane and continue to image the sample. The SBF/SEM approach has the ability to sample thousands of images by using scanning and cutting the tissue with this automatic process. The expertise of Renovo Neural Inc. in SBF/SEM is well established (Chung et al., 2013; Duan et al., 2014; Hammer et al., 2014; Nordstrom et al., 2015; Traka et al., 2013; and Deerinck et al., 2010). The thickness of serial sections generated through this process was 70 nm. Approximately 200-400 serially scanned micrographic images were collected from each region of interest. From these images, GPi terminals (labeled and unlabeled) were fully reconstructed using the 3D software application, *Reconstruct* (available at: synapses.clm.utexas.edu).

In brief, TIFF images of single sections acquired from Renovo were imported into *Reconstruct*, calibrated and aligned (aligning was done while ensuring that they were not distorted). The section thickness and pixel size were calibrated to measurements produced by Renovo for the respective image. Finally, the individual contours for the different analyzed objects (immunoreactive and non-immunoreactive terminal, synapse, and dendrite) were manually traced in each serial electron micrograph by using the *Reconstruct* software. The program calculated the dimensions of each object and generated a 3D representation based on the serial slice information.

In order to avoid bias in the selection of elements being reconstructed, the electron microscopic observer was blinded to the treatment (control versus MPTP-treated) and the GFP antibody described in 2.2.4.4 used in the tissue under analysis. Using this approach, the size (area) of these synapses, the volume of the dendrite (Den), and the volume of pallidothalamic terminals were randomly recorded in control and MPTP-treated animals. The *Reconstruct* software calculated the

flat surface area of a synapse to provide the area of the synapse in a two dimensional plane. The flat area is useful for objects that are known to be flat but may sometimes appear in the plane of section as well as perpendicular to it, as the case for synapses. On the other hand, the surface area is equal to the product of the trace length and the section thickness. Only cases in which the terminals were completely recovered through serial sections were 3D-reconstructed.

3.2.6 Analysis of material

GFP-immunostained VApc sections from normal and MPTP-treated monkeys were used for 3D reconstruction. Ten GPi terminals (labeled anterogradely or with ultrastructural features of S2 terminals described in Chapter 2) were randomly selected in one MPTP-treated and one control monkey. Each terminal and their postsynaptic targets were reconstructed with a 3D EM approach, through the use of serial ultrathin sections and the NIH software *Reconstruct* as described in the above section and previous studies from our laboratory (Villalba and Smith, 2010; Villalba and Smith, 2011; Villalba and Smith, 2013). Dendrites from projection neurons were separated from dendrites of interneurons based on the absence or presence of synaptic vesicles, respectively (Jones, 2007). From these reconstructed terminals, we measured their volume, counted the number of symmetric synapses and measured the flat and surface area of synapses, three structural features that are closely related to synaptic strength, transmitter release and metabolic activity of terminal boutons. The volume of the terminal, the cross-sectional diameter of the postsynaptic dendrite and the surface area of the symmetric synapses were automatically measured with the *Reconstruct* software.

Dendritic diameter

Three random sections from reconstructed dendrites in synaptic contact with a GPi terminal were chosen to estimate the cross-sectional diameter of the post-synaptic targets of GPi terminals. Dendrites were considered to be of the medium-size if the diameter of the dendrite was 0.5 µm – 1.0 µm and a large dendrite if it was greater than 1.0 µm (as described in Chapter 2).

3.3 Results

The extent of striatal dopamine depletion and nigral cell loss in the MPTP-treated animal used in this study is described in section 2.2.5.1 (Fig. 2.1). The whole extent of the caudate nucleus and putamen was almost completely devoid of tyrosine hydroxylase (TH) immunostaining. At the midbrain level, the ventral tier of the substantia nigra pars compacta (SNc) was severely damaged, whereas a significant number of TH-immunoreactive neurons and processes remained in the ventral tegmental area and dorsal tier SNc as seen in previous studies (Villalba et al., 2009).

3.3.1 General ultrastructural characteristics of pallidothalamic terminals in a control and a MPTP-treated monkey

The ultrastructural features of GPi terminals were investigated to determine structural differences amongst the terminal volume, synapse flat area, and synapse surface area in normal and MPTP-treated monkeys. A total of 20 GPi terminals that were GFP-labeled and unlabeled, their corresponding postsynaptic targets and their synapses were 3D-reconstructed in a control (n=10) (Fig. 3.1a-c) and MPTP-treated monkey (n=10) (Fig. 3.2 a-c). Occasionally, multiple GPi terminals formed synaptic contact with a single dendrite (Fig. 3.2a). The GPi terminal volume, the area of the synapse, and the average number of synapses/GPi terminal in one control and one MPTP-treated animal were measured and averaged from each monkey.

In the control monkey (Fig. 3.3a) the median volume of GPi boutons was 10.4 μm^3 (mean, 10.8 μm^3, interquartile range, 16.4 μm^3; n = 10). In the MPTP-treated monkey, the median volume was

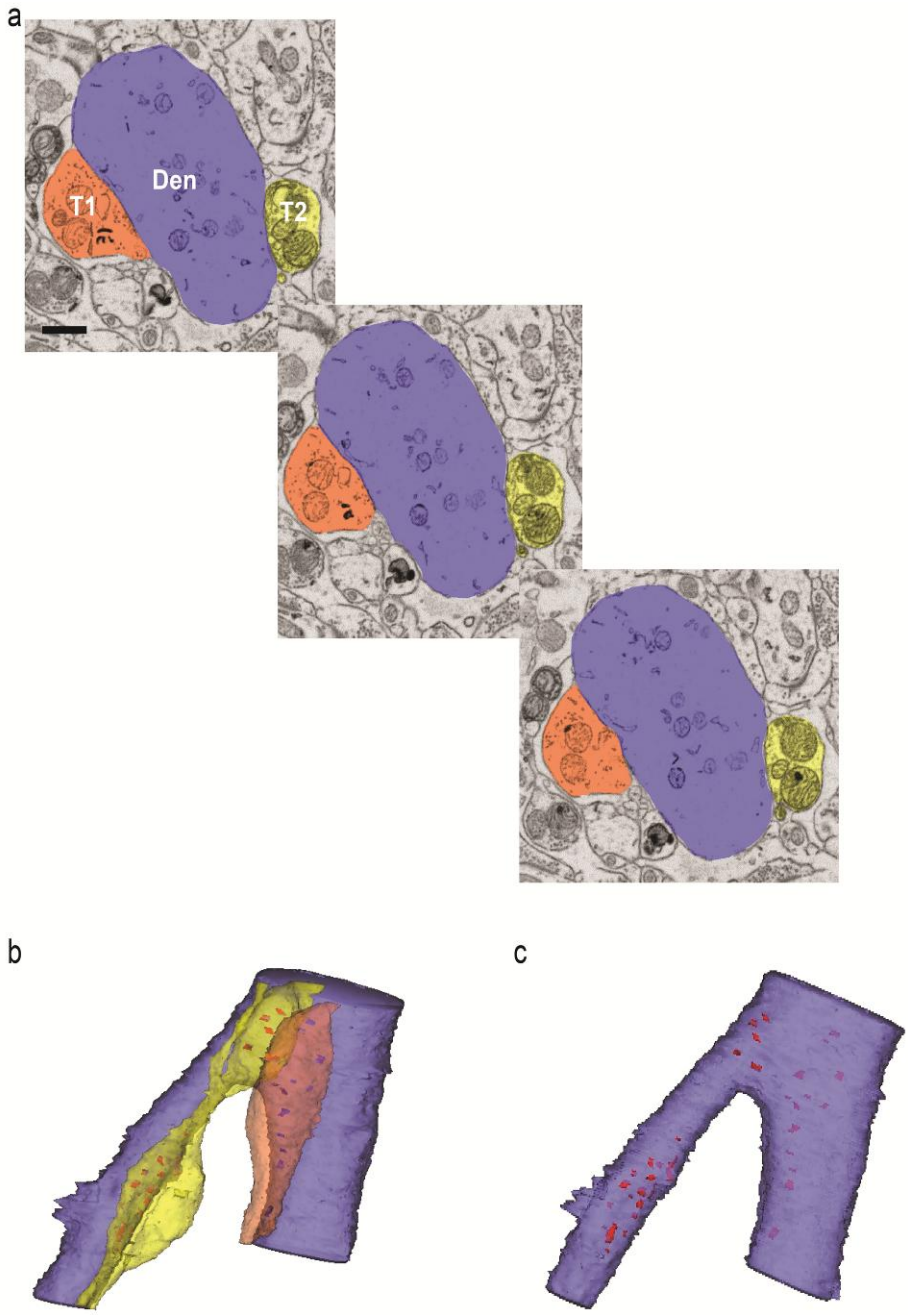

Figure 3.1. **Pallidothalamic terminals forming multiple synapses with a large dendrite in a control animal.**

(a) Serial electron micrographs of 2 GPi-like terminals (T1-organge, T2-yellow) in contact with a large dendrite (Den-purple) in the VApc of the control monkey. T2 displays GFP immunoreactivity indicating that it was anterogradely labeled by the AAV injection in the GPi. (b) 3D reconstructed images of T1, T2, the postsynaptic Den, and the symmetric synapses formed by the two terminals (red shapes). In (c), only the symmetric axo-dendritic synapses (red shapes) formed by T1 and T2 are shown. *Scale bar* = 2 μm in a.

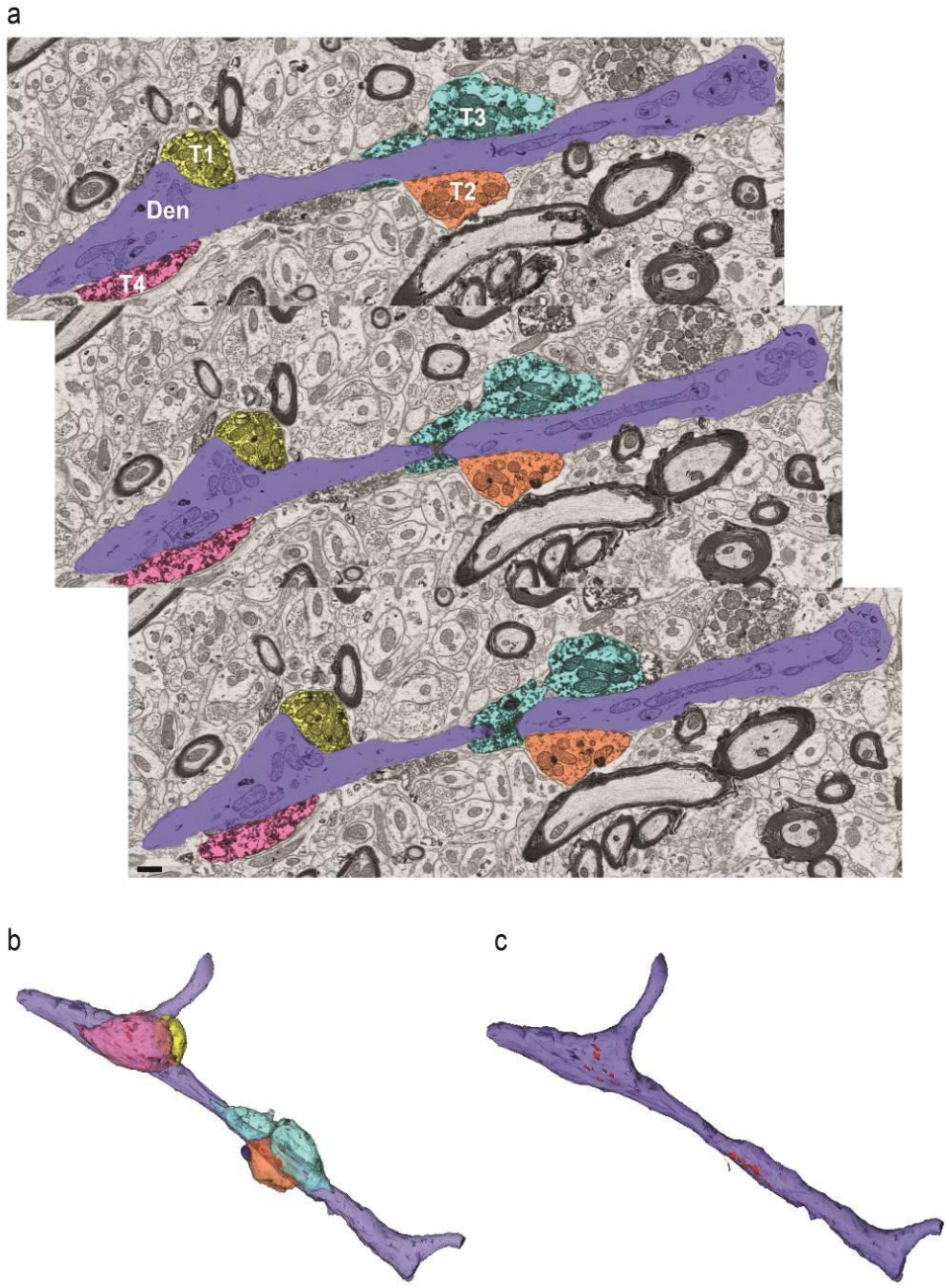

Figure 3.2. **Pallidothalamic terminals in contact with a large dendrite in a MPTP-treated animal.**

(a) Serial electron micrographs of four GFP immunostained GPi terminals (T1, T2, T3, and T4) in contact simultaneously with a large dendrite (Den) in the VApc. (b-c) 3D reconstruction of the four immunoreactive terminals (T1, T2, T3, T4) and their postsynaptic target dendrite (Den) and multiple symmetric synapses in a partially transparent image to allow visualization of the postsynaptic density's shown in a. Multiple synapses (shown in red) are formed by T1, T2, T3, and T4 onto the same large dendrite in (b). The image in c shows the morphology of the postsynaptic density's the dendrite receives from T1, T2, T3, and T4. In c all terminals have been removed from the image to better illustrate the SYNAPSE. *Scale bar in bottom panel of a* = 2 μm.

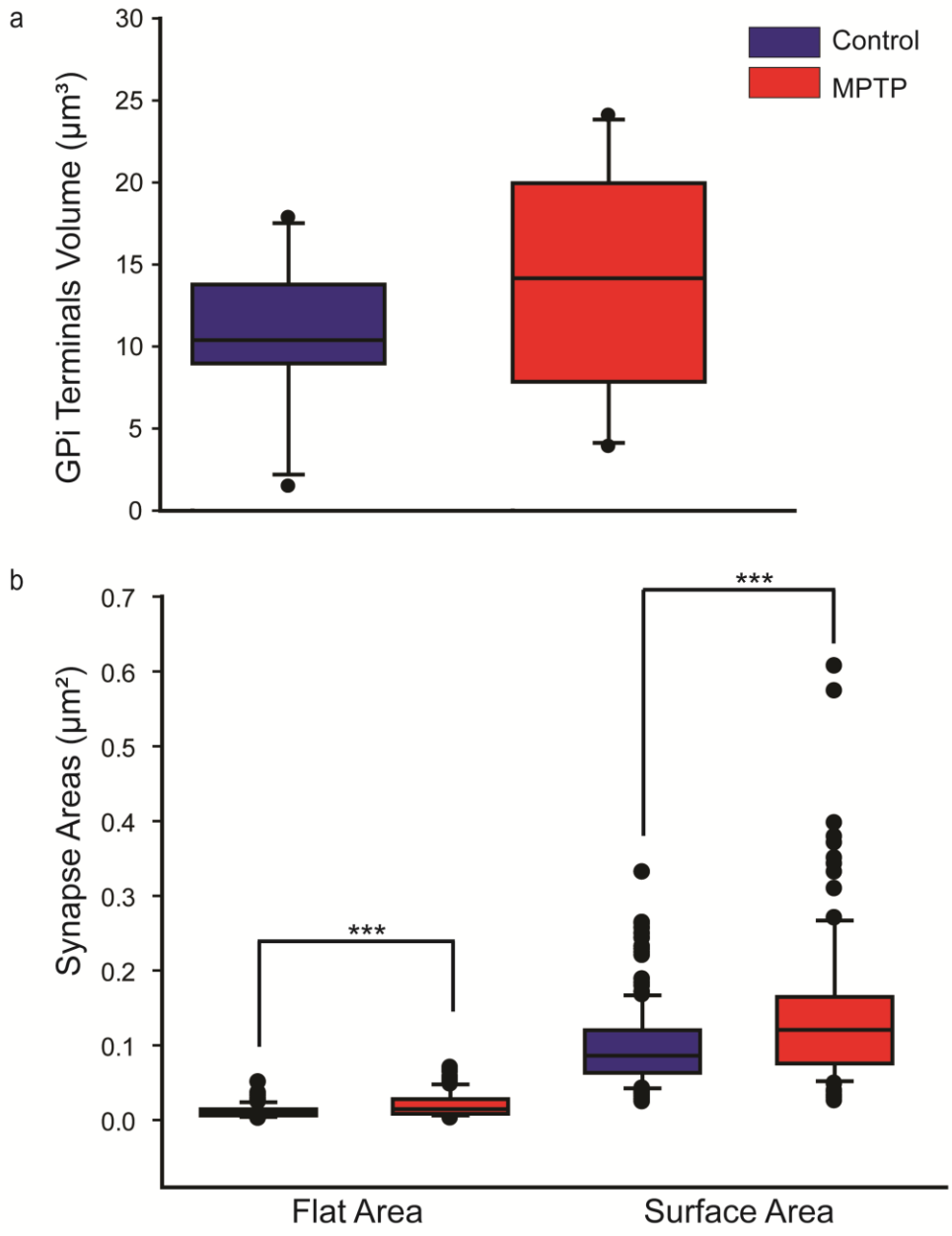

Figure 3.3. **Ultrastructural features of pallidothalamic terminals in control and MPTP-treated monkeys.**

(a-b) Box-whisker plot comparing the morphometric measurements (GPi terminal volume, synapse flat area, and synapse surface area) of structural elements at pallidothalamic GABAergic synapses using the 3D reconstruction method of serial ultrathin sections collected from 10 GPi terminals in each group from one control and one MPTP-treated animal. The units used for these measurements are indicated in the Y axis within parentheses. (b) In an MPTP monkey (n = 102 synapses) the synapse areas are significantly larger than the control (n = 166 synapse) (***, $P < 0.001$, student's t-test, for synapse flat area and synapse surface area).

14.2 μm³ (mean, 13.9 μm³; interquartile range, 20.2 μm³; n = 10). The volume of GPi terminals was increased in the MPTP-treated monkey. The flat area and surface area of synapses of GPi terminals in MPTP-treated monkeys were increased (Fig. 3.3b). This quantitative analysis of 3D-reconstructed pallidothalamic terminals suggested that: 1) the volume of GPi terminals may be larger in MPTP-treated monkeys and 2) the synapse areas of pallidothalamic terminals were larger in MPTP-treated monkeys (Fig. 3.3 b). Future analysis will include more animals in both groups.

The cross sectional diameters of dendritic profiles contacted by GPi terminals in control and MPTP-treated monkeys were tabulated. Consistent with data presented in Chapter 2, they were of the medium- and large-sized category (Table 3.1).

3.3.2 Number of Synapses per GPi Terminals in Control and Parkinsonian Monkeys

A total of 166 and 102 synapses were counted from the 10 fully reconstructed GPi terminals in the VApc of the control and the MPTP-treated monkey, respectively. The average number of synapses/GPi terminal was lower in the MPTP-treated monkey than in the control animal (Fig. 3.4a; Control: mean, 10.6; median, 14; interquartile range, 30; min–max, 5-35; n = 10; MPTP: mean, 10.3; median, 11; interquartile range, 15; min–max, 3-18; n = 10). The majority of synapses of single GPi terminals (Control: 9/10 terminals and MPTP: 7/10 terminals) converged on the same postsynaptic profile.

The number of synapses per GPi terminal might possible be correlated with GPi terminal volumes in control (R = 0.683; n = 10; P = 0.029; Fig. 3.4b) and MPTP-treated animals (R = 0.545; n = 10; P = 0.104; Fig. 3.4c). Weaker correlations were found between the average synapse surface areas and GPi terminal volumes in the control (R = 0.176; n = 10; Fig. 3.4d) and parkinsonian condition (R = 0.228; n = 10; Fig. 3.4e).

Table 3. 1 Post-synaptic target distribution of GPi terminals in a control and MPTP-treated monkey

		Average dendrite diameter (µm)	Dendrite category Small, Medium, or Large
Control	Dendrite T1	1.0	Medium Dendrite
	Dendrite T2	1.99	Large Dendrite
	Dendrite.T3	1.22	Large Dendrite
	Dendrite T4	0.68	Medium Dendrite
	Dendrite T5	1.36	Large Dendrite
	Dendrite T6	2.10	Large Dendrite
	Dendrite T7	2.70	Large Dendrite
	Dendrite T8	2.98	Large Dendrite
	Dendrite T9	0.98	Medium Dendrite
	Dendrite T9	0.94	Medium Dendrite
	Dendrite T10	1.71	Large Dendrite
MPTP	Dendrite T1-T4	1.69	Large Dendrite
	Dendrite2 T2	1.37	Large Dendrite
	Dendrite T5	1.04	Large Dendrite
	Dendrite2 T5	2.10	Large Dendrite
	Dendrite T6	1.30	Large Dendrite
	Dendrite T7	1.21	Large Dendrite
	Dendrite2 T7	0.64	Medium Dendrite
	Dendrite T8	1.22	Large Dendrite
	Dendrite T9	1.73	Large Dendrite
	Dendrite T10	0.83	Medium Dendrite

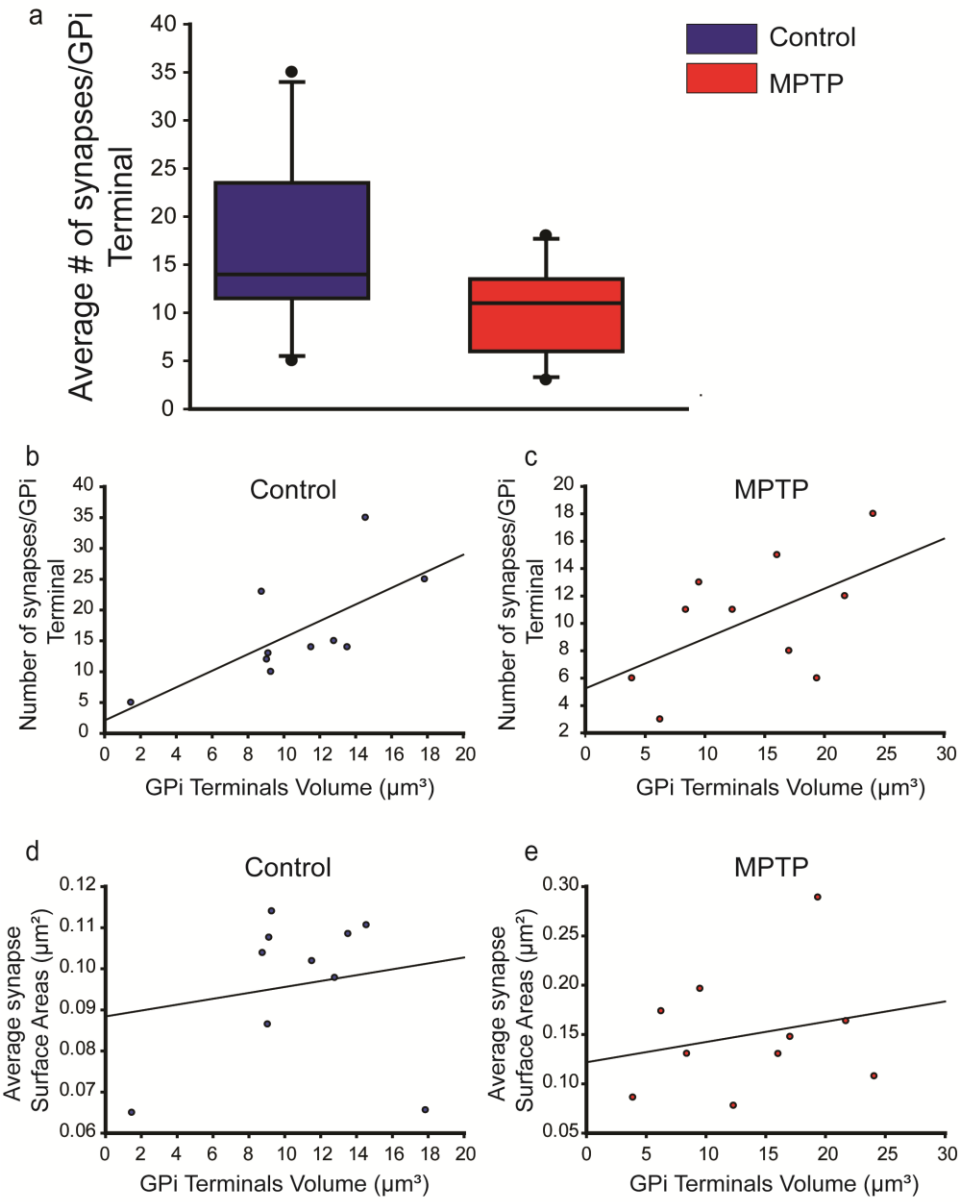

Figure 3.4. **Synapse analysis via scatter diagrams showing the correlation between GPi terminal volume (µm³) and the surface (µm²) of synapses at pallidothalamic GABAergic terminals in the VApc of one normal and one MPTP-treated animal.**

(a) Box-whisker plot comparing the average number of synapses per GPi terminal using the 3D reconstruction method of serial ultrathin sections collected from 10 GPi terminals in each group from one control and one MPTP-treated animal. (b-c) Correlation of the number of synapses per GPi terminal and GPi terminal volume in the VApc in one control (b) and one MPTP-treated animal (c) The number of synapses/GPi terminal was positively correlated with the GPi terminal volume (a; coefficient of correlation, R = 0.683) and MPTP-treated animals (b; R = 0.545). (d-e) Average synapse surface area plotted as a function of GPi terminal volume in the VApc in control (d) and parkinsonian monkeys (e). A slight correlation was found in the MPTP case (d; R = 0.176 and e; R = 0.228).

3.4 Discussion

These preliminary data suggest three major ultrastructural features related to the morphology and plasticity of pallidothalamic terminals in the primate motor thalamus, specifically the VApc, which may underlie functional differences in the pallidothalamic system between normal and parkinsonian monkeys: 1) the volume of the pallidothalamic terminals is enlarged in the MPTP monkey, 2) the average number of synapses per GPi terminal is decreased in the MPTP monkey, and 3) the flat and surface areas of synapses formed by GPi terminals are increased in the MPTP-treated monkey. Our preliminary data also suggest that the number of synapses per GPi terminal is positively correlated with the volume of pallidothalamic boutons. Altogether, these preliminary data suggest that the pallidothalamic terminals undergo significant structural changes in the parkinsonian state. These data illustrate the complex level of synaptic plasticity that governs thalamic GABAergic transmission under normal and parkinsonian conditions.

3.4.1 3D reconstruction utilizing SBF/SEM

To my knowledge, this is the first 3D reconstruction of pallidothalamic terminals in the VApc in control and parkinsonian monkeys. Because of the size of the terminals and the arrangement of the active zones, the use of single sections transmission electron microscopy (TEM) analysis becomes of little use to characterize the morphology of these elements. Unlike TEM, SBF/SEM provides the ability to collect large amounts of tissue and a minute thickness (30-70nm). Since pallidal terminals are large in size, a series of at least 100 serial images are necessary to fully reconstruct these terminals in primates. Because the SBF/SEM allows the acquisition of large amounts of data from specific regions of interest, this cutting edge methodology allows complete reconstruction of complex synaptic circuits and connectivity in the primate brain. One of the main goals of the present study was to assess the level of plasticity GPi terminals in the VApc undergo in the parkinsonian condition using the SBF/SEM method.

3.4.2 Anatomical and functional characteristics of pallidothalamic system

The preliminary findings of the present study suggest that GPi GABAergic pallidothalamic terminals undergo morphological changes in volume and in the number and size of synapses in the parkinsonian state.

Serial electron microscopic reconstruction demonstrated that all GPi terminals innervate their postsynaptic partner via multiple synapses (on average, approximately ten per terminal). These morphological data are in agreement with previous observations of single and 3D electron microscopic material (Bodor et al., 2008; Bokor et al., 2005; Fan et al., 2012; Ilinsky and Kultas-Ilinsky, 1990; Ilinsky et al., 1997; Kultas-Ilinsky and Ilinsky, 1990; Wanaverbecq et al., 2008). The size of the terminals and the arrangement of the multiple synapses formed by GPi terminals can influence synaptic release of transmitter, synaptic strength, neurotransmitter uptake and spillover amongst synapses (Bodor et al., 2008). The synapses formed by single GPi terminals tend to be closely spaced, similar to SNr terminals, and therefore creates a favorable condition for transmitter spillover (Bodor et al., 2008). Spillover among synapses results in larger charge transfer because of the slower decay of the synaptic currents and reduces the variability of the synaptic transmission (DiGregorio et al., 2002). The synapses of the mossy fiber-granule cell contact in the cerebellar cortex are known to become more separated during development (Cathala et al., 2005). In the glutamatergic system, this development of increased intersynaptic distance paired with a reduced likelihood that the neighboring postsynaptic densities are on the same granule cell favor a reduced spillover component of the EPSCs (Cathala et al., 2005), indicating that the exact spatial arrangement of the synapses formed by single terminals have strong influence on the extent of transmitter spillover. Data from the same synapses indicate that intersynaptic cross-talk between synapses of single boutons through spillover of GABA is able to maintain faithful synaptic transmission at high-frequency firing rates (Telgkamp et al., 2004), when vesicle fusion exceeds the rate of replenishment (Zucker and Regehr, 2002). A similar

consideration may apply to the multisite GPi terminals as well. Future studies should determine the average intersynaptic distance of GPi terminals and the effect it might have on neurotransmitter spillover using whole-cell recordings or patch-clamp.

The presence of multiple synapses on a terminal also allows for cross talk amongst synapses. There is thought to believe that communication across synapses can limit vesicle depletion at the GABAergic synapses in the cerebellum. This limitation of vesicles at the synapse has been shown to happen during prolonged high-frequency simulation (Telgkamp et al., 2004). It is possible that this effect is mediated by multisite terminals. The Purkinje cells in the cerebellum displayed a mean number of synapses (9.2), which was similar to previous studies shown in the rat and monkey SNR terminals (8.5) (Bodor et al., 2008). In this study, the multisite pallidothalamic terminals in the monkey have a similar mean, 16.6 in control and 10.3 in MPTP-treated animals.

Postsynaptic responses rely on the type of presynaptic terminals and the number and arrangement of synapses (Cathala et al., 2005). Combined anatomical and physiological data demonstrated that large, presumably multisite GABAergic terminals are present in the thalamus and exert strong inhibitory influence on their targets (Barthó et al., 2002; Bokor et al., 2005; Lavallée et al., 2005). Therefore, plasticity in the number of synapses can influence their postsynaptic target via other parameters such as GABA reuptake, GABA release, and GABA receptors, all of which weren't discussed here. Future studies that directly assess the number of GABA receptors at pallidothalamic synapses, and determine changes in the electrophysiological properties of pallidothalamic pathways under normal and parkinsonian conditions, are warranted to test this hypothesis. Similar to previous experiments in the RTN and the pretectal nucleus in rats that have looked at GABAergic inputs, other parameters that require in vitro electrophysiological techniques could investigate the number of release sites, probability of release, and quantal content of morphologically altered GPi terminals in the VApc of parkinsonian animals (Wanaverbecq et al., 2008).

3.4.3 Changes in number and size of GABAergic pallidothalamic synapses in parkinsonian monkeys

Data from previous studies that involved electron microscopy from single section studies and 3D EM indicated that thalamic activity is dependent on various input structures and that these input structures may differ in multiple morphometric features such as; the number of synapses a single terminal establishes on its postsynaptic partner (Bodor et al., 2008; Sakai et al., 1998; Wanaverbecq et al., 2008). It is therefore quite likely that other ultrastructural features such as the synaptic arrangement of thalamic afferents, intersynaptic distance, and length of individual synapses might influence active zone functionality. This in turn could aid in understanding the physiological roles of the GABAergic inputs from the pallidum to the thalamus. In line with rodent and primate data suggesting morphological changes of symmetric synapses in the thalamus (Barthó et al., 2002; Bodor et al., 2008; Wanaverbecq et al., 2008), our ultrastructural data demonstrate that the size of synaptic areas at pallidothalamic synapses is increased in the nonhuman primate model of PD, suggesting that pallidal inputs undergo plastic changes consistent with increased synaptic strength in parkinsonism (Bodor et al., 2008), although this remains to be directly tested.

To complete this work, additional pallidothalmic terminals (that allows for 25 terminals per group) will be analyzed, as previously mentioned, from one more control and one more MPTP-treated animal that have received the viral vector listed above. In addition, terminals will be separated into different categories based on their postsynaptic target (small, medium, or large dendrite) and similar parameters (i.e. surface area, number of synapses per GPi terminal, and volume of pallidal terminals) will be analyzed and compared to the parkinsonian animal in each category. Parsing the data in this fashion will be highly valuable in determining if the morphology of GPi terminals in contact with distal and proximal dendrites is different in control monkeys and MPTP-treated monkeys.

Chapter 4 : Conclusions & Implications

4.1 Summary of main findings

In traditional models of the pathophysiology of Parkinson's disease, dopamine loss in the striatum is thought to increase the GPi/SNr inhibition of the thalamus, thereby reducing the activity of (glutamatergic) thalamocortical projection neurons. However, the underlying anatomical and electrophysiological substrates of functional changes in the glutamatergic and GABAergic systems in the motor thalamus in the parkinsonian condition have not been fully characterized. This study is one of the very few ongoing research investigations that explore the morphological and structural changes of glutamatergic and GABAergic synapses in the motor thalamus of parkinsonian monkeys. The following conclusions can be drawn from our studies:

1) There is no significant change in the prevalence and overall pattern of synaptic connectivity of GABAergic terminals from GPi and RTN in both VApc and CM.

2) There is a significant reduction in the prevalence (in the VApc), and an increase in the cross-sectional area, of vGluT1-positive, putative corticothalamic terminals in CM, but not in VApc in MPTP-treated monkeys.

3) There is a trend towards an increase in the proportion of pallidal terminals in contact with vesicle-filled dendrites of GABAergic interneurons in both the VApc and CM in MPTP-treated monkeys.

4) Preliminary results suggest:

    i. the volume of the pallidothalamic terminals is enlarged in the MPTP-treated monkey;

    ii. the average number of synapses per GPi terminal is decreased in the MPTP-treated monkey; and

iii. the flat and surface areas of synapses formed by GPi terminals are increased in the MPTP-treated monkey.

4.2 Implications

4.2.1 Influence of synaptic plasticity in the corticothalamic system

This thesis demonstrates a reduced prevalence of corticothalamic terminals in VApc, and an increased volume of these boutons in both VApc and CM of parkinsonian monkeys. Together, these observations suggest that the corticothalamic system undergoes significant synaptic remodeling in the parkinsonian state. Based on previous studies, one can believe that this glutamatergic system might be undergoing a form of pruning and morphological remodeling. Cortical terminals in the striatum and STN undergo morphological changes in parkinsonian animals. For example, in the STN there is a decreased density of vGluT1 terminals and in the striatum, vGluT1 terminals get bigger in MPTP monkeys (Chu et al., 2017; Fan et al., 2012; Mathai et al., 2015; Villalba and Smith, 2011; Villalba et al., 2015; Villalba and Smith, 2017).

Furthermore, electrophysiological studies that investigated the physiological effects of optogenetic stimulation of corticothalamic terminals in the basal ganglia- and cerebellar-receiving regions of the motor thalamus in awake normal monkeys (Galvan et al., 2016b) led to a striking result. Contrary to the expectation that activation of corticothalamic afferents leads to prominent excitatory effects in most cells, they found that activation of corticothalamic terminals elicits slowly developing excitatory and inhibitory effects in equal proportions of thalamic neurons (Galvan et al., 2016b). A possible source of this inhibition could be the involvement of GABAergic interneurons in the thalamus. It will therefore be important to investigate the connectivity with corticothalamic terminals in more animal in both normal and parkinsonian states in the future.

While the CM showed less evidence of morphological plasticity, one cannot fully rule out alterations in the CM, since it has been found to experience neuronal loss in parkinsonian

conditions (Halliday et al., 2005; Halliday, 2009; Henderson et al., 2000a; Henderson et al., 2000b; Villalba et al., 2014). Electrophysiological data about the activity of CM neurons in primate models of PD still remains sparse. Although such analyzes have been performed in the parafascicular nucleus of 6-OHDA-treated rats, the data are controversial. Some authors reported evidence for neuronal hyperactivity (Aymerich et al., 2006; Hirsch et al., 2000; Lanciego et al., 2009; Orieux et al., 2000), while others did not find any change in the firing rate of Pf neurons in parkinsonian animals (Parr-Brownlie et al., 2009; Tseng, 2009). There is also the possibility that the lack of change in the density of vGluT1 terminals in CM may be due to their increased volume, as was found for vGluT1 terminals in the striatum of MPTP monkeys. In order to determine changes in the volume of vGluT1 terminals and to visualize these terminals to its entirety, 3D EM and stereological synaptic counts should be used to address this issue.

4.2.2 Reorganization of GABAergic interneurons and projection neurons in the basal ganglia receiving thalamus

The potential trend for increase in the prevalence of pallidal and cortical terminals in contact with thalamic GABAergic interneurons suggests that thalamic GABAergic microcircuits in the parkinsonian state may undergo reorganization. In the dopamine-depleted state, studies have shown an increased inhibitory output from GPi to the thalamus (Albin et al., 1989; DeLong, 1990; Galvan and Wichmann, 2008). Changes in the organization of pallidothalamic connectivity can also enhance the basal ganglia output. This inhibition of GABAergic interneurons by the GPi may disinhibit thalamocortical neurons; thereby increasing thalamic output to motor cortices. Since interneurons add to the complexity of the intrathalamic GABAergic network via their interaction with thalamocortical neurons, it is likely that an increase in terminals forming synaptic contact with interneurons could elude to increased thalamic inhibition therefore reduced excitatory thalamic output in the dopamine depleted state (Casale and McCormick, 2011; Deschênes et al., 1982a; Deschênes and Hu, 1990; Ilinsky and Kultas-Ilinsky, 1990; Ilinsky et al., 1999; Jones and Powell, 1969; Jones, 2001; Jones, 2002a; Kultas-Ilinsky and Ilinsky, 1991;

Kultas-Ilinsky et al., 2011). The reorganization of pallidal inputs to interneurons may be initiated as a compensatory mechanism to counterbalance the direct increased inhibitory influences of GPi inputs onto thalamocortical cells that has been described in the parkinsonian state. This change in synaptic organization could also contribute to the increased synchrony of thalamocortical neurons in parkinsonism.

Despite their high prevalence in the primate thalamus, the anatomy and synaptic integration of GABAergic interneurons in the microcircuitry of the motor thalamus is largely unknown and because of the limited tools available to selectively interrogate thalamic GABAergic interneurons in the primate brain, their role remains elusive in the normal and diseased brain. The development of genetically based approaches, similar to the dual viral vector method recently used to manipulate midbrain dopaminergic neurons (Alikaya et al., 2017; Stauffer et al., 2016), may help us to further understand the role of the intrathalamic GABAergic networks in regulating thalamocortical outflow in normal and diseased states.

4.2.3 Structural changes in GABAergic system in Parkinson's disease in the VApc

It is noteworthy that the lack of changes in the prevalence and pattern of synaptic connections of GABAergic pallidothalamic synapses does not rule out the possibility that the strength and functional properties of these synapses may be affected in parkinsonism. Recent studies in rodent models of PD have suggested that GABAergic synapses from the globus pallidus (i.e. GPe in primates) on STN neurons (Chu et al., 2017; Fan et al., 2012) undergo significant structural plasticity associated with changes in the strength of pallidosubthalamic synapses in a mouse model of parkinsonism. A common feature to both GPe and GPi GABAergic terminals is their large size, large number of mitochondria and the formation of multiple synapses with their postsynaptic targets (Bodor et al., 2008; Ilinsky et al., 1997; Kultas-Ilinsky and Ilinsky, 1990; Kultas-Ilinsky et al., 1997; Wanaverbecq et al., 2008). Based on data collected from GABAergic boutons that are morphologically similar to pallidothalamic GABAergic terminals (from

substantia nigra pars reticulata and anterior pretectal nucleus), the formation of multiple synapses may provide these terminals with unique short-term plastic properties that allow maintenance of tonic synaptic inhibition even at very high firing rates (Wanaverbecq et al., 2008), and creates favorable conditions for intersynaptic spillover of GABA and cross-talk between neighboring synapses (Bodor et al., 2008). Thus, the strength of the pallidothalamic system may be dynamically regulated by changes in the number, size and proximity of synapses formed by individual pallidothalamic terminals.

Changes in GABA receptor composition or expression or in GABA release may also affect the function of the pallidothalamic system in the parkinsonian state. It is known that the expression of the mRNA for the α1 subunit of GABA-A receptor is reduced in the basal ganglia-receiving territory of the thalamus in rodent models of PD (Caruncho et al., 1997; Chadha et al., 2000; Pan et al., 1983), which may be a consequence of increased synaptic release of GABA (Christie and de Blas, 2002). The impact of this mRNA down regulation on the pattern of subsynaptic expression of GABA-A receptors in the basal ganglia-receiving thalamic nuclei remains to be established.

4.3 Concluding Remarks

In summary, our results suggest that the corticothalamic and pallidothalamic projections to the VApc and CM undergo plastic remodeling in the parkinsonian state. Whether these changes are drivers of the pathophysiology of the basal ganglia-thalamocortical networks in PD or secondary to network alterations induced by progressive nigrostriatal dopamine degeneration remains unknown. Because the pathophysiology of the thalamocortical system in PD remains poorly understood, the functional significance of the ultrastructural data presented in this thesis remains to be established. However, the development of new genetic-based approaches to interrogate specific neuronal populations and selectively manipulate projection systems in the primate brain (Boyden et al., 2005; Chow et al., 2010; Eldridge et al., 2016; Farrell et al., 2013; Fenno et al.,

2011; Grayson et al., 2016; Nagai et al., 2016; Nagel et al., 2005; Roth, 2016; Sternson and Roth, 2014), and the use of high throughput 3D electron microscopy approaches capable of fully reconstructing complex synaptic networks, may help us to understand the functional significance of synaptic microcircuit plasticity in the development, maintenance and worsening of parkinsonism. .

4.4 Future Directions

Currently there is lack of understanding of the function of GABAergic interneurons in the primate thalamus. Previous studies have shown that these neurons regulate the processing of cortical afferent information in the thalamus (Fishell and Rudy, 2011; Inan and Anderson, 2014; Kawaguchi and Kondo, 2002; Tanaka et al., 2011), but it is still unclear as to what directly regulates these cells and how these cells directly affect thalamocortical cells. It is reasonable to believe that a disruption of the thalamic drive to cortical GABAergic networks may be an important component of the pathophysiology of the thalamocortical system in parkinsonism. Furthermore, it is still obscure as to whether GABAergic interneurons belong to a single population of cells in the primate thalamus. Development of genetic-based approaches may help us to further subcategorize these cells. (Cowan and Powell, 1956)

Although little change in the morphology and postsynaptic targets was observed in the CM it is imperative that one does not ignore the impact nor significance the degeneration that happens in the CM in PD may have in the basal ganglia-thalamocortical system. It is clear that the CM undergoes significant neuronal loss in the PD state, as mentioned above, however it is still unknown as to how this neuronal loss affects the relationships between the basal ganglia, thalamus, and cortex. Because of the strong connection between the striatum and the CM, it is likely that the neuronal loss causes some plasticity in the thalamostriatal system. Future studies aimed at elucidating the physiological and pharmacological properties of CM neurons vs. other

thalamic cells are essential to determine the basis for the selective vulnerability of CM neurons in Parkinson's disease.

Overall, there is a certain level of plasticity in the GABAergic and glutamatergic system in the motor thalamus, however; there is still information in regards to alterations in the connectivity of the three cellular types in the motor thalamus in the parkinsonian state that is unknown. In addition, there is a need to understand the relative importance and significance of layer V vs. layer VI corticothalamic systems and how they relate to different cell types in the thalamus. In this study, layer V cells were not parsed out from layer VI cells; therefore, future studies should aim to identify which corticothalamic cells are from layer V and which cells are from layer VI in the VApc and CM. In addition, 3D reconstruction of GABAergic interneurons and GPi terminals in the CM could provide more information in regards to the connectivity of these structures in the motor thalamus. Since alterations in presynaptic terminals morphology and ultrastructure can influence postsynaptic activity, future studies should investigate several postsynaptic mechanisms such as neurotransmitter uptake, spillover, and even more so neurotransmitter release in the parkinsonian state. Having a full understanding of the level of plasticity the presynaptic and postsynaptic elements that might happen as compensatory mechanisms when dopamine is lost could contribute to the understanding of the pathophysiology of Parkinson's disease.

Chapter 5: References

Abbott, L.F., Chance, F.S., 2005. Drivers and modulators from push-pull and balanced synaptic input. Prog Brain Res. 149**,** 147-55.

Abdi, A., et al., 2015. Prototypic and arkypallidal neurons in the dopamine-intact external globus pallidus. J Neurosci. 35**,** 6667-88.

Akintunde, A., Buxton, D.F., 1992. Differential sites of origin and collateralization of corticospinal neurons in the rat: a multiple fluorescent retrograde tracer study. Brain Res. 575**,** 86-92.

Akkal, D., Dum, R.P., Strick, P.L., 2007. Supplementary motor area and presupplementary motor area: targets of basal ganglia and cerebellar output. J Neurosci. 27**,** 10659-73.

Albin, R.L., Young, A.B., Penney, J.B., 1989. The functional anatomy of basal ganglia disorders. Trends Neurosci. 12**,** 366-75.

Alexander, G.E., DeLong, M.R., Strick, P.L., 1986. Parallel organization of functionally segregated circuits linking basal ganglia and cortex. Annual Review of Neuroscience. 9**,** 357-381.

Alexander, G.E., Crutcher, M.D., DeLong, M.R., 1990. Basal ganglia-thalamocortical circuits: parallel substrates for motor, oculomotor, "prefrontal" and "limbic" functions. Prog Brain Res. 85**,** 119-46.

Alikaya, A., Rack-Wildner, M., Stauffer, W.R., 2017. Reward and value coding by dopamine neurons in non-human primates. J Neural Transm (Vienna).

Anderson, M.E., Postupna, N., Ruffo, M., 2003. Effects of high-frequency stimulation in the internal globus pallidus on the activity of thalamic neurons in the awake monkey. J Neurophysiol. 89**,** 1150-60.

Ansah, T.A., et al., 2011. Age- and duration-dependent effects of MPTP on cortical serotonin systems. Neurosci Lett. 504**,** 160-4.

Arai, R., Jacobowitz, D.M., Deura, S., 1994. Distribution of calretinin, calbindin-D28k, and parvalbumin in the rat thalamus. Brain Res Bull. 33**,** 595-614.

Aymerich, M.S., et al., 2006. Consequences of unilateral nigrostriatal denervation on the thalamostriatal pathway in rats. European Journal of Neuroscience. 23**,** 2099-2108.

Balercia, G., et al., 1996. Neuronal and synaptic organization of the centromedian nucleus of the monkey thalamus: a quantitative ultrastructural study, with tract tracing and immunohistochemical observations. J Neurocytol. 25**,** 267-88.

Baron, M.S., et al., 2001. Course of motor and associative pallidothalamic projections in monkeys. J Comp Neurol. 429**,** 490-501.

Barroso-Chinea, P., et al., 2008. Glutamatergic pallidothalamic projections and their implications in the pathophysiology of Parkinson's disease. Neurobiol Dis. 31**,** 422-32.

Barth, T.M., Jones, T.A., Schallert, T., 1990. Functional subdivisions of the rat somatic sensorimotor cortex. Behav Brain Res. 39**,** 73-95.

Barthó, P., Freund, T.F., Acsády, L., 2002. Selective GABAergic innervation of thalamic nuclei from zona incerta. Eur J Neurosci. 16**,** 999-1014.

Bendotti, C., et al., 1990. Developmental expression of somatostatin in mouse brain. II. In situ hybridization. Brain Res Dev Brain Res. 53**,** 26-39.

Bergman, H., et al., 1994. The primate subthalamic nucleus. II. Neuronal activity in the MPTP model of parkinsonism. Journal of Neurophysiology. 72**,** 507-20.

Berretta, S., Parthasarathy, H.B., Graybiel, A.M., 1997. Local release of GABAergic inhibition in the motor cortex induces immediate-early gene expression in indirect pathway neurons of the striatum. J Neurosci. 17**,** 4752-63.

Bodor, A.L., et al., 2008. Structural correlates of efficient GABAergic transmission in the basal ganglia-thalamus pathway. Journal of Neuroscience. 28**,** 3090-102.

Bogenpohl, J., et al., 2012. Metabotropic glutamate receptor 4 in the basal ganglia of parkinsonian monkeys: Ultrastructural localization and electrophysiological effects of activation in the striatopallidal complex. Neuropharmacology.

Bogenpohl, J., et al., 2013. Metabotropic glutamate receptor 4 in the basal ganglia of parkinsonian monkeys: Ultrastructural localization and electrophysiological effects of activation in the striatopallidal complex. Neuropharmacol. 66**,** 242-52.

Bohr, I.J., et al., 2005. Cholinergic nicotinic receptor involvement in movement disorders associated with Lewy body diseases. An autoradiography study using [(125)I]alpha-conotoxinMII in the striatum and thalamus. Experimental Neurology. 191**,** 292-300.

Bokor, H., et al., 2005. Selective GABAergic control of higher-order thalamic relays. Neuron. 45**,** 929-40.

Bolam, J.P., et al., 2000. Synaptic organisation of the basal ganglia. J Anat. 196 (Pt 4)**,** 527-42.

Bosch-Bouju, C., Hyland, B.I., Parr-Brownlie, L.C., 2013. Motor thalamus integration of cortical, cerebellar and basal ganglia information: implications for normal and parkinsonian conditions. Front Comput Neurosci. 7**,** 163.

Bosch-Bouju, C., et al., 2014. Reduced reach-related modulation of motor thalamus neural activity in a rat model of Parkinson's disease. J Neurosci. 34**,** 15836-50.

Bostan, A.C., Dum, R.P., Strick, P.L., 2010. The basal ganglia communicate with the cerebellum. Proc Natl Acad Sci U S A. 107**,** 8452-6.

Bostan, A.C., Strick, P.L., 2010. The cerebellum and basal ganglia are interconnected. Neuropsychol Rev. 20**,** 261-70.

Bové, J., Perier, C., 2012. Neurotoxin-based models of Parkinson's disease. Neuroscience. 211**,** 51-76.

Boyden, E.S., et al., 2005. Millisecond-timescale, genetically targeted optical control of neural activity. Nat Neurosci. 8**,** 1263-8.

Brown, P., 2007. Abnormal oscillatory synchronisation in the motor system leads to impaired movement. Curr Opin Neurobiol. 17**,** 656-64.

Burgunder, J.M., Young, W.S., 1992. Expression of cholecystokinin and somatostatin genes in the human thalamus. J Comp Neurol. 324**,** 14-22.

Buzsaki, G., et al., 1990. Petit mal epilepsy and parkinsonian tremor: Hypothesis of a common pacemaker. Neuroscience. 36(1)**,** 1-14.

Callaway, E.M., Wiser, A.K., 1996. Contributions of individual layer 2-5 spiny neurons to local circuits in macaque primary visual cortex. Vis Neurosci. 13**,** 907-22.

Canavan, A.G., Nixon, P.D., Passingham, R.E., 1989. Motor learning in monkeys (Macaca fascicularis) with lesions in motor thalamus. Exp Brain Res. 77**,** 113-26.

Carpenter, M.B., Nakano, K., Kim, R., 1976. Nigrothalamic projections in the monkey demonstrated by autoradiographic technics. J Comp Neurol. 165**,** 401-15.

Carpenter, M.B., et al., 1981. Connections of the subthalamic nucleus in the monkey. Brain Res. 224**,** 1-29.

Caruncho, H.J., et al., 1997. Time course of striatal, pallidal and thalamic alpha 1, alpha 2 and beta 2/3 GABAA receptor subunit changes induced by unilateral 6-OHDA lesion of the nigrostriatal pathway. Brain Res Mol Brain Res. 48**,** 243-50.

Casale, A.E., McCormick, D.A., 2011. Active action potential propagation but not initiation in thalamic interneuron dendrites. J Neurosci. 31**,** 18289-302.

Castle, M., et al., 2005. Thalamic innervation of the direct and indirect basal ganglia pathways in the rat: Ipsi- and contralateral projections. J Comp Neurol. 483**,** 143-53.

Cathala, L., et al., 2005. Changes in synaptic structure underlie the developmental speeding of AMPA receptor-mediated EPSCs. Nat Neurosci. 8**,** 1310-8.

Chadha, A., et al., 2000. Effect of unilateral 6-hydroxydopamine lesions of the nigrostriatal pathway on GABA(A) receptor subunit gene expression in the rodent basal ganglia and thalamus. Neuroscience. 95**,** 119-26.

Charara, A., et al., 2005. Synaptic and extrasynaptic GABA-A and GABA-B receptors in the globus pallidus: an electron microscopic immunogold analysis in monkeys. Neuroscience. 131**,** 917-33.

Chen, H., et al., 2010. Neuronal firing in the ventrolateral thalamus of patients with Parkinson's disease differs from that with essential tremor. Chin Med J (Engl). 123**,** 695-701.

Chow, B.Y., et al., 2010. High-performance genetically targetable optical neural silencing by light-driven proton pumps. Nature. 463**,** 98-102.

Christie, S.B., de Blas, A.L., 2002. alpha5 Subunit-containing GABA(A) receptors form clusters at GABAergic synapses in hippocampal cultures. Neuroreport. 13**,** 2355-8.

Chronister, R.B., et al., 1976. The rodent neostriatum: a Golgi analysis. Brain Res. 108**,** 37-46.

Chu, H.Y., et al., 2017. Loss of Hyperdirect Pathway Cortico-Subthalamic Inputs Following Degeneration of Midbrain Dopamine Neurons. Neuron. 95**,** 1306-1318.e5.

Cicirata, F., et al., 1986. Functional organization of thalamic projections to the motor cortex. An anatomical and electrophysiological study in the rat. Neuroscience. 19**,** 81-99.

Clemence, A.E., Mitrofanis, J., 1992. Cytoarchitectonic heterogeneities in the thalamic reticular nucleus of cats and ferrets. J Comp Neurol. 322**,** 167-80.

Cowan, W.M., Powell, T.P., 1956. A study of thalamo-striate relations in the monkey. Brain. 79**,** 364-90.

Cox, C.L., 2014. Complex regulation of dendritic transmitter release from thalamic interneurons. Curr Opin Neurobiol. 29**,** 126-32.

Crunelli, V., Leresche, N., 1991. A role for GABAB receptors in excitation and inhibition of thalamocortical cells. Trends Neurosci. 14**,** 16-21.

Dauer, W., Przedborski, S., 2003. Parkinson's disease: mechanisms and models. Neuron. 39**,** 889-909.

Davis, G.C., et al., 1979. Chronic Parkinsonism secondary to intravenous injection of meperidine analogues. Psychiatry Res. 1**,** 249-54.

Day, M., et al., 2006. Selective elimination of glutamatergic synapses on striatopallidal neurons in Parkinson disease models. Nat Neurosci. 9**,** 251-9.

DeLong, M.R., 1971. Activity of pallidal neurons during movement. J Neurophysiol. 34**,** 414-27.

DeLong, M.R., 1990. Primate models of movement disorders of basal ganglia origin. Trends in Neuroscience. 13**,** 281-285.

Deschenes, M., Bourassa, J., Pinault, D., 1994. Corticothalamic projections from layer V cells in rat are collaterals of long-range corticofugal axons. Brain Research. 664**,** 215-9.

Deschênes, M., Landry, P., Clercq, M., 1982a. A reanalysis of the ventrolateral input in slow and fast pyramidal tract neurons of the cat motor cortex. Neuroscience. 7**,** 2149-57.

Deschênes, M., Roy, J.P., Steriade, M., 1982b. Thalamic bursting mechanism: an inward slow current revealed by membrane hyperpolarization. Brain Res. 239**,** 289-93.

Deschênes, M., Hu, B., 1990. Membrane resistance increase induced in thalamic neurons by stimulation of brainstem cholinergic afferents. Brain Res. 513**,** 339-42.

Deschênes, M., Veinante, P., Zhang, Z.W., 1998. The organization of corticothalamic projections: reciprocity versus parity. Brain Res Brain Res Rev. 28**,** 286-308.

Deutch, A.Y., 2006. Striatal plasticity in parkinsonism: dystrophic changes in medium spiny neurons and progression in Parkinson's disease. J Neural Transm Suppl. 67-70.

Devergnas, A., et al., 2014. Relationship between oscillatory activity in the cortico-basal ganglia network and parkinsonism in MPTP-treated monkeys. Neurobiol Dis. 68**,** 156-66.

Devergnas, A., et al., 2016. Anatomical localization of Cav3.1 calcium channels and electrophysiological effects of T-type calcium channel blockade in the motor thalamus of MPTP-treated monkeys. J Neurophysiol. 115**,** 470-85.

DiGregorio, D.A., Nusser, Z., Silver, R.A., 2002. Spillover of glutamate onto synaptic AMPA receptors enhances fast transmission at a cerebellar synapse. Neuron. 35**,** 521-33.

Donoghue, J.P., Parham, C., 1983. Afferent connections of the lateral agranular field of the rat motor cortex. J Comp Neurol. 217**,** 390-404.

Eidelberg, D., et al., 1997. Metabolic correlates of pallidal neuronal activity in Parkinson's disease. Brain. 120 (Pt 8)**,** 1315-24.

Eldridge, M.A., et al., 2016. Chemogenetic disconnection of monkey orbitofrontal and rhinal cortex reversibly disrupts reward value. Nat Neurosci. 19**,** 37-9.

Fabri, M., Burton, H., 1991. Ipsilateral cortical connections of primary somatic sensory cortex in rats. J Comp Neurol. 311**,** 405-24.

Fan, K.Y., et al., 2012. Proliferation of external globus pallidus-subthalamic nucleus synapses following degeneration of midbrain dopamine neurons. J Neurosci. 32**,** 13718-28.

Farrell, M.S., et al., 2013. A Gαs DREADD mouse for selective modulation of cAMP production in striatopallidal neurons. Neuropsychopharmacology. 38**,** 854-62.

Fenno, L., Yizhar, O., Deisseroth, K., 2011. The development and application of optogenetics. Annu Rev Neurosci. 34**,** 389-412.

Fishell, G., Rudy, B., 2011. Mechanisms of inhibition within the telencephalon: "where the wild things are". Annu Rev Neurosci. 34**,** 535-67.

Freeman, A., et al., 2001. Nigrostriatal collaterals to thalamus degenerate in parkinsonian animal models. Ann Neurol. 50**,** 321-9.

Gabbott, P.L., et al., 1986a. A quantitative investigation of the neuronal composition of the rat dorsal lateral geniculate nucleus using GABA-immunocytochemistry. Neuroscience. 19**,** 101-11.

Gabbott, P.L., et al., 1986b. GABA-immunoreactive neurons in the dorsal lateral geniculate nucleus of the rat: characterisation by combined Golgi-impregnation and immunocytochemistry. Exp Brain Res. 61**,** 311-22.

Galvan, A., et al., 2005. GABAergic modulation of the activity of globus pallidus neurons in primates: in vivo analysis of the functions of GABA receptors and GABA transporters. J Neurophysiol. 94**,** 990-1000.

Galvan, A., Wichmann, T., 2008. Pathophysiology of parkinsonism. Clin Neurophysiol. 119**,** 1459-74.

Galvan, A., et al., 2010. Localization and function of GABA transporters in the globus pallidus of parkinsonian monkeys. Experimental Neurology. 223**,** 505-15.

Galvan, A., et al., 2011. Localization and pharmacological modulation of GABA-B receptors in the globus pallidus of parkinsonian monkeys. Exp Neurol. 229**,** 429-39.

Galvan, A., et al., 2014a. Localization and Function of Dopamine Receptors in the Subthalamic Nucleus of Normal and Parkinsonian Monkeys. J Neurophysiol.

Galvan, A., et al., 2014b. Optogenetic modulation of corticothalamic interactions in monkeys in vivo. Society for Neuroscience Abstracts.

Galvan, A., et al., 2016a. Lack of Antiparkinsonian Effects of Systemic Injections of the Specific T-Type Calcium Channel Blocker ML218 in MPTP-Treated Monkeys. ACS Chem Neurosci. 7**,** 1543-1551.

Galvan, A., et al., 2016b. Effects of Optogenetic Activation of Corticothalamic Terminals in the Motor Thalamus of Awake Monkeys. J Neurosci. 36**,** 3519-30.

Gatev, P., Darbin, O., Wichmann, T., 2006. Oscillations in the basal ganglia under normal conditions and in movement disorders. Movement Disorders. 21**,** 1566-77.

Gerfen, C.R., 1984. The neostriatal mosaic: compartmentalization of corticostriatal input and striatonigral output systems. Nature. 311**,** 461-4.

Gerfen, C.R., Baimbridge, K.G., Thibault, J., 1987a. The neostriatal mosaic: III. Biochemical and developmental dissociation of patch-matrix mesostriatal systems. J Neurosci. 7**,** 3935-44.

Gerfen, C.R., Herkenham, M., Thibault, J., 1987b. The neostriatal mosaic: II. Patch- and matrix-directed mesostriatal dopaminergic and non-dopaminergic systems. J Neurosci. 7**,** 3915-34.

Gertler, T.S., Chan, C.S., Surmeier, D.J., 2008. Dichotomous anatomical properties of adult striatal medium spiny neurons. J Neurosci. 28**,** 10814-24.

Giolli, R.A., et al., 2001. Cortical and subcortical afferents to the nucleus reticularis tegmenti pontis and basal pontine nuclei in the macaque monkey. Vis Neurosci. 18**,** 725-40.

Goldberg, J.H., Farries, M.A., Fee, M.S., 2013. Basal ganglia output to the thalamus: still a paradox. Trends Neurosci. 36**,** 695-705.

Goldman-Rakic, P.S., Selemon, L.D., 1990. New frontiers in basal ganglia research. Introduction. Trends Neurosci. 13**,** 241-4.

Govindaiah, G., Cox, C.L., 2006. Metabotropic glutamate receptors differentially regulate GABAergic inhibition in thalamus. J Neurosci. 26**,** 13443-53.

Graybiel, A.M., Ragsdale, C.W., 1978. Histochemically distinct compartments in the striatum of human, monkeys, and cat demonstrated by acetylthiocholinesterase staining. Proc Natl Acad Sci U S A. 75**,** 5723-6.

Graybiel, A.M., et al., 1981. An immunohistochemical study of enkephalins and other neuropeptides in the striatum of the cat with evidence that the opiate peptides are arranged to form mosaic patterns in register with the striosomal compartments visible by acetylcholinesterase staining. Neuroscience. 6**,** 377-97.

Graybiel, A.M., Elde, R.P., 1983. Somatostatin-like immunoreactivity characterizes neurons of the nucleus reticularis thalami in the cat and monkey. J Neurosci. 3**,** 1308-21.

Grayson, D.S., et al., 2016. The Rhesus Monkey Connectome Predicts Disrupted Functional Networks Resulting from Pharmacogenetic Inactivation of the Amygdala. Neuron. 91**,** 453-66.

Groenewegen, H.J., 1988. Organization of the afferent connections of the mediodorsal thalamic nucleus in the rat, related to the mediodorsal-prefrontal topography. Neuroscience. 24**,** 379-431.

Grofová, I., Rinvik, E., 1974. Cortical and pallidal projections to the nucleus ventralis lateralis thalami. Electron microscopical studies in the cat. Anat Embryol (Berl). 146**,** 113-32.

Guehl, D., et al., 2003. Tremor-related activity of neurons in the 'motor' thalamus: changes in firing rate and pattern in the MPTP vervet model of parkinsonism. European Journal of Neuroscience. 17**,** 2388-400.

Haber, S.N., et al., 1990. Topographic organization of the ventral striatal efferent projections in the rhesus monkey: an anterograde tracing study. J Comp Neurol. 293**,** 282-98.

Haber, S.N., Calzavara, R., 2009. The cortico-basal ganglia integrative network: the role of the thalamus. Brain Res Bull. 78**,** 69-74.

Hadipour-Niktarash, A., et al., 2012. Extrastriatal D2-like receptors modulate basal ganglia pathways in normal and Parkinsonian monkeys. J Neurophysiol. 107**,** 1500-12.

Halliday, G.M., Macdonald, V., Henderson, J.M., 2005. A comparison of degeneration in motor thalamus and cortex between progressive supranuclear palsy and Parkinson's disease. Brain. 128**,** 2272-80.

Halliday, G.M., 2009. Thalamic changes in Parkinson's disease. Parkinsonism Relat Disord. 15 Suppl 3**,** S152-5.

Hammond, C., Bergman, H., Brown, P., 2007. Pathological synchronization in Parkinson's disease: networks, models and treatments. Trends Neurosci. 30**,** 357-64.

Hazrati, L.N., Parent, A., 1991. Contralateral pallidothalamic and pallidotegmental projections in primates: an anterograde and retrograde labeling study. Brain Res. 567**,** 212-23.

Henderson, J.M., et al., 2000a. Degeneration of the centré median-parafascicular complex in Parkinson's disease. Ann Neurol. 47**,** 345-52.

Henderson, J.M., et al., 2000b. Loss of thalamic intralaminar nuclei in progressive supranuclear palsy and Parkinson's disease: clinical and therapeutic implications. Brain. 123 (Pt 7), 1410-21.

Herkenham, M., 1979. The afferent and efferent connections of the ventromedial thalamic nucleus in the rat. J Comp Neurol. 183, 487-517.

Herkenham, M., 1980. Laminar organization of thalamic projections to the rat neocortex. Science. 207, 532-5.

Hikosaka, O., 1991. Basal ganglia--possible role in motor coordination and learning. Curr Opin Neurobiol. 1, 638-43.

Hirsch, E.C., et al., 2000. Metabolic effects of nigrostriatal denervation in basal ganglia. Trends Neurosci. 23, S78-85.

Hoover, J.E., Strick, P.L., 1993. Multiple output channels in the basal ganglia. Science. 259, 819-21.

Hutchison, W.D., et al., 1994. Differential neuronal activity in segments of globus pallidus in Parkinson's disease patients. Neuroreport. 5, 1533-7.

Hámori, J., et al., 1974. Triadic synaptic arrangements and their possible significance in the lateral geniculate nucleus of the monkey. Brain Res. 80, 379-93.

Ilinsky, I.A., Kultas-Ilinsky, K., Smith, K.R., 1982. Organization of basal ganglia inputs to the thalamus. A light and electron microscopic study in the cat. Appl Neurophysiol. 45, 230-7.

Ilinsky, I.A., Kultas-Ilinsky, K., 1984. An autoradiographic study of topographical relationships between pallidal and cerebellar projections to the cat thalamus. Exp Brain Res. 54, 95-106.

Ilinsky, I.A., 1990. Structural and connectional diversity of the primate motor thalamus: experimental light and electron microscopic studies in the rhesus monkey. Stereotact Funct Neurosurg. 54-55, 114-24.

Ilinsky, I.A., Kultas-Ilinsky, K., 1990. Fine structure of the magnocellular subdivision of the ventral anterior thalamic nucleus (VAmc) of Macaca mulatta: I. Cell types and synaptology. J Comp Neurol. 294, 455-78.

Ilinsky, I.A., Tourtellotte, W.G., Kultas-Ilinsky, K., 1993. Anatomical distinctions between the two basal ganglia afferent territories in the primate motor thalamus. Stereotact Funct Neurosurg. 60, 62-9.

Ilinsky, I.A., Yi, H., Kultas-Ilinsky, K., 1997. Mode of termination of pallidal afferents to the thalamus: a light and electron microscopic study with anterograde tracers and immunocytochemistry in Macaca mulatta. J Comp Neurol. 386**,** 601-12.

Ilinsky, I.A., Ambardekar, A.V., Kultas-Ilinsky, K., 1999. Organization of projections from the anterior pole of the nucleus reticularis thalami (NRT) to subdivisions of the motor thalamus: light and electron microscopic studies in the rhesus monkey. J Comp Neurol. 409**,** 369-84.

Inan, M., Anderson, S.A., 2014. The chandelier cell, form and function. Curr Opin Neurobiol. 26**,** 142-8.

Inase, M., et al., 1996. Origin of thalamocortical projections to the presupplementary motor area (pre-SMA) in the macaque monkey. Neurosci Res. 25**,** 217-27.

Ingham, C.A., et al., 1998. Plasticity of synapses in the rat neostriatum after unilateral lesion of the nigrostriatal dopaminergic pathway. Journal of Neuroscience. 18**,** 4732-43.

Jahanshahi, M., et al., 1995. Self-initiated versus externally triggered movements. I. An investigation using measurement of regional cerebral blood flow with PET and movement-related potentials in normal and Parkinson's disease subjects. Brain. 118 (Pt 4)**,** 913-33.

Jellinger, K.A., 1991. Pathology of Parkinson's disease. Changes other than the nigrostriatal pathway. Mol Chem Neuropathol. 14**,** 153-97.

Johnston, J.G., et al., 1990. Mechanisms of striatal pattern formation: conservation of mammalian compartmentalization. Brain Res Dev Brain Res. 57**,** 93-102.

Jones, B.E., Yang, T.Z., 1985. The efferent projections from the reticular formation and the locus coeruleus studied by anterograde and retrograde axonal transport in the rat. J Comp Neurol. 242**,** 56-92.

Jones, E.G., Powell, T.P., 1969. An electron microscopic study of the mode of termination of cortico-thalamic fibres within the sensory relay nuclei of the thalamus. Proc R Soc Lond B Biol Sci. 172**,** 173-85.

Jones, E.G., Leavitt, R.Y., 1974. Retrograde axonal transport and the demonstration of non-specific projections to the cerebral cortex and striatum from thalamic intralaminar nuclei in the rat, cat and monkey. J Comp Neurol. 154**,** 349-77.

Jones, E.G., 2001. The thalamic matrix and thalamocortical synchrony. Trends Neurosci. 24**,** 595-601.

Jones, E.G., 2002a. Thalamic organization and function after Cajal. Prog Brain Res. 136**,** 333-57.

Jones, E.G., 2002b. Thalamic circuitry and thalamocortical synchrony. Philos Trans R Soc Lond B Biol Sci. 357**,** 1659-73.

Jones, E.G., 2007. The Thalamus, Vol. 1 and 2, Cambridge University Press, New York.

Jongen-Rělo, A.L., Groenewegen, H.J., Voorn, P., 1993. Evidence for a multi-compartmental histochemical organization of the nucleus accumbens in the rat. J Comp Neurol. 337**,** 267-76.

Kakei, S., Na, J., Shinoda, Y., 2001. Thalamic terminal morphology and distribution of single corticothalamic axons originating from layers 5 and 6 of the cat motor cortex. Journal of Comparative Neurology. 437**,** 170-85.

Kammermeier, S., et al., 2014. Effects of stimulation of the internal globus pallidus on thalamic activity patterns in parkinsonian monkeys. Society for Neuroscience Annual meeting Abstracts.

Kammermeier, S., et al., 2016. Effects of high-frequency stimulation of the internal pallidal segment on neuronal activity in the thalamus in parkinsonian monkeys. J Neurophysiol. 116**,** 2869-2881.

Kaneoke, Y., Vitek, J.L., 1995. The motor thalamus in the parkinsonian primate: enhanced burst and oscillatory activities. Society for Neuroscience Abstracts. 21**,** 1428.

Kaufman, E.F., Rosenquist, A.C., 1985a. Afferent connections of the thalamic intralaminar nuclei in the cat. Brain Res. 335**,** 281-96.

Kaufman, E.F., Rosenquist, A.C., 1985b. Efferent projections of the thalamic intralaminar nuclei in the cat. Brain Res. 335**,** 257-79.

Kawaguchi, Y., Wilson, C.J., Emson, P.C., 1990. Projection subtypes of rat neostriatal matrix cells revealed by intracellular injection of biocytin. J Neurosci. 10**,** 3421-38.

Kawaguchi, Y., Kondo, S., 2002. Parvalbumin, somatostatin and cholecystokinin as chemical markers for specific GABAergic interneuron types in the rat frontal cortex. J Neurocytol. 31**,** 277-87.

Kim, K.M., Nakajima, S., Nakajima, Y., 1997. Dopamine and GABA receptors in cultured substantia nigra neurons: correlation of electrophysiology and immunocytochemistry. Neuroscience. 78**,** 759-69.

Kimura, A., et al., 2007. Axonal projections of single auditory neurons in the thalamic reticular nucleus: implications for tonotopy-related gating function and cross-modal modulation. Eur J Neurosci. 26**,** 3524-35.

Kimura, A., 2014. Diverse subthreshold cross-modal sensory interactions in the thalamic reticular nucleus: implications for new pathways of cross-modal attentional gating function. Eur J Neurosci. 39**,** 1405-18.

Kita, H., Kitai, S.T., 1991. Intracellular study of rat globus pallidus neurons: membrane properties and responses to neostriatal, subthalamic and nigral stimulation. Brain Res. 564**,** 296-305.

Kita, H., 2007. Globus pallidus external segment. Prog Brain Res. 160**,** 111-33.

Kliem, M.A., Wichmann, T., 2004. A method to record changes in local neuronal discharge in response to infusion of small drug quantities in awake monkeys. Journal of Neuroscience Methods. 138**,** 45-9.

Kliem, M.A., et al., 2007. Activation of nigral and pallidal dopamine D1-like receptors modulates basal ganglia outflow in monkeys. J Neurophysiol. 98**,** 1489-500.

Kliem, M.A., et al., 2009. Comparative Ultrastructural Analysis of D1 and D5 Dopamine Receptor Distribution in the Substantia Nigra and Globus Pallidus of Monkeys. Adv Behav Biol. 58**,** 239-253.

Kosar, E., Grill, H.J., Norgren, R., 1986. Gustatory cortex in the rat. II. Thalamocortical projections. Brain Res. 379**,** 342-52.

Krettek, J.E., Price, J.L., 1977. The cortical projections of the mediodorsal nucleus and adjacent thalamic nuclei in the rat. J Comp Neurol. 171**,** 157-91.

Kultas-Ilinsky, K., et al., 1983. Fine structure of nigral and pallidal afferents in the thalamus: an EM autoradiography study in the cat. J Comp Neurol. 216**,** 390-405.

Kultas-Ilinsky, K., et al., 1990. GABA and benzodiazepine receptors in the cat motor thalamus after lesioning of nigro- and pallidothalamic pathways. Brain Res. 511**,** 197-208.

Kultas-Ilinsky, K., Ilinsky, I.A., 1990. Fine structure of the magnocellular subdivision of the ventral anterior thalamic nucleus (VAmc) of Macaca mulatta: II. Organization of nigrothalamic afferents as revealed with EM autoradiography. J Comp Neurol. 294**,** 479-89.

Kultas-Ilinsky, K., Ilinsky, I.A., 1991. Fine structure of the ventral lateral nucleus (VL) of the Macaca mulatta thalamus: cell types and synaptology. J Comp Neurol. 314**,** 319-49.

Kultas-Ilinsky, K., et al., 1997. Pallidal afferent territory of the Macaca mulatta thalamus: neuronal and synaptic organization of the VAdc. J Comp Neurol. 386**,** 573-600.

Kultas-Ilinsky, K., Ilinsky, I.A., Verney, C., 2011. Glutamic acid decarboxylase isoform 65 immunoreactivity in the motor thalamus of humans and monkeys: γ-aminobutyric acidergic connections and nuclear delineations. J Comp Neurol. 519**,** 2811-37.

Kuo, J.S., Carpenter, M.B., 1973. Organization of pallidothalamic projections in the rhesus monkey. J Comp Neurol. 151**,** 201-36.

Kuroda, M., Price, J.L., 1991. Ultrastructure and synaptic organization of axon terminals from brainstem structures to the mediodorsal thalamic nucleus of the rat. J Comp Neurol. 313**,** 539-52.

Lacey, C.J., Bolam, J.P., Magill, P.J., 2007. Novel and distinct operational principles of intralaminar thalamic neurons and their striatal projections. J Neurosci. 27**,** 4374-84.

Lanciego, J.L., et al., 1998. Multiple axonal tracing: simultaneous detection of three tracers in the same section. Histochem Cell Biol. 110**,** 509-15.

Lanciego, J.L., et al., 2004. Thalamic innervation of striatal and subthalamic neurons projecting to the rat entopeduncular nucleus. Eur J Neurosci. 19**,** 1267-77.

Lanciego, J.L., et al., 2009. The search for a role of the caudal intralaminar nuclei in the pathophysiology of Parkinson's disease. Brain Res Bull. 78**,** 55-9.

Lanciego, J.L., Vázquez, A., 2012. The basal ganglia and thalamus of the long-tailed macaque in stereotaxic coordinates. A template atlas based on coronal, sagittal and horizontal brain sections. Brain Struct Funct. 217**,** 613-66.

Langston, J.W., et al., 1984. Selective nigral toxicity after systemic administration of 1-methyl-4-phenyl-1,2,5,6-tetrahydropyrine (MPTP) in the squirrel monkey. Brain Res. 292**,** 390-4.

Lavallée, P., et al., 2005. Feedforward inhibitory control of sensory information in higher-order thalamic nuclei. J Neurosci. 25**,** 7489-98.

Leblois, A., et al., 2007. Late emergence of synchronized oscillatory activity in the pallidum during progressive Parkinsonism. Eur J Neurosci. 26**,** 1701-13.

Lefaucheur, J.P., 2005. Motor cortex dysfunction revealed by cortical excitability studies in Parkinson's disease: influence of antiparkinsonian treatment and cortical stimulation. Clin Neurophysiol. 116**,** 244-53.

Leichnetz, G.R., Gonzalo-Ruiz, A., 1987. Collateralization of frontal eye field (medial precentral/anterior cingulate) neurons projecting to the paraoculomotor region, superior colliculus, and medial pontine reticular formation in the rat: a fluorescent double-labeling study. Exp Brain Res. 68**,** 355-64.

Leichnetz, G.R., Hardy, S.G., Carruth, M.K., 1987. Frontal projections to the region of the oculomotor complex in the rat: a retrograde and anterograde HRP study. J Comp Neurol. 263**,** 387-99.

Liu, X.B., Jones, E.G., 1999. Predominance of corticothalamic synaptic inputs to thalamic reticular nucleus neurons in the rat. J Comp Neurol. 414**,** 67-79.

Magnin, M., Morel, A., Jeanmonod, D., 2000. Single-unit analysis of the pallidum, thalamus and subthalamic nucleus in parkinsonian patients. Neuroscience. 96**,** 549-64.

Mallet, N., et al., 2012. Dichotomous organization of the external globus pallidus. Neuron. 74**,** 1075-86.

Martin, L.J., et al., 1991. The striatal mosaic in primates: patterns of neuropeptide immunoreactivity differentiate the ventral striatum from the dorsal striatum. Neuroscience. 43**,** 397-417.

Masilamoni, G., et al., 2010. (18)F-FECNT: validation as PET dopamine transporter ligand in parkinsonism. Experimental Neurology. 226**,** 265-73.

Masilamoni, G.J., et al., 2011. Metabotropic glutamate receptor 5 antagonist protects dopaminergic and noradrenergic neurons from degeneration in MPTP-treated monkeys. Brain. 134**,** 2057-73.

Masilamoni, G.J., Smith, Y., 2017. Chronic MPTP administration regimen in monkeys: a model of dopaminergic and non-dopaminergic cell loss in Parkinson's disease. J Neural Transm (Vienna).

Mathai, A., Smith, Y., 2011. The corticostriatal and corticosubthalamic pathways: two entries, one target. So what? Front Syst Neurosci. 5**,** 64.

Mathai, A., et al., 2015. Reduced cortical innervation of the subthalamic nucleus in MPTP-treated parkinsonian monkeys. Brain. 138**,** 946-62.

McCormick, D.A., Bal, T., 1994. Sensory gating mechanisms of the thalamus. Curr Opin Neurobiol. 4**,** 550-6.

McDowell, K., Chesselet, M.F., 2012. Animal models of the non-motor features of Parkinson's disease. Neurobiol Dis. 46**,** 597-606.

McFarland, N.R., Haber, S.N., 2000. Convergent inputs from thalamic motor nuclei and frontal cortical areas to the dorsal striatum in the primate. J Neurosci. 20**,** 3798-813.

McFarland, N.R., Haber, S.N., 2001. Organization of thalamostriatal terminals from the ventral motor nuclei in the macaque. J Comp Neurol. 429**,** 321-36.

McFarland, N.R., Haber, S.N., 2002. Thalamic relay nuclei of the basal ganglia form both reciprocal and nonreciprocal cortical connections, linking multiple frontal cortical areas. Journal of Neuroscience. 22**,** 8117-32.

McHaffie, J.G., et al., 2005. Subcortical loops through the basal ganglia. Trends Neurosci. 28**,** 401-7.

Meissner, W., et al., 2005. Subthalamic high frequency stimulation resets subthalamic firing and reduces abnormal oscillations. Brain. 128**,** 2372-82.

Meredith, G.E., Pennartz, C.M., Groenewegen, H.J., 1993. The cellular framework for chemical signalling in the nucleus accumbens. Prog Brain Res. 99**,** 3-24.

Meredith, G.E., et al., 1996. Shell and core in monkey and human nucleus accumbens identified with antibodies to calbindin-D28k. J Comp Neurol. 365**,** 628-39.

Middleton, F.A., Strick, P.L., 1994. Anatomical evidence for cerebellar and basal ganglia involvement in higher cognitive function. Science. 266**,** 458-61.

Middleton, F.A., Strick, P.L., 1996. Basal ganglia and cerebellar output influences non-motor function. Mol Psychiatry. 1**,** 429-33.

Middleton, F.A., Strick, P.L., 2002. Basal-ganglia 'projections' to the prefrontal cortex of the primate. Cerebral Cortex. 12**,** 926-35.

Mink, J.W., 1996. The basal ganglia: focused selection and inhibition of competing motor programs. Prog Neurobiol. 50**,** 381-425.

Mitchell, I.J., et al., 1989. Neural mechanisms underlying parkinsonian symptoms based upon regional uptake of 2-deoxyglucose in monkeys exposed to 1-methyl-4-phenyl-1,2,3,6-tetrahydropyridine. Neuroscience. 32**,** 213-26.

Molnar, G.F., et al., 2005. Differences in neuronal firing rates in pallidal and cerebellar receiving areas of thalamus in patients with Parkinson's disease, essential tremor, and pain. Journal of Neurophysiology. 93**,** 3094-101.

Na, J., Kakei, S., Shinoda, Y., 1997. Cerebellar input to corticothalamic neurons in layers V and VI in the motor cortex. Neurosci Res. 28**,** 77-91.

Nagai, Y., et al., 2016. PET imaging-guided chemogenetic silencing reveals a critical role of primate rostromedial caudate in reward evaluation. Nat Commun. 7**,** 13605.

Nagel, G., et al., 2005. Light activation of channelrhodopsin-2 in excitable cells of Caenorhabditis elegans triggers rapid behavioral responses. Curr Biol. 15**,** 2279-84.

Nambu, A., Llinaś, R., 1994. Electrophysiology of globus pallidus neurons in vitro. J Neurophysiol. 72**,** 1127-39.

Nambu, A., Tokuno, H., Takada, M., 2002. Functional significance of the cortico-subthalamo-pallidal 'hyperdirect' pathway. Neurosci Res. 43**,** 111-7.

Nayyar, T., et al., 2009. Cortical serotonin and norepinephrine denervation in parkinsonism: preferential loss of the beaded serotonin innervation. Eur J Neurosci. 30**,** 207-16.

Neafsey, E.J., et al., 1986a. The organization of the rat motor cortex: a microstimulation mapping study. Brain Res. 396**,** 77-96.

Neafsey, E.J., Hurley-Gius, K.M., Arvanitis, D., 1986b. The topographical organization of neurons in the rat medial frontal, insular and olfactory cortex projecting to the solitary nucleus, olfactory bulb, periaqueductal gray and superior colliculus. Brain Res. 377**,** 261-70.

Ni, Z.G., et al., 2000. Unilateral lesion of the nigrostriatal pathway induces a transient decrease of firing rate with no change in the firing pattern of neurons of the parafascicular nucleus in the rat. Neuroscience. 101**,** 993-9.

Nini, A., et al., 1995. Neurons in the globus pallidus do not show correlated activity in the normal monkey, but phase-locked oscillations appear in the MPTP model of parkinsonism. J Neurophysiol. 74**,** 1800-5.

Ohara, P.T., et al., 1983. Neural elements containing glutamic acid decarboxylase (GAD) in the dorsal lateral geniculate nucleus of the rat; immunohistochemical studies by light and electron microscopy. Neuroscience. 8**,** 189-211.

Ohara, P.T., Lieberman, A.R., 1985. The thalamic reticular nucleus of the adult rat: experimental anatomical studies. J Neurocytol. 14**,** 365-411.

Ohara, P.T., 1988. Synaptic organization of the thalamic reticular nucleus. J Electron Microsc Tech. 10**,** 283-92.

Ohye, C., et al., 1970. Effect of dorsal rhizotomy on postural tremor in the monkey. Experimental Brain Research. 10**,** 140-50.

Orieux, G., et al., 2000. Metabolic activity of excitatory parafascicular and pedunculopontine inputs to the subthalamic nucleus in a rat model of Parkinson's disease. Neuroscience. 97**,** 79-88.

Pahapill, P.A., Lozano, A.M., 2000. The pedunculopontine nucleus and Parkinson's disease. Brain. 123**,** 1767-83.

Pan, H.S., et al., 1983. Changes in [3H]muscimol binding in substantia nigra, entopeduncular nucleus, globus pallidus, and thalamus after striatal lesions as demonstrated by quantitative receptor autoradiography. J Neurosci. 3**,** 1189-98.

Parent, A., De Bellefeuille, L., 1983. The pallidointralaminar and pallidonigral projections in primate as studied by retrograde double-labeling method. Brain Res. 278**,** 11-27.

Parent, A., et al., 1983. The output organization of the substantia nigra in primate as revealed by a retrograde double labeling method. Brain Research Bulletin. 10**,** 529-37.

Parent, A., 1990. Extrinsic connections of the basal ganglia. Trends Neurosci. 13**,** 254-8.

Parent, A., Charara, A., Pinault, D., 1995. Single striatofugal axons arborizing in both pallidal segments and in the substantia nigra in primates. Brain Res. 698**,** 280-4.

Parent, A., Hazrati, L.N., 1995a. Functional anatomy of the basal ganglia. I. The cortico-basal ganglia-thalamo-cortical loop. Brain Res Brain Res Rev. 20**,** 91-127.

Parent, A., Hazrati, L.N., 1995b. Functional anatomy of the basal ganglia. II. The place of subthalamic nucleus and external pallidum in basal ganglia circuitry. Brain Res Brain Res Rev. 20**,** 128-54.

Parent, A., et al., 2000. Organization of the basal ganglia: the importance of axonal collateralization. Trends Neurosci. 23**,** S20-7.

Parent, M., Lévesque, M., Parent, A., 2001. Two types of projection neurons in the internal pallidum of primates: single-axon tracing and three-dimensional reconstruction. J Comp Neurol. 439**,** 162-75.

Parent, M., Parent, A., 2004. The pallidofugal motor fiber system in primates. Parkinsonism Relat Disord. 10**,** 203-11.

Parent, M., Parent, A., 2005. Single-axon tracing and three-dimensional reconstruction of centre median-parafascicular thalamic neurons in primates. J Comp Neurol. 481**,** 127-44.

Parkinson, J., 1817. An essay on the shaking palsy., Vol., W.a. Rowland, N. for Sherwood, and Jones, ed.^eds., London, pp. 66.

Parr-Brownlie, L.C., et al., 2009. Parafascicular thalamic nucleus activity in a rat model of Parkinson's disease. Exp Neurol. 217**,** 269-81.

Paré, D., Smith, Y., 1996. Thalamic collaterals of corticostriatal axons: their termination field and synaptic targets in cats. J Comp Neurol. 372**,** 551-67.

Passingham, R.E., et al., 1988. Premotor cortex in the rat. Behav Neurosci. 102**,** 101-9.

Percheron, G., et al., 1996. The primate motor thalamus. Brain Res Brain Res Rev. 22**,** 93-181.

Percheron, G., 1997. The motor thalamus. J Neurosurg. 87**,** 981-2.

Pessiglione, M., et al., 2005. Thalamic neuronal activity in dopamine-depleted primates: evidence for a loss of functional segregation within basal ganglia circuits. Journal of Neuroscience. 25**,** 1523-31.

Peters, A., Palay, S., Webster, H., 1991. The fine structure of the nervous system-Neurons and their supporting cells Vol., Oxford University Press, New York.

Pinault, D., Bourassa, J., Deschenes, M., 1995. The axonal arborization of single thalamic reticular neurons in the somatosensory thalamus of the rat. European Journal of Neuroscience. 7**,** 31-40.

Pinault, D., Deschênes, M., 1998. Projection and innervation patterns of individual thalamic reticular axons in the thalamus of the adult rat: a three-dimensional, graphic, and morphometric analysis. J Comp Neurol. 391**,** 180-203.

Pinault, D., 2004. The thalamic reticular nucleus: structure, function and concept. Brain Res Brain Res Rev. 46**,** 1-31.

Przedborski, S., et al., 2001. The parkinsonian toxin 1-methyl-4-phenyl-1,2,3,6-tetrahydropyridine (MPTP): a technical review of its utility and safety. J Neurochem. 76**,** 1265-74.

Raeva, S., Vainberg, N., Dubinin, V., 1999. Analysis of spontaneous activity patterns of human thalamic ventrolateral neurons and their modifications due to functional brain changes. Neuroscience. 88**,** 365-76.

Raju, D.V., et al., 2006. Differential synaptology of vGluT2-containing thalamostriatal afferents between the patch and matrix compartments in rats. J Comp Neurol. 499**,** 231-43.

Raju, D.V., et al., 2008. Differential synaptic plasticity of the corticostriatal and thalamostriatal systems in an MPTP-treated monkey model of parkinsonism. European Journal of Neuroscience. 27**,** 1647-58.

Rascol, O., et al., 1992. Supplementary and primary sensory motor area activity in Parkinson's disease. Regional cerebral blood flow changes during finger movements and effects of apomorphine. Arch Neurol. 49**,** 144-8.

Rascol, O., et al., 1994. Normal activation of the supplementary motor area in patients with Parkinson's disease undergoing long-term treatment with levodopa. J Neurol Neurosurg Psychiatry. 57**,** 567-71.

Raz, A., Vaadia, E., Bergman, H., 2000. Firing patterns and correlations of spontaneous discharge of pallidal neurons in the normal and the tremulous 1-methyl-4-phenyl-1,2,3,6-tetrahydropyridine vervet model of parkinsonism. J Neurosci. 20**,** 8559-71.

Redgrave, P., Prescott, T.J., Gurney, K., 1999. The basal ganglia: a vertebrate solution to the selection problem? Neuroscience. 89**,** 1009-23.

Reep, R.L., et al., 1984. Afferent connections of medial precentral cortex in the rat. Neurosci Lett. 44**,** 247-52.

Reep, R.L., Goodwin, G.S., Corwin, J.V., 1990. Topographic organization in the corticocortical connections of medial agranular cortex in rats. J Comp Neurol. 294**,** 262-80.

Rico, A.J., et al., 2010. A direct projection from the subthalamic nucleus to the ventral thalamus in monkeys. Neurobiol Dis. 39**,** 381-92.

Rieck, R.W., Carey, R.G., 1985. Organization of the rostral thalamus in the rat: evidence for connections to layer I of visual cortex. J Comp Neurol. 234**,** 137-54.

Rochet, J.C., 2012. New insights into lysosomal dysfunction in Parkinson's disease: an emerging role for ATP13A2. Mov Disord. 27**,** 1092.

Rochet, J.C., Hay, B.A., Guo, M., 2012. Molecular insights into Parkinson's disease. Prog Mol Biol Transl Sci. 107**,** 125-88.

Rolland, A.S., et al., 2007. Metabolic activity of cerebellar and basal ganglia-thalamic neurons is reduced in parkinsonism. Brain. 130**,** 265-75.

Roth, B.L., 2016. DREADDs for Neuroscientists. Neuron. 89**,** 683-94.

Rouiller, E.M., et al., 1998. Dual morphology and topography of the corticothalamic terminals originating from the primary, supplementary motor, and dorsal premotor cortical areas in macaque monkeys. Journal of Comparative Neurology. 396**,** 169-85.

Rouiller, E.M., Welker, E., 2000. A comparative analysis of the morphology of corticothalamic projections in mammals. Brain Research Bulletin. 53**,** 727-41.

Rovó, Z., Ulbert, I., Acsády, L., 2012. Drivers of the primate thalamus. J Neurosci. 32**,** 17894-908.

Royce, G.J., Mourey, R.J., 1985. Efferent connections of the centromedian and parafascicular thalamic nuclei: an autoradiographic investigation in the cat. J Comp Neurol. 235**,** 277-300.

Sadikot, A.F., Parent, A., François, C., 1992a. Efferent connections of the centromedian and parafascicular thalamic nuclei in the squirrel monkey: a PHA-L study of subcortical projections. J Comp Neurol. 315**,** 137-59.

Sadikot, A.F., et al., 1992b. Efferent connections of the centromedian and parafascicular thalamic nuclei in the squirrel monkey: a light and electron microscopic study of the thalamostriatal projection in relation to striatal heterogeneity. J Comp Neurol. 320**,** 228-42.

Sakai, S.T., Grofova, I., Bruce, K., 1998. Nigrothalamic projections and nigrothalamocortical pathway to the medial agranular cortex in the rat: single- and double-labeling light and electron microscopic studies. J Comp Neurol. 391**,** 506-25.

Sakai, S.T., Inase, M., Tanji, J., 1999. Pallidal and cerebellar inputs to thalamocortical neurons projecting to the supplementary motor area in Macaca fuscata: a triple-labeling light microscopic study. Anat Embryol (Berl). 199**,** 9-19.

Sakai, S.T., et al., 2000. Pallidal and cerebellar afferents to pre-supplementary motor area thalamocortical neurons in the owl monkey: a multiple labeling study. J Comp Neurol. 417**,** 164-80.

Sakai, S.T., Inase, M., Tanji, J., 2002. The relationship between MI and SMA afferents and cerebellar and pallidal efferents in the macaque monkey. Somatosensory & Motor Research. 19**,** 139-48.

Sarnthein, J., Jeanmonod, D., 2007. High thalamocortical theta coherence in patients with Parkinson's disease. Journal of Neuroscience. 27**,** 124-31.

Scatton, B., et al., 1983. Reduction of cortical dopamine, noradrenaline, serotonin and their metabolites in Parkinson's disease. Brain Res. 275**,** 321-8.

Schell, G.R., Strick, P.L., 1984. The origin of thalamic inputs to the arcuate premotor and supplementary motor areas. J Neurosci. 4**,** 539-60.

Schneider, C.A., Rasband, W.S., Eliceiri, K.W., 2012. NIH Image to ImageJ: 25 years of image analysis. Nat Methods. 9**,** 671-5.

Schneider, J.S., Rothblat, D.S., 1996. Alterations in intralaminar and motor thalamic physiology following nigrostriatal dopamine depletion. Brain Research. 742**,** 25-33.

Sherman, S.M., Friedlander, M.J., 1988. Identification of X versus Y properties for interneurons in the A-laminae of the cat's lateral geniculate nucleus. Exp Brain Res. 73**,** 384-92.

Sherman, S.M., Guillery, R.W., 2001. Exploring the Thalamus, Vol., Academic Press, San Diego.

Sherman, S.M., Guillery, R.W., 2002. The role of the thalamus in the flow of information to the cortex. Philos Trans R Soc Lond B Biol Sci. 357**,** 1695-708.

Sherman, S.M., 2004. Interneurons and triadic circuitry of the thalamus. Trends Neurosci. 27**,** 670-5.

Sherman, S.M., 2005. Thalamic relays and cortical functioning. Prog Brain Res. 149**,** 107-26.

Sherman, S.M., Guillery, R.W., 2011. Distinct functions for direct and transthalamic corticocortical connections. J Neurophysiol. 106**,** 1068-77.

Sherman, S.M., 2012. Thalamocortical interactions. Current Opinion in Neurobiology. 22**,** 575-9.

Shi, T., Apkarian, A.V., 1995. Morphology of thalamocortical neurons projecting to the primary somatosensory cortex and their relationship to spinothalamic terminals in the squirrel monkey. J Comp Neurol. 361**,** 1-24.

Shindo, K., Shima, K., Tanji, J., 1995. Spatial distribution of thalamic projections to the supplementary motor area and the primary motor cortex: a retrograde multiple labeling study in the macaque monkey. J Comp Neurol. 357**,** 98-116.

Shink, E., Smith, Y., 1995. Differential synaptic innervation of neurons in the internal and external segments of the globus pallidus by the GABA- and glutamate-containing terminals in the squirrel monkey. J Comp Neurol. 358**,** 119-41.

Shink, E., et al., 1996. The subthalamic nucleus and the external pallidum: two tightly interconnected structures that control the output of the basal ganglia in the monkey. Neuroscience. 73**,** 335-57.

Shink, E., Sidibé, M., Smith, Y., 1997. Efferent connections of the internal globus pallidus in the squirrel monkey: II. Topography and synaptic organization of pallidal efferents to the pedunculopontine nucleus. J Comp Neurol. 382**,** 348-63.

Sidibe, M., et al., 1997. Efferent connections of the internal globus pallidus in the squirrel monkey: I. Topography and synaptic organization of the pallidothalamic projection. Journal of Comparative Neurology. 382**,** 323-47.

Sidibe, M., Pare, J.F., Smith, Y., 2002. Nigral and pallidal inputs to functionally segregated thalamostriatal neurons in the centromedian/parafascicular intralaminar nuclear complex in monkey. Journal of Comparative Neurology. 447**,** 286-99.

Sidibé, M., Smith, Y., 1996. Differential synaptic innervation of striatofugal neurones projecting to the internal or external segments of the globus pallidus by thalamic afferents in the squirrel monkey. J Comp Neurol. 365**,** 445-65.

Sirota, M.G., Swadlow, H.A., Beloozerova, I.N., 2005. Three channels of corticothalamic communication during locomotion. Journal of Neuroscience. 25**,** 5915-25.

Smith, Y., Parent, A., 1986. Differential connections of caudate nucleus and putamen in the squirrel monkey (Saimiri sciureus). Neuroscience. 18**,** 347-71.

Smith, Y., Seguela, P., Parent, A., 1987. Distribution of GABA-immunoreactive neurons in the thalamus of the squirrel monkey (Saimiri sciureus). Neuroscience. 22**,** 579-91.

Smith, Y., Sidibe, M., 2003. The Thalamus. In: Neuroscience in Medicine. Vol., P.M. Conn, ed.^eds. Humana Press Inc., Totowa, NJ.

Smith, Y., et al., 2004. The thalamostriatal system: a highly specific network of the basal ganglia circuitry. Trends Neurosci. 27**,** 520-7.

Smith, Y. (Ed.) 2008. The Thalamus, in Neuroscience in Medicine. Human Press: Totowa, NJ.

Smith, Y., et al., 2009. The thalamostriatal systems: anatomical and functional organization in normal and parkinsonian states. Brain Res Bull. 78**,** 60-8.

Smith, Y., et al., 2012. Parkinson's disease therapeutics: new developments and challenges since the introduction of levodopa. Neuropsychopharmacology. 37**,** 213-46.

Smith, Y., et al., 2014a. The thalamostriatal system in normal and diseased states. Front Syst Neurosci. 8**,** 5.

Smith, Y., Wichmann, T., DeLong, M.R., 2014b. Corticostriatal and mesocortical dopamine systems: do species differences matter? Nat Rev Neurosci. 15**,** 63.

Soares, J., et al., 2004. Role of external pallidal segment in primate parkinsonism: comparison of the effects of 1-methyl-4-phenyl-1,2,3,6-tetrahydropyridine-induced parkinsonism and lesions of the external pallidal segment. J Neurosci. 24**,** 6417-26.

Stauffer, W.R., et al., 2016. Dopamine Neuron-Specific Optogenetic Stimulation in Rhesus Macaques. Cell. 166**,** 1564-1571.e6.

Stepniewska, I., Preuss, T.M., Kaas, J.H., 2007. Thalamic connections of the dorsal and ventral premotor areas in New World owl monkeys. Neuroscience. 147**,** 727-45.

Steriade, M., 2001. The GABAergic reticular nucleus: a preferential target of corticothalamic projections. Proceedings of the National Academy of Sciences of the United States of America. 98**,** 3625-7.

Sternson, S.M., Roth, B.L., 2014. Chemogenetic tools to interrogate brain functions. Annu Rev Neurosci. 37**,** 387-407.

Strick, P.L., 1985. How do the basal ganglia and cerebellum gain access to the cortical motor areas? Behavioural Brain Research. 18**,** 107-23.

Surmeier, D.J., Song, W.J., Yan, Z., 1996. Coordinated expression of dopamine receptors in neostriatal medium spiny neurons. J Neurosci. 16**,** 6579-91.

Tanaka, Y.H., et al., 2011. Local connections of layer 5 GABAergic interneurons to corticospinal neurons. Front Neural Circuits. 5**,** 12.

Taverna, S., Ilijic, E., Surmeier, D.J., 2008. Recurrent collateral connections of striatal medium spiny neurons are disrupted in models of Parkinson's disease. J Neurosci. 28**,** 5504-12.

Telgkamp, P., et al., 2004. Maintenance of high-frequency transmission at purkinje to cerebellar nuclear synapses by spillover from boutons with multiple release sites. Neuron. 41**,** 113-26.

Tepper, J.M., et al., 2010. Heterogeneity and diversity of striatal GABAergic interneurons. Front Neuroanat. 4**,** 150.

Tokuno, H., Kimura, M., Tanji, J., 1992. Pallidal inputs to thalamocortical neurons projecting to the supplementary motor area: an anterograde and retrograde double labeling study in the macaque monkey. Exp Brain Res. 90**,** 635-8.

Tseng, G.F., Royce, G.J., 1986. A Golgi and ultrastructural analysis of the centromedian nucleus of the cat. J Comp Neurol. 245**,** 359-78.

Tseng, K.Y., 2009. Facing the lack of anti-phase oscillation in the parafascicular nucleus after dopamine depletion. Experimental Neurology. 219**,** 62-5.

Tsumori, T., et al., 2002. Synaptic organization of GABAergic projections from the substantia nigra pars reticulata and the reticular thalamic nucleus to the parafascicular thalamic nucleus in the rat. Brain Res. 957**,** 231-41.

Uylings, H.B., van Eden, C.G., 1990. Qualitative and quantitative comparison of the prefrontal cortex in rat and in primates, including humans. Prog Brain Res. 85**,** 31-62.

Villalba, R.M., Lee, H., Smith, Y., 2009. Dopaminergic denervation and spine loss in the striatum of MPTP-treated monkeys. Exp Neurol. 215**,** 220-7.

Villalba, R.M., Smith, Y., 2010. Striatal spine plasticity in Parkinson's disease. Front Neuroanat. 4**,** 133.

Villalba, R.M., Smith, Y., 2011. Differential structural plasticity of corticostriatal and thalamostriatal axo-spinous synapses in MPTP-treated Parkinsonian monkeys. J Comp Neurol. 519**,** 989-1005.

Villalba, R.M., Smith, Y., 2013. Differential striatal spine pathology in Parkinson's disease and cocaine addiction: a key role of dopamine? Neuroscience. 251**,** 2-20.

Villalba, R.M., Wichmann, T., Smith, Y., 2014. Neuronal loss in the caudal intralaminar thalamic nuclei in a primate model of Parkinson's disease. Brain Struct Funct. 219**,** 381-94.

Villalba, R.M., Mathai, A., Smith, Y., 2015. Morphological changes of glutamatergic synapses in animal models of Parkinson's disease. Front Neuroanat. 9**,** 117.

Vitek, J.L., Ashe, J., Kaneoke, Y., 1994. Spontaneous neuronal activity in the motor thalamus: alteration in pattern and rate in parkinsonism. Society for Neuroscience Abstracts. 20**,** 561.

Vitek, J.L., et al., 2012. External pallidal stimulation improves parkinsonian motor signs and modulates neuronal activity throughout the basal ganglia thalamic network. Exp Neurol. 233**,** 581-6.

Voloshin, M., et al., 1994. Electrophysiological investigation of thalamic neuronal mechanisms of motor disorders in parkinsonism: an influence of D2ergic transmission blockade on excitation and inhibition of relay neurons in motor thalamic nuclei of cat. Neuroscience. 62**,** 771-81.

Voorn, P., Gerfen, C.R., Groenewegen, H.J., 1989. Compartmental organization of the ventral striatum of the rat: immunohistochemical distribution of enkephalin, substance P, dopamine, and calcium-binding protein. J Comp Neurol. 289**,** 189-201.

Wanaverbecq, N., et al., 2008. Contrasting the functional properties of GABAergic axon terminals with single and multiple synapses in the thalamus. J Neurosci. 28**,** 11848-61.

Wichmann, T., DeLong, M.R., 1993. Pathophysiology of parkinsonian motor abnormalities. Adv Neurol. 60**,** 53-61.

Wichmann, T., DeLong, M.R., 1996. Functional and pathophysiological models of the basal ganglia. Curr Opin Neurobiol. 6**,** 751-8.

Wichmann, T., et al., 1999. Comparison of MPTP-induced changes in spontaneous neuronal discharge in the internal pallidal segment and in the substantia nigra pars reticulata in primates. Experimental Brain Research. 125**,** 397-409.

Wichmann, T., Kliem, M.A., DeLong, M.R., 2001. Antiparkinsonian and behavioral effects of inactivation of the substantia nigra pars reticulata in hemiparkinsonian primates. Experimental Neurology. 167**,** 410-424.

Wichmann, T., DeLong, M.R., 2003. Pathophysiology of Parkinson's disease: the MPTP primate model of the human disorder. Ann N Y Acad Sci. 991**,** 199-213.

Wichmann, T., Soares, J., 2006. Neuronal firing before and after burst discharges in the monkey basal ganglia is predictably patterned in the normal state and altered in parkinsonism. Journal of Neurophysiology. 95**,** 2120-33.

Willis, A.M., et al., 2015. Open-loop organization of thalamic reticular nucleus and dorsal thalamus: a computational model. J Neurophysiol. 114**,** 2353-67.

Wilson, C.J., Phelan, K.D., 1982. Dual topographic representation of neostriatum in the globus pallidus of rats. Brain Res. 243**,** 354-9.

Wu, Y., Richard, S., Parent, A., 2000. The organization of the striatal output system: a single-cell juxtacellular labeling study in the rat. Neurosci Res. 38**,** 49-62.

Wörgötter, F., et al., 2002. The influence of the corticothalamic projection on responses in thalamus and cortex. Philos Trans R Soc Lond B Biol Sci. 357**,** 1823-34.

Zahm, D.S., Brog, J.S., 1992. On the significance of subterritories in the "accumbens" part of the rat ventral striatum. Neuroscience. 50**,** 751-67.

Zhang, L., Jones, E.G., 2004. Corticothalamic inhibition in the thalamic reticular nucleus. J Neurophysiol. 91**,** 759-66.

Zirh, T.A., et al., 1998. Patterns of bursting occurring in thalamic cells during parkinsonian tremor. Neuroscience. 83**,** 107-21.

Zucker, R.S., Regehr, W.G., 2002. Short-term synaptic plasticity. Annu Rev Physiol. 64**,** 355-405.